

Studies on Fabrication of Bilayer Scaffolds Incorporating Antibacterial and Antioxidant Agents for Wound Healing Applications

THESIS

Submitted in partial fulfilment
of the requirements for the degree of
DOCTOR OF PHILOSOPHY

By
MOHAMMED MONSOOR SHAIK

Under the Supervision of
Prof. Meenal Kowshik



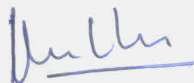
BITS Pilani
Pilani | Dubai | Goa | Hyderabad

**BIRLA INSTITUTE OF TECHNOLOGY AND SCIENCE,
PILANI
2018**

BIRLA INSTITUTE OF TECHNOLOGY AND SCIENCE, PILANI

CERTIFICATE

This is to certify that the thesis entitled “**Studies on Fabrication of Bilayer Scaffolds Incorporating Antibacterial and Antioxidant Agents for Wound Healing Applications**” submitted by **Mr. Mohammed Monsoor Shaik** ID No **2011PXHF0404G** for award of Ph.D. of the Institute embodies original work done by him under my supervision.



Signature of the Supervisor

Prof. Meenal Kowshik

Date: 10th Oct 2018

Acknowledgements

First and foremost I offer my sincerest gratitude to my supervisor, Dr Meenal Kowshik, who has supported me throughout my thesis with her knowledge and patience whilst believing me. I thank her for reinforcing the values of independence and perseverance all through my career at BITS. I attribute the level of my PhD degree to her encouragement and effort without her this thesis, too, would not have been completed or written. One simply could not wish for a better or friendlier supervisor.

I am grateful to Prof. Souvik Bhattacharyya, Vice Chancellor, BITS Pilani and Prof. Raghu Rama, Director, BITS Pilani K K Birla Goa Campus for providing necessary facilities and financial support as “Institute Research Fellowship” to fulfill my research dreams. I would like to extend my thanks to Prof. Bijendra Nath Jain (former Vice Chancellor), Prof. K. E. Raman and Prof. Sanjeev K Agarawal (former director BITS Pilani K K Birla Goa Campus) for their constant support.

I would like to extend my gratitude towards Prof. Dibakar Chakraborty, Convener, Doctoral Research Committee (DRC) and other DRC members for their co-operation. I express heartiest thanks to Dr. Angshuman Sarkar for teaching the animal cell culture techniques and guidance throughout my thesis as a member of Doctoral Advisory Committee (DAC). I also consider it a privilege to record my respect to Prof. Vijayshree Nayak, for her support as a member of my DAC. I would also extend my thanks to the entire faculty at department of Biological Sciences, for their support and encouragement.

In my daily work I have been blessed with a friendly and cheerful group of fellow students who made my stay in BITS a wonderful joyful experience. I am grateful to my friends Dr. Ajay Ghosh Chalasani, Dr. Pallavee Srivastava, Dr. Shruti Balaji, Dr. Archana Sharma, Dr. Ketaki Deshmukh, Dr. Rajesh Pasumarthi, Dr. Kshipra Naik, Dr. Ramya Ramachandran, Dr. Deepti Das, Dr. Vilas Desai and Dr. Raeesh Shaik for making my stay memorable. I thank my fellow research group members, Pranjita Zantye, Reshma, Pooja, and Dr. Gauri for their help in various ways. I am thankful to Kamana ma'am, Mahadev, and Mahalingam for their help in day to day lab activities.

I am thankful to Dr. Jyuthika Rajwade and Dr. Sachin Jadhav, Agharkar Research Institute, Pune for their help in animal studies, which played a crucial role in concluding my research.

It is now my turn to thank my family who stood by my side for completion of my thesis work. I would like to greatly acknowledge the constant motivating support I received from my parents Moosamiah Shaik and Musarath Banu. I extend my support to my siblings, Fahimida, Mujahid, and Maseeha for their support and encouragement. I would also like to extend my gratitude towards my fiancé, Eleonora Messa for her love, inspiration, support and motivation.

Abstract

Chitosan (CS) incorporated silver (Ag) scaffolds were synthesized with varying concentrations of Ag (1, 2, and 3 % w/w) by using a novel melt-down neutralization technique followed by solvent curing and freeze drying. The slow and steady melting of the frozen chitosan solution allows uniform neutralization of the scaffold, resulting in even distribution of Ag throughout the CS matrix. The synthesized scaffolds (CS-Ag) were characterized by X-ray diffraction, Fourier transform infrared spectroscopy, thermogravimetric analysis, and scanning electron microscopy. The *in vitro* degradation of the scaffold was studied using the enzyme, lysozyme for 28 days. The *in vitro* release kinetics of Ag shows an initial high release followed by slow and sustained release. The CS–Ag scaffolds exhibit excellent antibacterial properties against representative Gram-positive (*Staphylococcus aureus*) and Gram-negative (*Escherichia coli*) bacterial cultures. The antibacterial activity of scaffolds increases with the concentration of Ag. The *in vitro* biocompatibility of the CS–Ag scaffolds was studied using HaCaT cells (keratinocytes) by the MTT assay. The scaffolds are biocompatible and support cell adhesion and proliferation without exhibiting any toxicity. The CS–Ag scaffolds are proposed as promising candidates for treating bacterial infections in tissue engineering applications.

Scaffolds with different concentrations (0.5, 1 and 2% w/w) of antioxidants (SM/ CM/ EA) incorporated within the collagen (CO) and CS matrix were synthesized with an aim to incorporate antioxidant properties within the supporting matrix. The structural characterization of the scaffolds was carried out by XRD and FTIR, which confirmed the presence of antioxidants (SM/ CM/ EA) within the CS-CO matrix. The synthesized scaffolds exhibited sustained release of antioxidants in phosphate buffered saline for 120 h. The scaffolds were biocompatible and supported the growth of COS7 (fibroblast) cells. The CS-CO scaffolds incorporated with antioxidants and seeded with cells were subjected to UV irradiation for 10, 20, and 30 minutes, and cell viability was recorded by the MTT assay immediately and 24 h after incubation. All the three antioxidant incorporated scaffolds exhibit excellent cell revival at both the time points; with the order of efficiency being SM>CM>EA. These scaffolds with the potential to address oxidative stress may be strategic in managing chronic wounds.

The bilayer scaffolds were fabricated by incorporating a layer upon layer arrangement of CS-Ag3 and the 2 % (w/w) antioxidant (SM/ CM/ EA) incorporated within CS-CO matrix, with an aim to impart antibacterial as well as antioxidant activity. The *in vivo*

studies on bilayer scaffolds were carried out in Wistar rat models at 3, 7 and 10 days post injury and the skin excisions were studied for wound contraction, histology (H&E staining), and lipid peroxidation (anti-malondialdehyde). The bilayer scaffold with antioxidants accelerated the process of wound healing with no inflammatory cells, proliferation of fibroblast, neovascularization and collagen deposition, where as the control exhibited excessive inflammation throughout the healing process. The bilayer scaffolds containing Ag/SM exhibited complete wound contraction by day 10 and had a structure similar to normal skin with complete re-epithelialization. While the bilayer scaffolds with Ag/CM and Ag/EA exhibited 91 % and 84 % wound contraction. Thus, the bilayer scaffold with antioxidant and antimicrobial properties can promote wound healing and is proposed as a potential tissue engineering material for managing chronic wounds.

Brief Contents

Sr. No.	Title	Page
1	Introduction and Literature of Review	1
2	Synthesis and Characterization of Silver Incorporated Chitosan Scaffolds	20
3	Synthesis and Characterization of Antioxidant Incorporated Chitosan-Collagen Scaffolds	39
4	Fabrication of Bilayer Scaffolds and Their <i>In vivo</i> Applications	63
5	Summary of Results and Conclusion	76
6	Future Scope of Work	79
7	List of Publications and Presentations	100
8	Brief Biography of the Candidate	102
9	Brief Biography of the Supervisor	103

Table of Contents

	Page
Thesis Title Page (Annexure I)	
Certificate from Supervisor (Annexure II)	
Acknowledgements	
Abstract.....	i
Brief contents.....	iii
Table of Contents.....	iv
List of Tables.....	vii
List of Figures.....	viii
List of Abbreviations/Symbols.....	xii
Chapter 1: Introduction and Literature Review	
1.1 Tissue engineering	1
1.1.1 Cells	1
1.1.2 Bioreactor.....	2
1.1.3 Scaffolds/Matrices	3
1.1.4 Bioactive molecules	4
1.2 Biomaterials in tissue engineering	5
1.3 Skin tissue engineering	7
1.3.1 Anatomy of skin.....	8
1.4 Wound healing	8
1.5 Types of Wounds	10
1.6 Factors affecting wound healing.....	10
1.6.1 Infections.....	11
1.6.2 Oxidative stress.....	12
1.7 Wound care medications.....	13
1.8 Gaps in Existing Research	18

Chapter 2: Synthesis and Characterization of Silver Incorporated Chitosan Scaffolds

2.1 Introduction.....	20
2.2 Materials and Methods.....	22
2.2.1 Chemicals and materials	22
2.2.2 Synthesis of CS-Ag scaffolds	22
2.2.3 Characterization	23
2.3 Results and Discussion:	26
2.3.1 XRD analysis	29
2.3.2 FTIR analysis	30
2.3.3 Thermal stability by TGA.....	31
2.3.4 <i>In-vitro</i> degradation of scaffolds.....	32
2.3.5 Anti-bacterial studies	33
2.3.6 <i>In vitro</i> Ag release studies.....	35
2.3.7 Biocompatibility studies	36
2.4 Conclusion	38

Chapter 3: Synthesis and Characterization of Antioxidant Incorporated Chitosan-Collagen Scaffolds

3.1 Introduction.....	39
3.2 Materials and methods	41
3.2.1 Materials	41
3.2.2 Synthesis of antioxidant (SM/CM/EA) incorporated collagen chitosan scaffolds	41
3.2.3 Characterization	42
3.3 Results and Discussion:	44
3.3.1 Synthesis of the CS-CO scaffolds.....	44
3.3.2 Physico-chemical characterization of the scaffolds	45

3.3.3 Release kinetics of the antioxidants from the antioxidant incorporated scaffolds	52
3.3.4 <i>In vitro</i> biocompatibility of the scaffolds.....	55
3.3.5 Application/ anti-oxidant activity of scaffolds	58
3.4 Conclusion	62

Chapter 4: Fabrication of Bilayer Scaffolds and Their *In vivo* Applications

4.1 Introduction.....	63
4.2 Materials and methods	64
4.2.1 Materials	64
4.2.2 Synthesis and fabrication of bilayer scaffolds	64
4.2.3 Swelling studies.....	64
4.2.4 Assessment of functional performance of the bilayer scaffolds	65
4.2.5 Statistical analysis.....	67
4.3 Results and discussion:	67
4.3.1 Estimation of the rate of wound healing (wound closure).....	68
4.3.2 Histological examination of skin excisions	71
4.3.3 Immunohistochemical staining	72
4.4 Conclusion	74

List of Tables

Table	Title	Page
Chapter 1		
1.1	Factors affecting wound healing	11

List of Figures

Figure	Title	Page
Chapter 1		
1.1	Factors involved in tissue engineering	3
1.2	Graphical representation of wound healing process	9
1.3	Graphical representation of wound healing in the chronic wounds	10
1.4	Structure of SM (A), CM (B) and EA (C)	16
Chapter 2		
2.1 (A)	Standard curve of D-Glucosamine by ninhydrin assay	27
2.1 (B)	Reduced viscosity of chitosan solutions at varying concentrations. Intrinsic viscosity of the CS is shown in the inset as the intercept value	27
2.2	CS scaffolds neutralized with NaOH without melt-down (A), and with melt-down (B) technique	28
2.3	SEM micrographs showing the porosity of the CS (A), CS-Ag1, CS-Ag2 and CS-Ag3 scaffolds (scale bar – 100 μ M)	29
2.4	XRD diffractograms of CS, CS-Ag1, CS-Ag2 and CS-Ag3 scaffolds	30
2.5	FT-IR spectra of CS, CS-Ag1, CS-Ag2 and CS-Ag3 scaffolds	31
2.6	TGA curves of CS, CS-Ag1, CS-Ag2 and CS-Ag3 scaffolds	32
2.7	Degradation studies of CS, CS-Ag1, CS-Ag2 and CS-Ag3 scaffolds using lysozyme treatment for a period of 7 to 28days	33
2.8	Antibacterial effect of CS and CS-Ag (1,2,3) scaffolds against <i>E.coli</i> (A) and <i>S.aureus</i> (B)	33
2.9	Growth of bacterial cells around the CS scaffolds incubated with bacterial suspension for 24 h. No growth is observed around CS-Ag scaffolds.	34
2.10	Ag release rate from the CS-Ag scaffolds over a period of seven days	35
2.11	SEM micrographs of HaCaT cell attachment and proliferation on	36

	CS (A), CS-Ag1, CS-Ag2 and CS-Ag3 scaffolds (scale bar- 10 μ M)	
2.12	Cell viability by MTT assay on CS, CS-Ag1, CS-Ag2 and CS-Ag3	37
<hr/>		
Chapter 3		
<hr/>		
3.1	SEM micrographs of CS-CO scaffolds (A) along with 2 % w/w SM (B), CM (C) and EA (D), incorporated CS-CO scaffolds (scale bar – 200 μ M)	45
3.2	XRD pattern of CS and CS-CO scaffolds exhibiting the semi-amorphous nature of the polymers	46
3.3	XRD pattern of the CS-CO-SM _(0.5) , CS-CO-SM ₍₁₎ and CS-CO-SM ₍₂₎ scaffolds along with the CS-CO scaffolds and SM	47
3.4	XRD patterns of the CS-CO-CM _(0.5) , CS-CO-CM ₍₁₎ and CS-CO-CM ₍₂₎ scaffolds along with the CS-CO scaffolds and CM	47
3.5	XRD pattern of the CS-CO-EA _(0.5) , CS-CO-EA ₍₁₎ and CS-CO-EA ₍₂₎ scaffolds along with the CS-CO scaffolds and EA	48
3.6	FTIR spectra of CS-CO scaffolds along with CO, and CS polymers	49
3.7	FT-IR spectra of the CS-CO-SM _(0.5) , CS-CO-SM ₍₁₎ and CS-CO-SM ₍₂₎ scaffolds along with the CS-CO scaffolds and SM	50
3.8	FT-IR spectra of the CS-CO-CM _(0.5) , CS-CO-CM ₍₁₎ and CS-CO-CM ₍₂₎ scaffolds along with the CS-CO scaffolds and CM	51
3.9	FT-IR spectra of the CS-CO-EA _(0.5) , CS-CO-EA ₍₁₎ and CS-CO-EA ₍₂₎ scaffolds along with the CS-CO scaffolds and EA	52
3.10 (A)	<i>In vitro</i> release kinetics of SM (%) from the CS-CO-SM _(0.5) , CS-CO-SM ₍₁₎ and CS-CO-SM ₍₂₎ at different time intervals	53
3.10 (B)	<i>In vitro</i> release kinetics of CM (%) from the CS-CO-CM _(0.5) , CS-CO-CM ₍₁₎ and CS-CO-CM ₍₂₎ at different time intervals	54
3.10 (C)	<i>In vitro</i> release kinetics of EA (%) from the CS-CO-EA _(0.5) , CS-CO-EA ₍₁₎ and CS-CO-EA ₍₂₎ at different time intervals	54
3.11	<i>In vitro</i> cytotoxicity studies of the CS-CO, CS-CO-SM _(0.5) , CS-CO-SM ₍₁₎ and CS-CO-SM ₍₂₎ scaffolds on COS-7 cells at different time intervals	55

3.12	<i>In vitro</i> cytotoxicity studies of the CS-CO, CS-CO-CM _(0.5) , CS-CO-CM ₍₁₎ and CS-CO-CM ₍₂₎ scaffolds on COS-7 cells at different time intervals	56
3.13	<i>In vitro</i> cytotoxicity studies of the CS-CO, CS-CO-EA _(0.5) , CS-CO-EA ₍₁₎ and CS-CO-EA ₍₂₎ scaffolds on COS-7 cells at different time intervals	56
3.14	SEM images indicating cell adhesion, growth and proliferation of COS7 cells on CS-CO scaffolds (A) along with 2% w/w SM (B), CM (C), and EA (D) incorporated in CS-CO scaffolds (scale bar – 10 μM)	57
3.15	Cytocompatibility of COS-7 cells seeded on SM (0.5, 1, 2 % w/w) scaffolds and exposed to UV light for 10, 20 and 30 min. Cell viability was recorded after incubating for 0h (A) and 24h (B) post UV exposure. $p < 0.05$ of SM (0.5, 1 and 2 %) scaffolds compared with the CO(CS) scaffold	59
3.16	Cytocompatibility of COS-7 cells seeded on CM (0.5, 1, 2 % w/w) scaffolds and exposed to UV light for 10, 20 and 30 min. Cell viability was recorded after incubating for 0h (A) and 24h (B) post UV exposure. $p < 0.05$ of SM (0.5, 1 and 2 %) scaffolds compared with the CO(CS) scaffold	60
3.17	Cytocompatibility of COS-7 cells seeded on EA (0.5, 1, 2 % w/w) scaffolds and exposed to UV light for 10, 20 and 30 min. Cell viability was recorded after incubating for 0h (A) and 24h (B) post UV exposure. $p < 0.05$ of SM (0.5, 1 and 2 %) scaffolds compared with the CO(CS) scaffold	61

Chapter 4

4.1	Swelling behavior of bilayer scaffolds incorporated with Ag/antioxidants (EA; CM; SM) along with BS-C in PBS at 37° C for 1, 2, 4, 8, 12 and 24 h (data are expressed as standard error of mean).	68
4.2	Representative images of the Wistar rats skin wounds after the administration of BS-C, BS-Ag-EA, BS-Ag-CM, BS-Ag-SM scaffolds and natural healing (control) on days 3, 7, and 10 days	69

	post injury	
4.3	Graphical representation of the wound contraction in Wistar rats after the application of BS-C, BS-Ag-EA, BS-Ag-CM, BS-Ag-SM scaffolds and natural healing (control) at 3, 7, and 10 days post injury. All values represent the means and SD; $n = 3$	70
4.4	Histological evaluation of skin grafts treated with of BS-C, BS-Ag-EA, BS-Ag-CM, BS-Ag-SM scaffolds and natural healing (control) after 3, 7, and 10 days post injury. (Black arrow-inflammatory infiltration; Yellow arrow-epithelialization; Red arrow-fibrogenesis; Green arrow-granulation)	71
4.5 (A)	Immunohistochemistry staining of anti-MDA performed on the skin grafts treated with BS-C, BS-Ag-EA, BS-Ag-CM, BS-Ag-SM scaffolds and natural healing (control) after 3, 7, and 10 days post injury	73
4.5 (B)	Graphical representation of Relative colour intensity of MDA in BS-C, BS-Ag-EA, BS-Ag-CM, and BS-Ag-SM scaffolds in context to natural healing (control), analyzed using ImageJ software	73

List of Abbreviations/ Symbols

η - Intrinsic viscosity
ATR – Attenuated total reflection
a.u – Arbitrary unit
Ag – Silver
AgNO₃ – Silver nitrate
ATP – Adenosine triphosphate
BS-Ag-CM – Bilayer scaffold with silver and curcumin
BS-Ag-EA – Bilayer scaffold with silver and ellagic acid
BS-Ag-SM – Bilayer scaffold with silver and silymarin
BS-C – Bilayer scaffold control
CM – Curcumin
CO – Collagen
CO₂ – Carbon dioxide
COS7 – Monkey kidney fibroblast
cps – counts per second
CS – Chitosan
DI – Deionized water
DMEM – Dulbecco's Modified Eagle's medium
DMSO – Dimethyl sulfoxide
DNA – Deoxyribonucleic acid
EA – Ellagic acid
ECM – Extracellular matrix
EtOH – Ethanol
FAAS – Flame atomic absorption spectroscopy
FBS – Fetal bovine serum
FTIR – Fourier transform Infrared
GAGs – Glycosaminoglycans

GPX – Glutathione peroxidase
GPX – Glutathione peroxidase
GST – Glutathione-S-transferase
H₂O – Water
H₂O₂ – Hydrogen peroxide

HaCaT – Human epidermal keratinocytes
HO-1 – heme oxygenase 1
IR – Infrared
JCPDS – Joint Committee on Powder Diffraction Standards
MDA – Malondialdehyde
MH – Muller Hinton
MMPs – Matrix metalloproteases
MTCC – Microbial Type Culture Collection and Gene Bank
MTT – 3-(4,5-dimethylthiazol-2-yl)-2,5-diphenyltetrazolium bromide
NaOH – Sodium hydroxide
NCCS – National Centre for Cell Science
NCIM – National Chemical Laboratory
PBS – Phosphate buffered saline
ppm – parts per million
ROS – Reactive oxygen species
SEM – Scanning electron microscopy
SM – Silymarin
SOD – Superoxide dismutase
SWF – Simulated wound fluid
TGA – Thermogravimetric analysis
UV – Ultraviolet
XRD – X-ray diffraction

Chapter 1: Introduction and Literature Review

1.1 Tissue engineering

In the early 90s' the increase in the demand for the organs/tissues and the complications arising due to lack of donors, transplant rejection, immunogenic suppressive treatments, etc., has led to the development of tissue engineering as an alternative in modern medicine. Tissue engineering by definition “applies the principles of engineering and life sciences towards the development of biological substitutes that can restore, maintain or improve the tissue functions” (Langer and Vacanti 1993). In other words tissue engineering deals with the application of engineering methods in life sciences by using biological mimics towards the development of structural and functional relationships of a damaged tissue. Tissue engineering is an interdisciplinary field which covers a broader range of applications in transplantation biology, drug delivery, biomedical engineering, and regenerative medicine. The advances in the field of tissue engineering have gained importance for the development of materials with functional characteristics. The incorporation of drugs/growth factors into biological substitutes and controlling their release behavior increase the therapeutic potential of the tissue engineering in the field of drug delivery (Stratton et al. 2016). Each tissue has different cells, some cells have the ability to completely renew (skin, mucosal lining, bone marrow etc.) while others are non-regenerative after differentiation. Tissue engineering methods have provided a platform for the stem cells to transform in to tissue types such as, heart muscle and nerves which are non regenerative in nature. The term regenerative medicine is often used synonymously with tissue engineering, although those involved in regenerative medicine emphasis more on the use of stem cells to produce tissues (Howard et al. 2008).

Generally, tissue engineering involves four major components which are cells, a matrix or scaffold, a bioreactor, and bioactive molecules. The *in vitro* involvement of all the components may or may not be necessary as the fabrication of tissue engineered products purely depend upon the type of application. As each tissue in the body contains different cell types and functions, the design of the tissue engineering materials mainly depends on the cellular and structural properties of the materials (Chaudhari et al. 2016).

1.1.1 Cells

Cells are the building blocks of life as described by Virchow in 1858, “*Omnis cellula e cellula...*” meaning that cells arise from pre-existing cells. Every tissue consists of a

variety of cell types, the progenitor cells for the tissue engineering product can be either stem cells with the ability to differentiate into multiple cell types or the neighboring cells from the implant site. Based upon the nature of the implant, the tissue engineering matrices are classified as acellular or cellular (Dhandayuthapani et al. 2011).

1.1.1.1 Acellular matrices

Tissue engineering products with decellularized matrices, which encourage the regeneration of the tissue solely by residing at the implantation site are known as acellular matrix. Various decellularized matrices derived from intestinal submucosa, amniotic membrane, heart valves, liver, etc., have been widely used to regenerate the functional tissues and organs (Hoshiba et al. 2010). These products aim to stimulate the local environment by recruiting the neighboring cells as progenitor cells to repair tissues, and hence do not face the regulatory and scientific challenges of cell based matrices. Investigations on decellularized matrices which are derived from a variety of tissues, and biopolymers have shown to facilitate the remodeling of many different tissues such as cartilage, skin, bone, bladder, blood vessels, heart etc., in both preclinical animal studies and in human clinical applications (Burdick et al. 2013).

1.1.1.2 Cellular matrices

The cellular matrices involve inclusion of cells into the matrix, prior to the implantation. The cells may be directly added on to the matrix during the implantation or allowed to grow in a *in vitro* bioreactor by providing necessary growth factors and other biochemical signals for their differentiation in to the desired tissue of interest. The use of progenitor stem cells in cellular matrices helps in cases where specialized cells within the organs have been damaged due to disease, or due to extensive tissue loss leading to organ dysfunction. The utilization of passive *in vitro* differentiation of specialized stem cells into tissue specific cells on the matrix will act as a step further in tissue regeneration. The challenges associated with *in vitro* growth of the tissue include the limitations with respect to differentiation and remodeling of stem cells. (Banerjee 2017).

1.1.2 Bioreactor

A bioreactor in tissue engineering can be defined as a device that provides physical and chemical stimulants to the cells thereby modulating their biological process. These biological processes can vary depending upon the type of application, as some signals will encourage stem cells to differentiate in to desired cell phenotype and some will

modulate the cells to produce extracellular matrix (ECM). The bioreactors increase the uniformity and reproducibility of the biological process in a regulated *in vitro* environment.

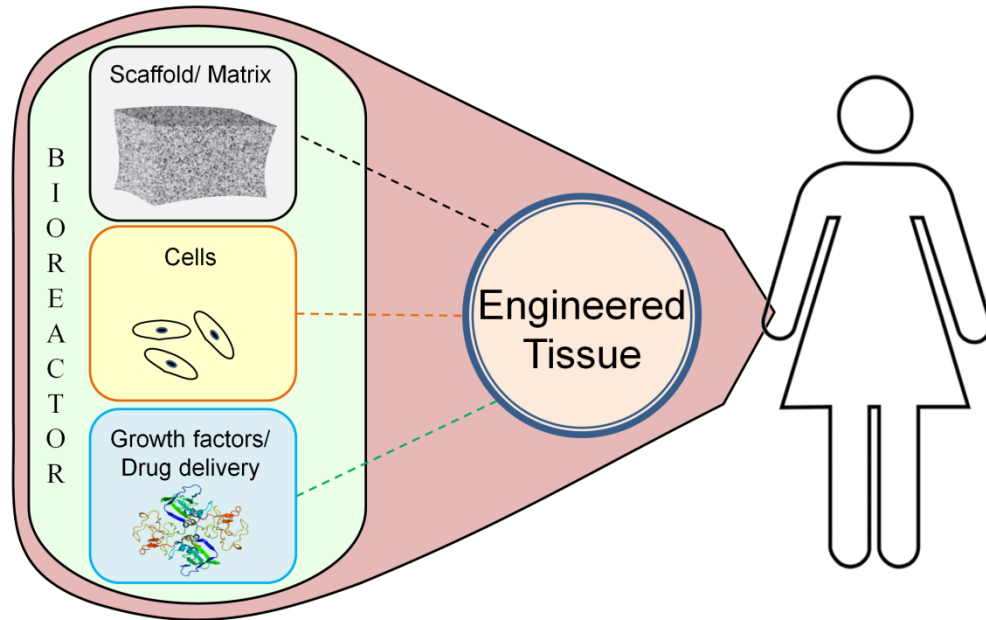


Figure 1.1 Factors involved in tissue engineering

1.1.3 Scaffolds/Matrices

A matrix or scaffold is one of the main objects of tissue engineering that mimics the native ECM, while structurally inducing the cells to form into functional tissues. Almost all mammalian cells are contact dependent as they adhere to the ECM to provide structural and functional properties of the particular tissue. The ECM is a network of fibrous proteins, proteoglycans, and glycosaminoglycans (GAGs) which are critical for wound repair after injury (Sell et al. 2010). Some components of the ECM also bind to the growth factors, and act as a reservoir of active molecules that can be rapidly mobilized following injury to stimulate cell proliferation and migration (Yue 2014, Lu et al. 2011). The rate of deposition of ECM components and their expression levels vary according to the age, illness, gender etc. of the individual (Coolen et al. 2010). The same is reflected in the wound healing process.

The development of 3 dimensional porous scaffolds can provide mechanical support to the cells allowing vascularisation while maintaining the shape of the tissue. Based on the application, scaffolds can be permanent or temporary. The permanent scaffolds use non

biodegradable polymers such as poly(methyl methacrylate) and high-density polyethylene, which are biologically stable. These scaffolds require constant strength to maintain the shape of the tissue and remain incorporated during the life time of the patient (Kim et al. 2012). The temporary scaffolds are biodegradable in nature and degrade within a predetermined period of time leaving only the newly grown tissue. The in situ degradation of the scaffold can occur through physical, chemical and biological processes, and mainly depends on the intrinsic properties of the polymers involved in the fabrication. It is essential that the degradation and restoration rates match the rate of tissue growth *in vitro* and *in vivo* for biodegradable or restorable materials (Ulery, Nair, and Laurencin 2011). Tissue engineered scaffolds are porous in nature and are designed with high porosity, surface area and interconnected geometrical structures. The porous structure of scaffold facilitates cell migration while also allowing them to have specific cell-cell interactions. The micro-porosity of the scaffold is important for the growth of blood capillaries, uniform cell distribution, and the cell-matrix interactions. The optimum porosity of the scaffold varies according to the tissue type. A decrease in pore size leads to the occlusion of the pores by the cells which will affect the nutrients and oxygen supply to the deeper areas of the scaffold (Loh and Choong 2013, Annabi et al. 2010). An ideal scaffold does not exist as different cell types require diverse bioactive characteristics with respect to mechanical and chemical properties of the matrix, which directs them towards specific tissue phenotypes.

1.1.4 Bioactive molecules

The bioactive molecules have a therapeutic potential and are entrapped or attached to the polymeric matrix for their release into the site of implant. Controlled delivery strategies are important in increasing the efficacy of the drug while releasing the optimum dosage for long periods. The release kinetics of the bioactive molecules from the scaffold depends on its affinity towards the polymer matrix, dissolution parameters of the drug, and diffusion coefficient. Biomolecules such as, prostaglandin, bovine serum albumin, insulin etc., and metal ions such as silver (Ag), gold, etc., have been widely used in the tissue engineering applications (Ji et al. 2011). Several studies on natural and synthetic polymers incorporated with growth factors such as vascular endothelial growth factor, platelet derived growth factor, bone morphogenetic protein 2, etc., have shown a sustained release profile thereby increasing the bioactivity of the tissue engineering matrices (Wei et al. 2006, Murphy et al. 2000, Jeon et al. 2007). Strategies such as

incorporation of cells or plasmid DNA in the scaffolds which in turn secrete or promote the growth factors within the cells have been actively explored (Sokolsky-Papkov et al. 2007). The controlled release of the biomolecules plays an important role as the irregularities in the release kinetics will hinder the cell proliferation and differentiation (Nair and Laurencin 2005, Rambhia and Ma 2015). The incorporation of one or more biomolecules with different functional activities and controlling their release behavior independently will have a great impact in the field of tissue engineering.

1.2 Biomaterials in tissue engineering

Biomaterials play an important role in tissue regeneration and repair by acting as frameworks (scaffolds) by mimicking the ECM. Biomaterials are broadly defined as the materials that augment or replace the tissue in order to maintain or improve the quality of life of the individual (O'brien 2011). Various polymers have been widely used as biomaterials for the fabrication of medical devices and tissue-engineering scaffolds. Polymeric biomaterials are classified into natural and synthetic polymers based on their origin. Polymers such as poly(lactic acid), poly(glycolic acid), polycaprolactone etc., which are chemically synthesized are referred to as synthetic polymers. They exhibit high versatility and under controlled conditions the properties like porosity, degradation time, mechanical strength etc., can be tailored for specific applications. The synthetic polymers generally have lower biocompatibility and at higher concentration can cause inflammatory responses *in vivo* (Dhandayuthapani et al. 2011, Gunatillake and Adhikari 2003).

Naturally derived polymer materials are extracted from plants, animals or human tissues. Natural polymers are attractive options for tissue engineering applications due to their similarity with ECM components, good biocompatibility, low toxicity, and minimal immunogenicity, which helps in better matrix-cell interactions. The widely studied natural polymers include collagen, gelatin, chitosan, alginate, starch, and cellulose (Dang and Leong 2006, Malafaya, Silva, and Reis 2007).

Collagen is a major component of the ECM, which provides mechanical support to the tissue. There are different types of collagen present in the human body, and are distributed across different tissues. Twenty nine types of collagen have been characterized and all display triple-stranded helical structure with type I (in skin and bone), type II (cartilage), type III (blood vessels walls) and type IV (basal lamina) being the most

abundant (Myllyharju and Kivirikko 2004). Although many types of collagen have been characterized, only a few are used to produce collagen based biomaterials. Type I collagen which comprises about 90% of the total collagen in the human body is majorly used in the field of tissue-engineering (Parenteau-Bareil, Gauvin, and Berthod 2010). Several studies on collagen based biomaterials have shown that it exhibits good biocompatibility, low immunogenicity, mechanical integrity, in terms of stiffness and elasticity. Integration of other biomaterials with collagen contributes towards the increase in mechanical strength as well as cellular functions such as migration, proliferation and differentiation (Harley et al. 2007, Powell and Boyce 2009).

Chitosan is widely used in the tissue engineering due to its biocompatibility, biodegradability, and non-antigenicity. CS is the deacetylated form of chitin, a natural polysaccharide which is present in the exoskeleton of shrimps and insects. It is a linear polysaccharide composed of β (1-4) linked D-glucosamine molecules with variable number of randomly located N-acetyl-glucosamine groups. The ratio of sum of D-glucosamine to N-acetyl-glucosamine is defined as degree of deacetylation. The molecular weight and degree of deacetylation are important factors which influence the solubility, degradation kinetics, mechanical strength and charge. CS has a positive charge due to the presence of the amino functional group, which could be suitably modified to impart desired properties (Madhally and Matthew 1999). Charge based polymers have an advantage in drug delivery as they can bind bioactive molecules facilitating targeted delivery at the wound site. Scaffolds fabricated with CS in combination with other biomaterials exhibit increased mechanical strength and have been used for a wide range of applications such as cartilage, chest wall and bone regeneration (Ma et al. 2003, Li et al. 2005, Correia et al. 2011).

Alginate is the most abundant naturally occurring anionic polysaccharide commonly found in brown algae. Structurally, alginate is a copolymer of two uronic acids, β -D-mannuronic acid and α -L-guluronic acid monomers linked by a 1-4 glycosidic bond. Alginate has been widely used in various tissue engineering and drug delivery applications as it exhibits properties such as, biocompatibility, biodegradability, non-antigenicity and chelating ability. While alginate alone is mechanically weak to be used as a structural tissue engineering scaffold, it has shown significant promise when copolymerized with other degradable polymers (Ulery, Nair, and Laurencin 2011, Sun and Tan 2013).

Gelatin is a natural polymeric protein derived by the hydrolysis of fibrous insoluble collagen. Structurally, gelatin molecules show similarity to collagen and contain repeated amino acids sequences of glycine, proline, and hydroxyproline. Gelatin based scaffolds are biodegradable and promote tissue regeneration which has been achieved in various tissue types such as cardiac, skin, bone, cartilage and kidney (Heydarkhan-Hagvall et al. 2008, Ghasemi-Mobarakeh et al. 2008).

Polymers such as silk fibroin, elastin, starch etc., have poor mechanical strength while their use in tissue engineering applications and drug delivery are reported as composites with other biomaterials. Polymeric biomaterials are able to degrade after they have served their function. This led to the advancement of modern medicine where biomaterial based scaffolds have been researched for the delivery of varied cell types such as, chondrocytes, osteoblasts, myoblasts, fibroblasts, keratinocytes, and adipose-derived stem cells (Ulery, Nair, and Laurencin 2011, Chaudhari et al. 2016). The polymer or co-polymeric blends with high tensile strength are used to achieve adequate mechanical properties to engineer bone or cartilage (Edgar et al. 2016, Cao, Dou, and Dong 2014, Li et al. 2005, Cheng et al. 2010, Han et al. 2014, Kim, Ahn, et al. 2011). The wide range of biomaterials provide opportunities for development of tissue engineering materials for applications in the regeneration of cartilage, skin, cornea, bone etc.

1.3 Skin tissue engineering

Current advances in tissue engineering have led to the development of improved skin substitutes which are commercially available. The use of stem cell based organ systems in third degree burns to counter the scarcity of autologous skin grafts is one of the earliest approaches of regenerative medicine (Pellegrini et al. 1999). The majority of current research in skin tissue engineering focuses on the synthesis of complex three-dimensional polymeric scaffolds containing functional biomolecules to support the growth of autologous cells, leading to regeneration. In order to be translated into clinical applications, systems based on bioengineered skin with the ability to grow tissues by retaining their functionality, including stemness are needed (Singh, Singh, and Han 2016). The ultimate goal of skin tissue engineering is to rapidly produce skin constructs that can offer complete regeneration of functional skin including all the layers of the skin and the skin appendages (Böttcher-Haberzeth, Biedermann, and Reichmann 2010, Balañá, Charreau, and Leirós 2015).

1.3.1 Anatomy of skin

Skin is the largest anatomical organ in the human body whose primary function is to act as a barrier to mechanical impacts, temperature, micro-organisms, radiation and chemicals. Skin consists of two layers: the epidermis and the dermis. The epidermis is the primary layer (avascular) which provides mechanical protection and consists of keratinocytes and stratified squamous epithelium attached to the dermis via intertwining collagen fibers, referred to as the basement membrane. The dermis is considered as the core of the skin, as it contains blood vessels that nourish the skin with oxygen and nutrients. The dermis majorly consists of fibroblast cells and two layers of connective tissue. Beneath the dermis lies the hypodermis or subcutaneous fatty tissue. It is not strictly a part of the skin, although it is difficult to distinguish between the hypodermis and dermis (Breitkreutz et al. 2013). The epidermal ECM has basal lamina whereas the dermal ECM comprises of fibrillar collagens and associated proteins. This heterogeneity of the ECM distribution in the skin extends beyond cell adhesion and facilitates an array of cell autonomous and non-autonomous processes (Watt and Fujiwara 2011). As skin is the outermost anatomical barrier of the human body it experiences injuries such as abrasions, ruptures, penetrating wounds etc., during routine activities. The superficial wounds heal fast as compared to deeper wounds, in which all the layers of the skin are compromised. Along with protection, skin has two other major functions which are regulation and sensation. Wounds affect all the functions of the skin, and at times may result in serious consequences.(Sen et al. 2009).

1.4 Wound healing

Disruption of cellular and anatomical continuity of tissue is defined as wound. The natural response to restore the structural and functional aspect of an injured tissue occurs through the process of wound healing. Wound healing is a complex process which occurs in three major phases: inflammation, proliferation and maturation which are often overlapping. These phases are divided based upon the different cellular and biochemical factors involved during the process. The inflammatory response begins with dilation of the blood vessels to increase the vascular permeability of neutrophils, macrophages and lymphocytes into the wound site. Neutrophils clear the wound area to prevent infections arising due to exogenous and endogenous microorganisms. Macrophages play an essential role in wound healing by eliminating the debris, bacteria and also releasing factors that in turn stimulates angiogenesis. During this stage, the wound appears red, hot,

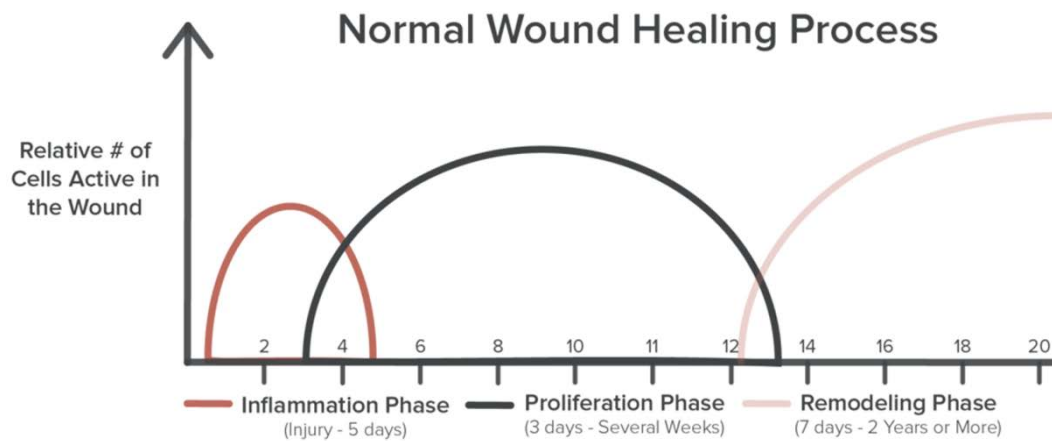


Figure 1.2 Graphical representation of wound healing process.

(Adapted from: <https://www.renovoderm.tech/the-product/>)

swollen, and pain is commonly observed. The duration of inflammation generally varies according to the tissue type and the intensity of the wound. T-lymphocytes migrate into the wound during the late inflammatory phase and secrete lymphokines such as, heparin-binding epidermal growth factor, basic fibroblast growth factor, etc. During the proliferative phase, the formation of collagen, ECM, fibroblasts and a new network of blood vessels begins which collectively are referred to as granulation tissue. The epidermal cells on the wound edges undergo structural transformation like detachment from the neighboring cells and basement membrane, to migrate across the wound surface. These cells finally resurface the wound, a process known as 'epithelialization'. The fibroblasts secrete the ECM components like collagen, elastin, fibronectin, glycosaminoglycans, and proteases. As the proliferation of fibroblasts increases, the number of inflammatory cells decreases as the factors that support inflammation are inactivated. In the proliferative phase the wound edges move centripetally, facilitating the decrease in the size of the wound eventually closing it completely. The contraction of the wound depends on the degree of tissue laxity and shape of the wound. During the maturation phase, once the wound has closed remodeling occurs where type III collagen is replaced by type I collagen, while hyaluronic acid and glycosaminoglycans are replaced by proteoglycans. Fibronectin gradually disappears and the water is resorbed from the scar. These events allow collagen fibers to lie close together and facilitate the cross-linking of the collagen ultimately decreasing scar thickness (Gonzalez et al. 2016).

1.5 Types of Wounds

There are different types of wounds which an individual can sustain throughout the life, as part of the daily activities. Many minor wounds are superficial and are limited to the outer layers of the skin, which need simple treatment to heal, while the wounds that are deeper, reaching the underlying tissues and organs, experience delayed healing and at times may be life threatening.

Depending on the healing time of a wound, they are classified as acute or chronic.

Acute - Acute wound is an injury that heals at a predictable and expected rate of time, and with no complications. The wound healing process is linear as described earlier. These wounds are further classified based on the cause (abrasions, punctures, incision etc.), size, and the depth (skin layers) of the wound (Sen et al. 2009).

Chronic – Chronic wounds do not heal in the standard time frame and may linger for weeks, months or even years. The reason a wound becomes chronic is that the body's ability to deal with the damage is overcome by local and systemic factors. Any acute wound can progress to a chronic wound as a result of poor blood supply, oxygen, nutrients or hygiene. Acute wounds should also be properly treated to avoid infection, and inflammation (Guest, Vowden, and Vowden 2017).

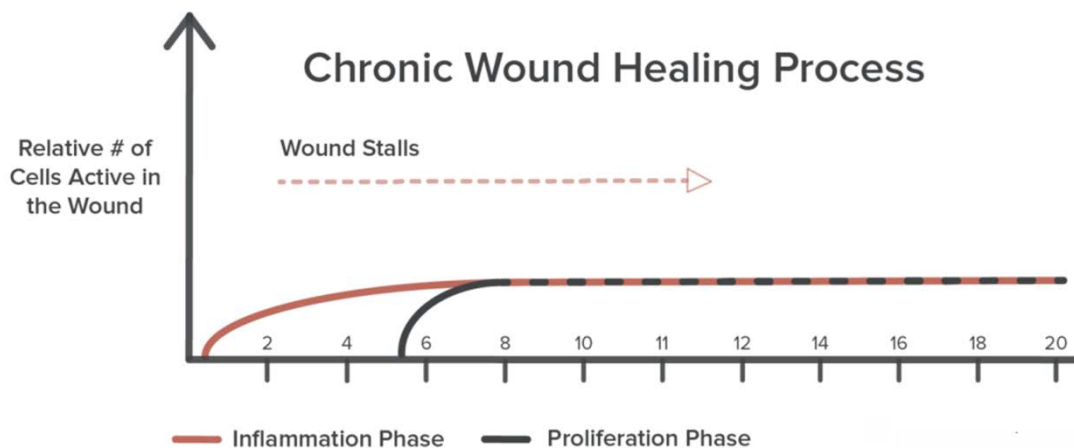


Figure 1.3 Graphical representation of wound healing in the chronic wounds.

(Adapted from: <https://www.renovoderm.tech/the-product/>)

1.6 Factors affecting wound healing

The wound healing process is not always linear and often can progress both forwards or backwards through the phases depending upon local and systemic factors acting on the

wound. Local factors such as oxygenation, infections, foreign body etc., can directly influence the characteristics of the wound. Whereas, systemic factors such as age, stress, illness, alcoholism, etc., depends upon the health of the individual, and his or her ability to heal. Many of these factors are related, and the systemic factors act through the local effects, affecting wound healing (Guo and DiPietro 2010, Diegelmann and Evans 2004).

1.6.1 Infections

The bacterial infections are one of the major factors which delay the wound healing process, contributing to chronicity, morbidity, and mortality. Bacteria adhere to the wound site and colonize leading to the complex situation referred to as infection. Infections burden the wound site by depleting the nutrients and inflow of oxygen, while increasing the amount of wound exudates. These bacteria release endotoxins which can induce prolonged elevation of pro-inflammatory cytokines (interleukin-1, TNF- α) and damage the tissue by recruiting more inflammatory cells.

Local Factors	Systemic Factors
Oxygenation Infection Oxidative stress Foreign body Venous sufficiency	<ul style="list-style-type: none"> • Age and gender • Sex hormones • Stress • Ischemia • Diseases: diabetes, keloids, fibrosis, hereditary healing disorders, jaundice, uremia • Obesity • Medications: glucocorticoid steroids, non-steroidal anti-inflammatory drugs, chemotherapy • Alcoholism and smoking • Immunocompromised conditions: cancer, radiation therapy, AIDS • Nutrition

Table 1.1 Factors Affecting Wound Healing

In the absence of effective defense mechanisms, inflammation phase is prolonged, damaging the neighboring cells, and the biochemical factors which help in the healing process. The prolonged inflammation can also lead to over expression of proteases including matrix metalloproteases (MMPs), which can degrade the ECM. The increase in the protease content exhausts the level of the naturally occurring protease inhibitors at the wound site. This imbalance in the protease and its inhibitors can rapidly degrade the growth factors which are necessary for the wound healing process (Guo and DiPietro 2010, Edwards and Harding 2004). Bacteria that colonize chronic wounds often form polymicrobial communities called biofilms. These complex structures are composed of microbial cells embedded in secreted polymer matrix, which provides optimal environment for bacterial cell survival, enabling their escape from host immune surveillance/defense and providing resistance to antibiotic treatment. Biofilms represent foci of infection and bacterial resistance within the wound and protect the bacteria from the effects of antimicrobial agents, especially antibiotics and antiseptics. Although biofilms are prevalent in chronic wounds, and significantly delay re-epithelialization in animal models, the precise mechanism of how they delay healing remains unclear (James et al. 2008).

1.6.2 Oxidative stress

Although wounds may have different origins, those which fail to heal are often characterized by chronically inflamed wound bed. It is widely understood that the inability of the chronic wound to heal is caused by both cellular and molecular abnormalities occurring within the wound bed. During inflammatory phase of wound healing, neutrophils and macrophages secrete large amounts of reactive oxygen species (ROS) along with pro-inflammatory cytokines and MMPs. The ROS directly attacks invading bacteria, and kill them. This type of inflammation is a natural part of the wound healing process which helps in the defense mechanism and is problematic only if prolonged for longer durations. ROS play a role, not only in disinfection during the inflammatory phase, but also in other phases including migration, proliferation, and angiogenesis through ROS signaling (Schäfer and Werner 2008, Dunnill et al. 2017). Inflammatory cells accumulated inside the chronic wounds triggered by infections and cell extravasations produce elevated levels of ROS for longer durations creating an imbalance in the redox potential. Redox homeostasis is the balance between ROS generation systems and their scavenging counterparts (antioxidant). When the production

of ROS exceeds the anti-oxidant capacity, the imbalance in the wound can generate oxidative stress. The elevated levels of ROS can potentially damage the structural elements of ECM and cell membranes, in turn leading to apoptosis of the cells in the surrounding tissues. In addition to these direct negative effects, ROS together with pro-inflammatory cytokines induce the production of proteases that can degrade the ECM and growth factors necessary for normal cellular function (Demidova-Rice, Hamblin, and Herman 2012, Ha et al. 2010). Thus, strict control of ROS levels is required to avoid their detrimental effects and to ensure their beneficial roles.

1.7 Wound care medications

Wound care has evolved over time, from the use of natural crude products in ancient ages to modern day dressings based upon better understanding of the wounds and the wound healing process. The application of antibacterial compounds like honey, Ag etc., to treat wounds reduced after the discovery of antibiotics. Antibiotics revolutionized the field of medicine as they proved to be bactericidal to a significantly large population of bacteria. However, their indiscriminate usage has resulted in decreased efficacy and development of resistant strains, which arise mainly by altering the cell structure and/or cell metabolism. As a result, during the past few decades, Ag has regained attention as an antimicrobial agent as it can kill bacteria which are resistant to many modern day antibiotics (Tsang et al. 2015). Initially, the use of Ag as AgNO₃ (silver nitrate) solution or silver sulfadiazine cream was specifically focused for the treatment of burns along with wound dressings (Gayle et al. 1978). Subsequently, different Ag based combinations gained attention for the treatment of chronic wounds. Ag is reported to demonstrate efficacy on planktonic microorganisms both within the *in vitro* and *in vivo* environments. When Ag is incorporated on medical implants, its antimicrobial property is also effective in reducing biofilms (Naik and Kowshik 2014, Besinis et al. 2017). Ag ions have been shown to be effective over 600 microorganisms including bacteria (both Gram-positive and negative), fungi and viruses; however, the precise mechanism of their mode of antimicrobial action is not yet fully understood (Dakal et al. 2016, Malarkodi et al. 2013). Several studies suggest that Ag has multiple modes of action to kill bacteria by targeting various components of bacterial metabolism, unlike antibiotics. Though elemental Ag appears to be antibacterial, its cation form (Ag⁺) is highly reactive due to an increase in its charge. Ionic Ag interacts with the cell membranes as the positive surface charge of the Ag ion can electrostatically interact with the negatively charged cell wall of the

bacteria. The Ag ions then bind various functional groups such as thiol, sulfhydryl, imidazole, and carboxyl groups present in the cell wall leading to protein unfolding and breakdown (Abbaszadegan et al. 2015). These changes in the cell wall structure affect the integrity of the lipid bilayer and permeability of the cell membrane resulting in its disruption (Ghosh et al. 2012). The Ag ions also impair the uptake of potassium channels in bacterial cells. The increase in the membrane permeability increases the loss by leakage of intracellular components including ions, proteins, reducing sugars and the cellular energy reservoir, ATP (Lok et al. 2006, Kim, Lee, et al. 2011). Ag ions inhibit the respiratory pathway of bacteria by binding to the functional groups of the electron transport chain components thereby interfering with the electrochemical gradient. This interference with metabolism of the bacteria as ATP synthesis will not progress, resulting in cell death (Thombre et al. 2016).

The Ag ions after adhesion to the cell membrane can penetrate the bacterial cells through porins (water-filled channels), which are present in outer membrane and can result in several cellular dysfunctions (Li, Nikaido, and Williams 1997). They interact with cellular components and biomolecules such as proteins, lipids, and DNA affecting all the vital cellular functions (Habash et al., 2014; Singh et al., 2015). The Ag ions interfere with the translation process by denaturing the ribosomes and ribonucleic acids thereby inhibiting protein synthesis (Morones et al., 2005; Jung et al., 2008; Rai et al., 2012). The Ag ions alter the 3D structure of proteins, by blocking the active binding sites, interfering with the disulfide bonds and forming stable bonds with the functional groups leading to overall functional defects in the microorganism (Lok et al., 2006).

Additionally, Ag ions have been used alone or in combination with antibiotics. In order to increase the antimicrobial efficacy against pathogenic strains, Ag ions used in combination with the antibiotics have displayed synergistic antimicrobial effect (Morones-Ramirez et al. 2013, Deng et al. 2016).

Apart from the microbial infections, another important factor which delays the wound healing process is oxidative stress. The imbalance between the ROS (oxidative systems) and their scavenging counterparts affects the wound if prolonged for longer durations. The antioxidants which are involved in fine tuning the ROS can be enzymatic or non-enzymatic in nature. The physiological antioxidative enzymes include superoxide dismutase (SOD), glutathione peroxidase (GPX), peroxiredoxins and catalase, while ascorbic acid, glutathione, carotenoids and polyphenolic compounds function as non-

enzymatic antioxidants (Kurahashi and Fujii 2015). The non-enzymatic antioxidants react with ROS stoichiometrically and become radicals themselves, though less reactive. These oxidized non-enzymatic antioxidants are less damaging than the radicals they scavenge. The antioxidant enzymes work together to reduce the oxidized non-enzymatic antioxidants, and the cycle continues (Kagan and Tyurina 1998). Several studies on the expression of antioxidants in chronic wounds indicate that it is lower than the normal levels leading to redox imbalance. Herein, molecules with free radical scavenging potential can come to the rescue as in addition to exhibiting antioxidant properties they also contribute towards the expression of endogenous antioxidant enzymes thereby augmenting the wound healing process (Martin, 1996).

Polyphenolic compounds are secondary metabolites of plants, synthesized as natural defense part of defense against the radicals in extreme environmental stress conditions. They exhibit antioxidant property by quenching the ROS and inhibiting lipid peroxidation (Shahidi, Janitha, and Wanasundara 1992, Yu et al. 2015). Several studies on phenolic compounds have also demonstrated anti-aging, anti-inflammatory, anti-cancer, anti-microbial and anti-proliferative activities (Rasouli, Farzaei, and Khodarahmi 2017, El Gharras 2009). Some polyphenols like quercetin, myricetin, rutin, etc., have shown to influence the gene expression by down-regulating the MMPs thereby reducing inflammation (Pereira and Bartolo 2016, Sin and Kim 2005). Polyphenolic compounds induce the expression of antioxidant encoding genes by interacting with the antioxidant response element that is present in the gene promoter region (Rasouli, Farzaei, and Khodarahmi 2017). The positive effects of polyphenols on cardiovascular diseases, liver damage, diabetics etc., are indirectly related to the anti-oxidant nature of the compounds (El Gharras 2009). Although polyphenols are known for their accessibility, specificity and low toxicity, their rapid metabolism and low bioavailability are certain limitations (Brglez Mojzer et al. 2016). Polyphenols have played a major role in wound healing as their use was recorded from ancient times as crude extracts. Their use in modern medicine has been accelerated as many aspects of their chemical and biological activities were identified and evaluated (Mandal and Mandal 2011). The polyphenols which are used in the current study are described below.

Silymarin (SM), is a polyphenolic flavonoid isolated from fruits and seeds of the milk thistle plant, *Silybum marianum*. SM is clinically used as a drug for treating liver diseases because of its hepatoprotective property. In addition, it exhibits strong antioxidant, anti-

inflammatory and anticancer activities. Investigations on SM as an anti-inflammatory and antioxidant agent have shown positive effects on the wound healing process in animal models. SM acts as a powerful antioxidant by inhibiting the OH⁻ radicals and inducing the production of a number of endogenous antioxidants, including GSH, SOD, catalase, and GPX (Surai 2015). Topical application of SM in the treatment of diabetic wounds has shown that it inhibits the inflammatory nuclear transcription factor κ B, and promotes the synthesis of anti-inflammatory cytokines, such as IL-10, IL-12 etc., thereby enhancing tissue regeneration (Meeran et al. 2006, Chang et al. 2006). Topical administration of SM in rats has shown to increase the proliferation of fibroblast, collagen synthesis, and angiogenesis. The antioxidant and anti-inflammatory abilities of the SM are also demonstrated in UVB-induced skin damage (Gazak, Walterova, and Kren 2007).

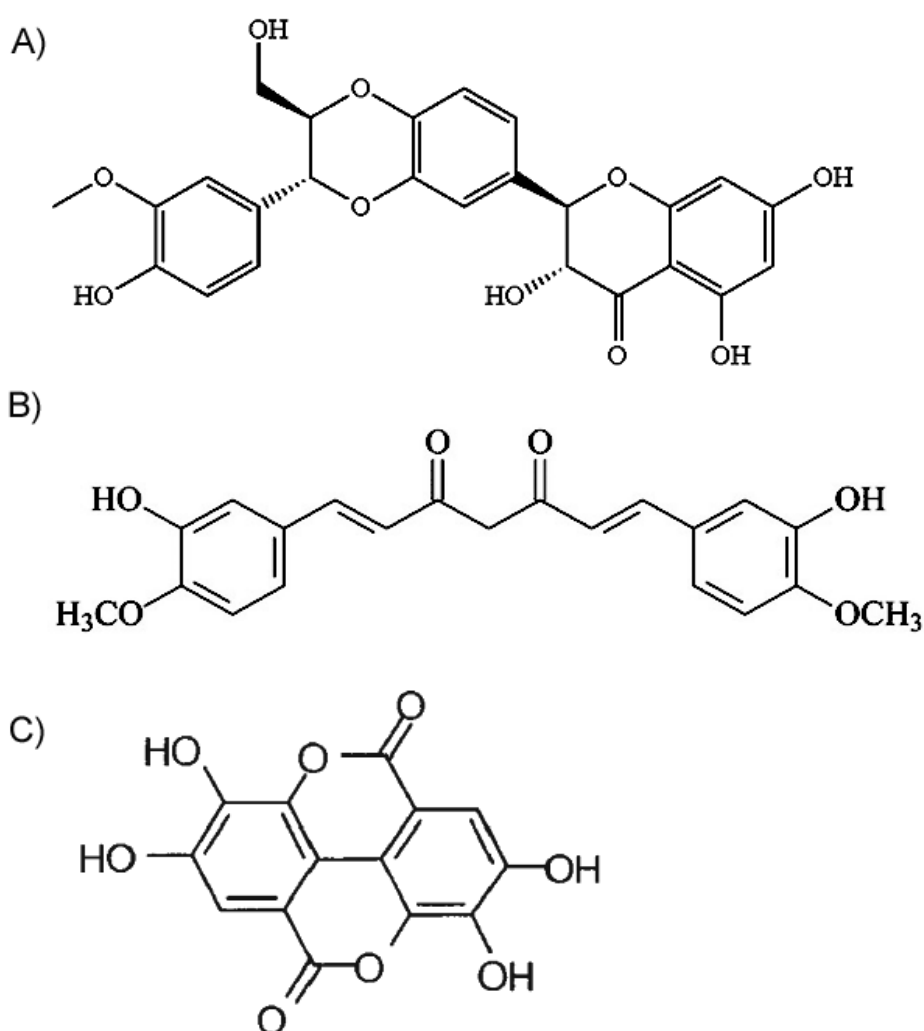


Figure 1.4 Structures of SM (A), CM (B) and EA (C).

Curcumin (CM), the most active component of the rhizome of *Curcuma longa* L. (common name: turmeric), has been traditionally studied for its medicinal properties. It has potent anti-oxidant and anti-inflammatory effects, which play a crucial role in the wound healing process. The structure of CM (1,7-bis(4-hydroxy-3-methoxyphenyl)-1,6-heptadiene-3,5-dione) was first described by Lampe and Milobedska in 1910. CM exhibits anti-cancer, anti-aging and wound healing properties. CM when administered orally or when applied topically to wounds reduces the oxidative stress while at the same time enhancing the activity of the antioxidant enzymes including superoxide dismutase, catalase and glutathione peroxidase in rat models (Reddy and Lokesh, 1994; Subudhi and Chainy, 2010). Various studies have demonstrated the infiltration of myofibroblasts into wound sites when treated with CM (Mohanty et al. (2012)). Infiltration of fibroblasts is essential for granulation tissue formation, collagen production and its deposition (Epstein et al., 1999; Loughlin and Artlett, 2011; Martin, 1997). Studies have shown an increase in the wound contraction rate as an evidence for curcumin's ability of accelerating wound healing. Due to its hydrophobicity, CM is poorly absorbed during oral administration as compared to topical application at the wound site. Hence, topical application of CM has more pronounced effects on wound healing compared to its oral administration (Liu et al. 2016). Novel formulations of curcumin are being explored in order to overcome drawbacks such as low bioavailability, rapid metabolism, poor solubility etc., to maximize the application potential.

Ellagic acid (EA) is a bioactive polyphenolic compound found abundantly in numerous fruits, vegetables and seeds of pomegranate; walnuts etc. EA possess a wide range of biological activities like antioxidant, inhibition of lipid peroxidation, anti-inflammatory and anti-carcinogenic properties. The structure of EA is 2,3,7,8-Tetrahydroxy-chromeno[5,4,3-cde]chromene-5,10-dione (Kilic, Yeşiloğlu, and Bayrak 2014). High molecular weight polyphenols are the major contributors of antioxidant properties as they have several hydroxyl functional groups in their structure, with a greater ability to donate the hydrogen atom and support the unpaired electron. *In vivo* studies on EA fed rats have shown down regulation of iNOS, COX-2, TNF- α and IL-6 through NF- κ B repression by exerting anti-inflammatory properties (Umesalma and Sudhandiran 2010). EA reduces the oxidative stress by effectively lowering the levels of plasma lipids; scavenging the O_2^- and OH $^\cdot$; and inhibiting lipid and DNA peroxidation (Takagi et al. 1995). EA also exerts

its protective effect by inhibiting the overproduction of free radicals by NADPH oxidase and up-regulating cellular antioxidant defenses (Lee et al. 2010).

In summary, the major factors affecting the wound healing process as described earlier are infections and oxidative stress. The strategies to incorporate antioxidant compounds (SM, CM, EA) into the polymeric matrix with a sustained release behavior will address the issues of low bioavailability and rapid metabolism of the polyphenols while reducing the oxidative stress. The uniform entrapment of antibacterial agent will provide better antibacterial effect at low concentrations, thereby reducing the mammalian cell toxicity. The fabrication of the scaffold with intra-dermal nature is significantly important in skin tissue engineering as the advancements primarily focus on mimicking the native nature of the ECM. The simultaneous incorporation of antibacterial and antioxidant compounds into the scaffolds, both with independent release behavior, will help in increasing the efficacy of the scaffold in chronic wounds.

1.8 Gaps in Existing Research

The Advances in the wound care management is important, as increase in the occurrence of chronic wounds that are hard to heal are constantly increasing with a current global estimate of around 50 million patients. The statistics of the global healthcare market as of 2015 is US \$8 billion and will be projected to reach the US \$10 billion by the end of 2020. The increase in lifestyle diseases such as diabetes has intensified the focus on faster wound healing products. Chronic wounds take considerable time to heal and therefore advanced wound care products have emerged as a standard solution for treating chronic wounds. The major factors which delay the wound healing process are bacterial infections and oxidative stress. Antimicrobial compounds have been extensively used in wound care to control infections. This has led to an increase in the antibiotic resistance bacteria, which has become a major challenge in wound healing. Currently a lot of research is focused on developing newer antimicrobial compounds with multimodal mechanism of actions to kill the bacteria. Ag has a broad antimicrobial spectrum and has been widely used in tissue engineering scaffolds. Although there are reports on Ag based biomaterials such as CS, CO, alginate etc., a lot needs to be done with respect to the synthesis modes using techniques which will lead to homogenous distribution of Ag. The uniform entrapment/distribution of the Ag into the polymeric matrix will ensure an even release thereby increasing its efficiency. The techniques used in scaffold fabrication such as ionic

gelation, freeze drying, electrospinning etc., can be combined with new strategies in order to ensure sustained release of the bioactive molecules.

Oxidative stress is also an important contributing factor of chronic wounds as it delays the healing process by disturbing the redox potential of the injured tissue. Polyphenolic antioxidants in their pure form have been used in treatment of wounds, but their use in tissue engineering has not been fully explored.

Biomaterials are often important components of tissue engineering strategies because they mimic the native ECM of tissues and direct cell behavior, while contributing to the structure and function of new tissue. Multilayer scaffolds provide an opportunity to coat different layers within the scaffold with different medically relevant biomolecules thereby providing an ecosystem for favorable interactions with the niche cells. Skin substitutes are often focused on developing tissue-engineered products with antibacterial or antioxidant compounds or the compounds which possess both the properties, while the use of both compounds for wound healing applications is not reported. The use of antimicrobial compounds along with antioxidants in tissue engineering will address the microbial infections and oxidative stress, which are considered key factors in delaying the healing process. Though their release has to be controlled in such a way that the normal physiological functions do not interfere with one another. Hence, in the present study, the idea was to design a bilayer scaffold incorporating antibacterial (Ag) and antioxidant (SM/ EA/ CM) compounds in two different layers, with an attempt to block the bacterial adhesion from the outer environment while addressing the oxidative stress inside the wounds. The localization of the compounds in separate matrix may help in reducing the conflict between the compounds and contribute to their synergistic effects in the healing process. The Polymeric multilayer formulations can have a significant impact on advancing the fields of cellular and tissue engineering.

In the view of above proposed gaps in the literature, the following objectives have been proposed:

1. Synthesis of bilayer scaffolds with layer by layer arrangement of CS-Ag; and CS-CO-R (where, R = CM/ EA/ SM).
2. Characterization of scaffold by determining its physical and chemical properties.
3. Studies on the *in vivo* biocompatibility of the bilayer scaffold with specific animal models.

Chapter 2: Synthesis and Characterization of Silver Incorporated Chitosan Scaffolds

2.1 Introduction

Preventing bacterial contamination and treating wound infections have been a major challenge in wound care management. Many bacteria release metallo-proteases and other mediators of inflammation, leading to local tissue damage (Edwards and Harding 2004, Diegelmann and Evans 2004). Certain pathogenic bacteria tend to form biofilms which provide them with protection against host defense mechanisms. Bacterial communities colonize and secrete exopolysaccharides facilitating biofilm formation, which offers resistance to bacteria by preventing the entry of antibacterial drugs. Organisms within biofilms can be 500 times less sensitive to antibiotics than planktonic forms (James et al. 2008). Approaches like supplementation of antibacterial compounds into the wound site helps in dealing with reducing the bacterial load and eradicating further infections. Ag has been a potent antibacterial compound for ages, the use of which diminished with the discovery of antibiotics. The increase in bacterial resistance to the antibiotics has renewed the interest in Ag (Demidova-Rice, Hamblin, and Herman 2012). Ag exhibits germicidal effects by effectively killing microorganisms without causing harm to higher organisms. Ag ions electrostatically interact with the negatively charged bacterial cell wall, thereby disrupting the cell membrane and biomolecules such as proteins, enzymes, electron transport chain components and DNA. Furthermore, the Ag radicals interact with the cell membrane and affect its permeability, causing the leakage of the cytoplasm leading to cell death (Abbaszadegan et al. 2015, Malarkodi et al. 2013, Tsang et al. 2015). Ag is also known to prevent the formation of biofilms, a major challenge in wound healing. The Ag ions facilitate biofilm dispersion by interfering with EPS and also down regulating the genes which are responsible for quorum sensing signaling (Singh et al. 2015, Besinis et al. 2017). Recent studies on the synthesis of Ag based compounds have focused to enhance the availability of Ag to bacterial cells thereby increasing the antibacterial efficacy. The use of Ag in treating chronically infected wounds when compared to traditional antibiotics has been increased, due the multimodal action of Ag ions in bacterial inhibition (Jain et al. 2009, Abbaszadegan et al. 2015, Dakal et al. 2016).

In general, the wound healing process involves many cellular and acellular (ECM; biochemical) components which combine to repair and restore the injured tissue. ECM plays an important role in wound healing process; this led to the creation of substitutes

which can stimulate or replace the ECM by using biopolymers (Lu et al. 2011). The biopolymers which mimic the native ECM are biocompatible in nature and helps in adhesion and proliferation of the neighboring cells. Various polymeric materials used in tissue engineering as matrices, scaffolds, films, hydrogels etc., are based up on the type of tissue and the area of application. Polymeric scaffolds are drawing great attention due to their unique properties such as high porosity, biocompatibility, chemical versatility and good mechanical properties (Dhandayuthapani et al. 2011, Stratton et al. 2016). Among the various biopolymers, chitosan (CS) has gained much attention as a bio-composite material in various tissue engineering applications due to its large scale availability, non-toxicity, biodegradability, and biocompatibility characteristics. Chitosan is a linear biopolymer of linked β (1, 4)-glucosamine (2-amino-2deoxy-D-glucose) and *N*-acetyl-D-glucosamine, a de-acetylated form of chitin and a major component of crustacean outer skeletons. The plethora of applications of chitosan, especially in the field of tissue engineering is due to the possibility of chemical modifications in its structure, and can blend with various polymers to generate materials with novel properties and functions (Madihally and Matthew 1999, Han et al. 2014, Correia et al. 2011, Li et al. 2005). To enhance the therapeutic potential of the polymeric matrices, incorporation of bioactive molecules with varied applications has been widely actively explored. Several studies on the incorporation of antimicrobial compounds such as, antibiotics, quaternary ammonium compounds, heavy metal compounds (e.g. Ag, tributyltin and mercury) and halogens into the polymeric matrix have shown to inhibit the microbial infections (Guo et al. 2015).

Efficient antibacterial activity of the scaffolds can be achieved through a sustained release of the Ag for a prolonged period of time (Rambhia and Ma 2015). The release kinetics of Ag ions guide antibacterial efficacy and affect factors like dosage limitation which are important for preventing mammalian cell toxicity (Pundir, Badola, and Sharma 2017). Several Ag immobilized dressings using bio-compatible polymer matrices have been reported to show antibacterial efficacy against both Gram-positive and Gram-negative bacteria without any mammalian cytotoxicity (Guzman, Dille, and Godet 2012).

The aim of the study is to incorporate the antibacterial compound (Ag) into polymeric (CS) matrix thereby eradicating the bacterial infections arising due to the exogenous and endogenous modes while enhancing the wound healing. In this study we used AgNO₃ as antibacterial precursor, to uniformly entrap Ag into the CS polymeric matrix by using novel melt-down neutralization for controlled release of Ag ions. The scaffolds were

prepared by using melt-down neutralization, followed by polymer curing and freeze drying. The synthesized scaffolds were physically characterized and further evaluated for their antibacterial potential. The *in vitro* biocompatibility of the composite scaffolds on human keratinocyte (HaCaT) cells was studied.

2.2 Materials and Methods

2.2.1 Chemicals and materials

CS with >75% degree of deacetylation, silver nitrate, tris, calcium chloride dihydrate, MTT (3-(4,5-dimethylthiazol-2-yl)-2,5-diphenyltetrazolium bromide), dulbecco's modified eagle medium (DMEM), foetal bovine serum (FBS), antibiotic-antimycotic, phosphate buffer saline (PBS), and Muller Hilton broth/agar (MHB/A) were purchased from HiMedia, India. The acetic acid, nitric acid, dimethyl sulfoxide (DMSO), sodium hydroxide (NaOH), diethyl ether, acetone were brought from SD Fine Chem. Ltd, India, and ethanol from Changshu Yangyuan Chemical, China. All solvents and solutions were used as received, without further purification.

2.2.2 Synthesis of CS-Ag scaffolds

Ag incorporated CS scaffolds were prepared by dissolving 300 mg of CS in 10 ml of 1% acetic acid solution containing Ag at concentrations of 1, 2 and 3 % (wt/wt), respectively. This was followed by the addition of 0.25 % glutaraldehyde and the suspension was stirred for 4 h. The viscous gel formed was poured in 50 mm petri plates and frozen at -80 °C. The samples were thawed at 8 °C and a solution of 0.1 M NaOH in ethanol was slowly added to precipitate the chitosan and obtain a gel. The gels were repeatedly washed with distilled water until the pH of the wash water remained neutral. These gels were frozen at -80 °C for 12 h and thawed at 4 °C for 3 h. Solvent curing of the gel was carried out by soaking the scaffolds in a solution of diethyl ether:acetone (1:1) for 30 min. The solvent cured gels were given five cycles of freeze–thawing to achieve optimum porosity and interconnectivity. Finally, the gels were lyophilized using a freeze dryer (CHRIST alpha 1–2 LD plus). CS (control) scaffolds were synthesized using the same protocol but without the addition of silver. The CS scaffolds synthesized with 1, 2, and 3 % Ag has been denoted as CS-Ag1, CS-Ag2, and CS-Ag3, respectively.

2.2.3 Characterization

2.2.3.1 Determination of CS Deacetylation

The degree of deacetylation of chitosan was determined by the ninhydrin assay (Prochazkova, Vårum, and Ostgaard 1999, Curotto and Aros 1993). D-glucosamine was used as the standard and the standard curve was plotted from 0.01 to 0.05 mg/mL of D-glucosamine prepared in 1% w/v acetic acid. Chitosan solution (0.1 mg/mL) was prepared by dissolving it in 1% acetic acid and stirring continuously at 25°C for 6 h. Specific amounts of standard and chitosan solution were taken in a test tube and the volume was made up to 1ml by adding 0.02M acetate buffer (pH 5.5). Subsequently, 2 ml of Ninhydrin reagent was added to the tubes, vortexed for 20 seconds and placed in a boiling water bath for 10 min. After the solutions had cooled down, the absorbance was recorded at 570 nm using an UV visible spectrophotometer (Shimadzu, UV-2450 MODEL).

2.2.3.2 Determination of average molecular weight of CS

The molecular weight of chitosan samples was determined using the Mark-Houwink equation (Wang et al. 1991, Kasai 2007).

$$[\eta] = KM^\alpha$$

Where $[\eta]$ is the intrinsic viscosity, M is Molecular weight, K and α are the constants of a particular polymer solvent system and temperature. Different concentrations of chitosan solutions (0.1%, 0.2%, 0.3%, 0.4%, and 0.5% w/v) were prepared in 0.2 M acetic acid and 0.1 M sodium acetate buffer solution. The solution was filtered to remove insoluble materials. The Ubbelohde type capillary viscometer was used to measure the flow time of the solutions through the capillary in a constant temperature bath at 25 °C. Three measurements were made for each sample. The running times of the solution and solvent were recorded as seconds (s) and specific viscosity calculated. The reduced viscosity was calculated for different concentrations of polymer using the specific viscosity data. The intrinsic viscosity was obtained by extrapolating the reduced viscosity on reduced viscosity vs. concentration plot to zero concentration. The literature values of K and α are 0.104×10^{-3} and 1.12, respectively.

2.2.3.3 XRD

The crystallinity of the scaffold material was determined by XRD analyses carried out using Rigaku Miniflex II with Cu-K α ($\lambda=1.5406\text{\AA}$) as the X-ray source and 2θ angle of 10° to 60° . The crystallite size of Ag was calculated using Scherrer equation.

$$D = \frac{K \lambda}{\beta \cos\theta}$$

Where D= Domain crystallite size; K = Scherrer constant; β = Full Width at Half Maximum (in radians) and θ = Half 2θ of the maximum intensity peak.

2.2.3.4 FTIR analysis

Infrared spectra were measured using an FT-IR spectrophotometer (Shimadzu IRAffinity-1S) coupled to a computer with analysis software. The scaffolds were analyzed by using attenuated total reflectance (ATR) sampling technique.

2.2.3.5 Thermal behavior by TGA

The TGA analysis was carried out using a thermogravimetric system (Shimadzu, DTG-60) with an electronically processed temperature control unit and a TA data station. About 2 mg of the sample was placed in the balance system equipment and the temperature was raised from 30° to 550°C at a heating rate of 10°C per minute. The mass of the sample pan was continuously recorded by taking first-order derivative of the raw weight loss of the TGA curves and calculating the area under respective polymer degradation temperature peak.

2.2.3.6 *In-vitro* degradation of scaffolds

In-vitro degradation of the scaffolds was carried out using the enzyme, lysozyme which catalyzes the hydrolysis of β (1, 4) linkages between N-acetyl-D-glucosamines. The lysozyme solution was prepared by dissolving 500 $\mu\text{g/L}$ in phosphate buffer saline. The scaffolds (10mm diameter; 2mm thickness) were placed in the six well plates containing 2ml of enzyme buffer solution and incubated at 37°C . The enzyme solution was changed once every 7 days and the rate of degradation was monitored for 28 days. The study was carried out in triplicates.

2.2.3.7 Anti-bacterial activity

The antibacterial activity of the scaffolds was tested against Gram-positive (*S.aureus* MTCC 737) and Gram-negative (*E.coli* NCIM 2345) bacteria using the disc diffusion assay in Muller Hilton agar. The bacteria were seeded (1×10^6 cells/ml) into warm and molten Muller Hilton agar, mixed gently and poured into petri plates. The scaffolds were embedded into the agar and the plates were allowed to solidify. The plates were incubated at 37 °C for 24 h and observed for zones of inhibition.

The bactericidal activity of the scaffolds was tested by incubating them in non- treated 6 well plates containing Mueller Hilton broth inoculated with 10^6 cells/ml of *E.coli* and *S.aureus*, respectively. The plates were incubated at 37 °C for 24 h and observed for growth of the bacteria. In order to check for bacteria adhering/harboring on to the scaffold, the scaffolds were transferred to MH agar plates, incubated at 37 °C for 24 h and observed for growth of adherent bacteria. All the experiments were performed in triplicates.

2.2.3.8 In-vitro Release Studies

The Ag release kinetics of the CS-Ag scaffolds were studied by cutting the scaffolds into discs of 10 mm diameter and immersing in 10 mL of simulated wound fluid (SWF-2% bovine serum albumin, 0.02 M calcium chloride dihydrate, 0.4 M sodium chloride, 0.08 M tris in de-ionized water, pH 7.5) at 37°C for 7 days (Pawar et al.). Spent SWF was replaced every 24h with an equal volume of fresh SWF. Ag was estimated by adding 5ml of 1N nitric acid to the spent SWF solution and analysing using a flame atomic absorption spectrophotometer (FAAS) (Shimadzu atomic absorption spectrophotometer AA-7000). All the studies are performed in triplicates.

2.2.3.9 Cell Viability Assessment

Cell viability assay is important in tissue engineering, to assess the number of viable cells attached and grown on the scaffolds. As HaCaT cells are aneuploid Human Keratinocyte cell lines (Boukamp, Petrussevska et al. 1988) and are derived from the keratinocytes, present in epidermal region of the skin, they were used for carrying out the MTT assay. For the cell viability studies, the CS and CS-Ag scaffolds were washed 3 times with phosphate buffer saline and placed in non-treated 6 well plates containing complete media (90% DMEM, 10% FBS, and 70 µL of Antibiotic Antimycotic Solution 100X liquid w/10,000 U Penicillin, 10mg Streptomycin and 25 µg Amphotericin B per ml in 0.9%

normal saline). They were allowed to soak for 4-6 h, followed by inoculation with HaCaT cells (1×10^5 cells/mL) and incubation in humidified CO₂ incubator (5% CO₂/95% air) for 24, 48 and 72 h, respectively. For the samples which were incubated for 72 h, the spent medium was replaced with fresh medium after 48 h. At the end of the respective incubation period, the media was removed and the scaffolds were washed with PBS (pH 7.2). MTT (500 μ L of 0.5mg/mL in PBS) was added to the wells and incubated for 4-6h for the formation of insoluble formazon crystals. DMSO (1.5 mL) was added and the cell suspension was incubated for 15 min to solubilize the formazon crystals. The absorbance of the supernatant was measured at 570 nm using DMSO as the blank. Three parallel replicates were analysed for each scaffold.

2.2.3.10 Scaffold morphology and cell attachment

The scaffold morphology and internal pore imaging was captured using a Scanning Electron Microscope (JEOL JSM-6390) operated at 10 kV. For the cell attachment studies, HaCaT cells were allowed to grow on the scaffolds for 24 h. The cells were fixed by placing the scaffolds in 2.5% glutaraldehyde solution overnight. The scaffolds were dehydrated using an ethanol gradient (20, 30, 50, 70, 90 and 100%) wherein, the scaffolds were maintained at each concentration for 10 min. The gold sputtering of the dehydrated scaffolds was carried out using vacuum controlled gold sputter coater (SPI-MODULE).

2.3 Results and Discussion:

Charge based polymers are generating a lot of interest in the field of biomedicine due to its ability to electrostatically interact with bioactive molecules. CS is positively charged polysaccharide obtained after deacetylation of chitin. The physiochemical and biological properties such as, crystallinity, hydrophilicity, degradataion and cellular response of the CS majorly depend upon the molecular weight and degree of deacetylation. Several reports suggested that the functional based diversity of CS have increased with degree of deacetylation while increasing the overall positive charge on the polymer allowing it to conjugate with the bioactive molecules (Madihally and Matthew 1999). The degree of the deacetylation of the CS molecules is ~71 % as determined by using ninhydrin assay [Figure 2.1 (A)]. The average molecular weight of CS as determined by using Mark-Houwink equation is about 26 Kilo Daltons [Figure 2.1(B)].

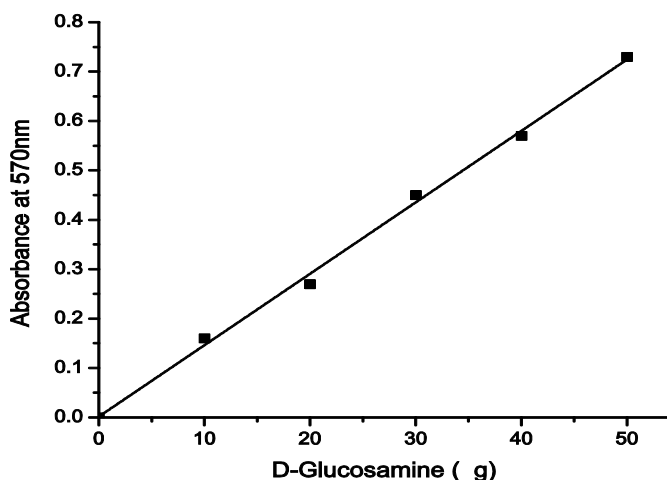


Figure 2.1 (A) Standard curve of D-Glucosamine by ninhydrin assay.

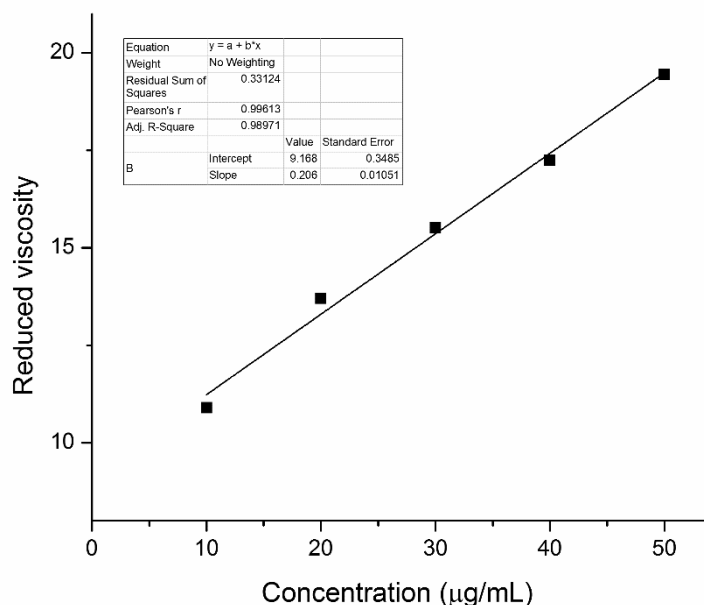


Figure 2.1 (B) Reduced viscosity of chitosan solutions at varying concentrations. Intrinsic viscosity of the CS is shown in the inset as the intercept value.

The CS-Ag scaffolds were synthesized using the technique of melt-down neutralization, followed by solvent curing and freeze drying. CS was dissolved in acetic acid to obtain a homogenous solution. The solution was frozen at -80°C followed by thawing at 8°C during which neutralization with sodium hydroxide in ethanol was carried out. Addition of alkali to the frozen samples helps in slow and controlled neutralization of the melting chitosan solution. The presence of ethanol increases the flexibility of the scaffold by rehydrating it from the strong alkaline affect, thereby exhibiting better biocompatibility

(He et al. 2011). The temperature of neutralization and the concentration of the alkali were crucial determinants of the shape and uniformity of the scaffolds. The descending temperature (thawing) of the frozen gel resulted in uniform molding of the scaffolds whereas surface deformities were observed in samples where freezing was not applied [Figure 2.2 (A, B)]. The gels were washed with deionized water to neutralize the pH and to remove the NaOH from the precipitated gels. The moulded gel was cured using acetone and diethyl ether followed by repeated freeze-thawing. Solvent curing has been shown to increase the mechanical stability of the resulting scaffold, and freeze-thawing was used to obtain uniform pore size and distribution (Orrego and Valencia 2009, Intranuovo et al. 2014). The ice nuclei comprise the void space between the polymers. At low temperatures the ice nucleation is faster resulting in the formation of smaller ice nuclei.

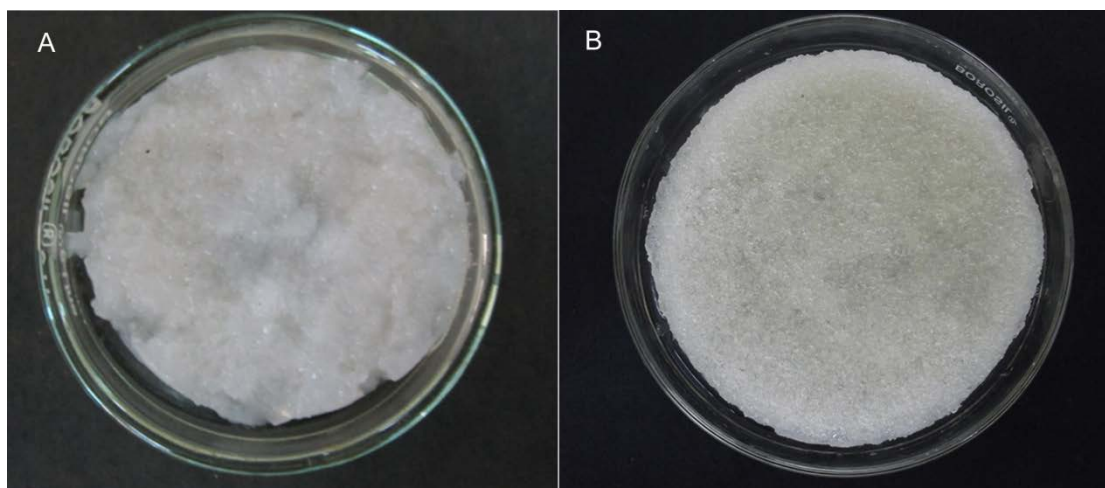


Figure 2.2 CS scaffolds neutralized with NaOH without melt-down (A), and with melt-down (B) technique.

Most of the reported methods for synthesis of CS scaffolds directly carry out freeze drying of the neutralized hydrogel. Studies on poly (vinyl alcohol) (PVA) hydrogels have shown that freeze thawing helps in the physical reorganization of the pores resulting in interconnectivity (Ricciardi et al. 2005, Gupta, Webster, and Sinha 2011). Similarly, freezing of collagen scaffolds is reported to have resulted in formation of scaffolds with smaller pore size (Haugh, Murphy, and O'Brien 2009). In this study, solvent curing was followed by freeze thawing to obtain an optimum pore size which directly influences cellular activity. Freeze thawing reorganizes the internal pore diameter as the ice crystals forms and thaws thus creating a uniform void space (pore). The SEM images of the scaffolds exhibiting open pore structure with a high degree of interconnectivity are shown

in Figure 2.3. The polymer structure was intact with no visible difference on incorporation of Ag within the CS matrix. The average pore size of the synthesized CS and Ag-CS scaffolds was between 100-200 μm .

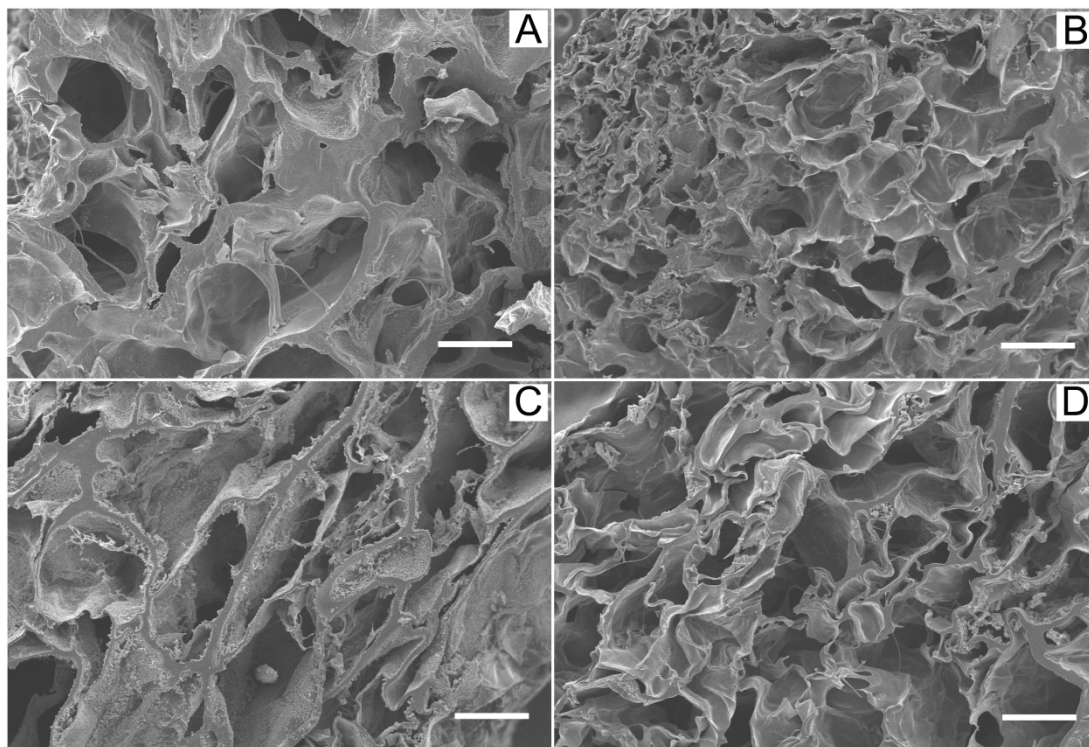


Figure 2.3 SEM micrographs showing the porosity of the CS (A), CS-Ag1, CS-Ag2 and CS-Ag3 scaffolds (scale bar – 100 μm).

The optimal scaffold pore size that allows maximal entry of cells and their adhesion varies with cell types. For example, endothelial cells show favourable attachment to pores in the range of 20-80 μm , osteoblasts require pores larger than 100 μm for bone formation whereas, keratinocytes require pore sizes between 80 to 150 μm (Doillon et al. 1986, Han et al. 2010).

2.3.1 XRD analysis

The crystalline patterns of the CS and CS-Ag scaffolds were identified by the presence of signature peaks for both the Ag and CS using an X-ray diffractometer. The overlaying data for the different scaffolds are shown in Figure 2.4. The broad peak at 2θ of 19.60 indicates the semi-crystalline nature of the CS with orthorhombic crystal structure (JCPDS no.39-1894). Similar diffraction patterns were reported for chitosan acetate films neutralized with sodium hydroxide as the reducing agent. The 2θ peaks at 38.06, 44.10,

64.60 and 77.54 correspond to hkl values of (111), (200), (220), and (311) respectively, of elemental Ag (JCPDS card number 04–0783) (López-Carballo et al. 2012).

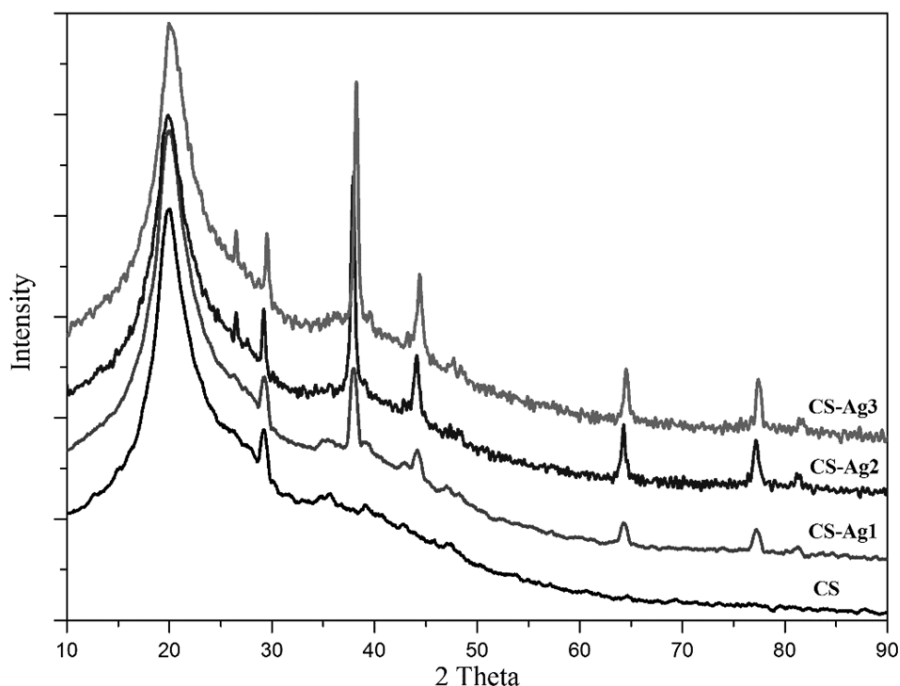


Figure 2.4 XRD diffractograms of CS, CS-Ag1, CS-Ag2 and CS-Ag3 scaffolds.

The intensity of the Ag peaks increases with increase in concentration of Ag. The average crystallite size of the Ag present in all the three CS-Ag samples is ~21nm as calculated using Scherrer formula.

2.3.2 FTIR analysis

FTIR spectra of CS and CS-Ag scaffolds are shown in Figure 2.5. The broad absorption peak at $3400\text{--}3200\text{ cm}^{-1}$ is the merged characteristic bands for OH and NH_2 groups. The FTIR spectra of CS show N-H bending at 1632 cm^{-1} , and N-H angular deformation in the CO-NH plane at 1543 cm^{-1} (Saraswathy et al. 2001, Mallikarjuna et al. 2011). In case of CS-Ag, the CO-NH plane of CS is shifted to 1560 cm^{-1} and NH bending to 1650 cm^{-1} . This has been attributed to the interaction of Ag with amine group of CS (Govindan et al. 2012). FTIR spectra of CS and CS-Ag scaffolds are shown in Figure 2.5. The broad absorption peak at $3400\text{--}3200\text{ cm}^{-1}$ is the merged characteristic bands for OH and NH_2 groups. The FTIR spectra of CS show N-H bending at 1632 cm^{-1} , and N-H angular deformation in the CO-NH plane at 1543 cm^{-1} (Saraswathy et al. 2001, Mallikarjuna et al. 2011). In case of CS-Ag, the CO-NH plane of CS is shifted to 1560 cm^{-1} and NH bending

to 1650 cm^{-1} . This has been attributed to the interaction of Ag with amine group of CS (Govindan et al. 2012).

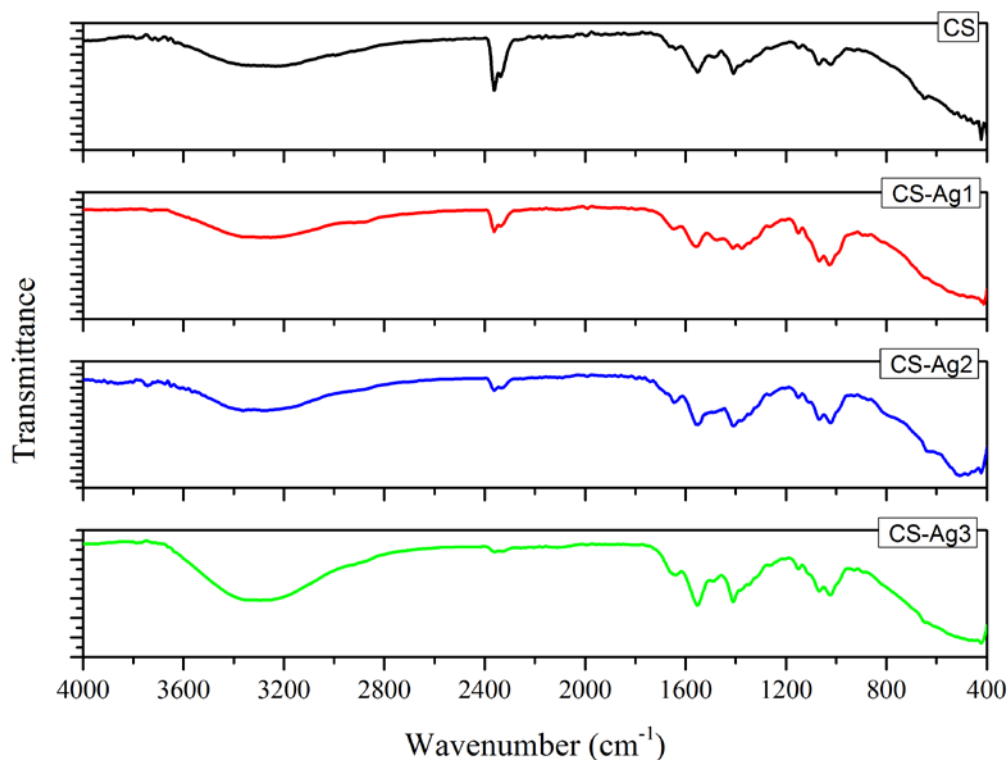


Figure 2.5 FT-IR spectra of CS, CS-Ag1, CS-Ag2 and CS-Ag3 scaffolds.

FTIR spectra of CS and CS-Ag scaffolds are shown in Figure 2.5. The broad absorption peak at $3400\text{--}3200\text{ cm}^{-1}$ is the merged characteristic bands for OH and NH_2 groups. The FTIR spectra of CS show N-H bending at 1632 cm^{-1} , and N-H angular deformation in the CO-NH plane at 1543 cm^{-1} (Saraswathy et al. 2001, Mallikarjuna et al. 2011). In case of CS-Ag, the CO-NH plane of CS is shifted to 1560 cm^{-1} and NH bending to 1650 cm^{-1} . This has been attributed to the interaction of Ag with amine group of CS (Govindan et al. 2012).

2.3.3 Thermal stability by TGA

Thermo-gravimetric analysis is performed to determine the thermal stability and the degradation pattern of a material. Various physical and chemical properties of the material were measured as a function of increasing temperature (Thakur, Thakur, and Gupta 2013). Figure 2.6, illustrates the thermo-gravimetric analysis of CS and CS-Ag scaffolds. The initial weight loss from 50°C to 100°C is due to the loss of moisture content from the scaffolds, and is more in the CS scaffold as compared to the CS-Ag

scaffolds. The second weight loss is due to scission of the ether linkage in the CS backbone between 200°C - 300°C for the CS and CS-Ag scaffolds. The degradation

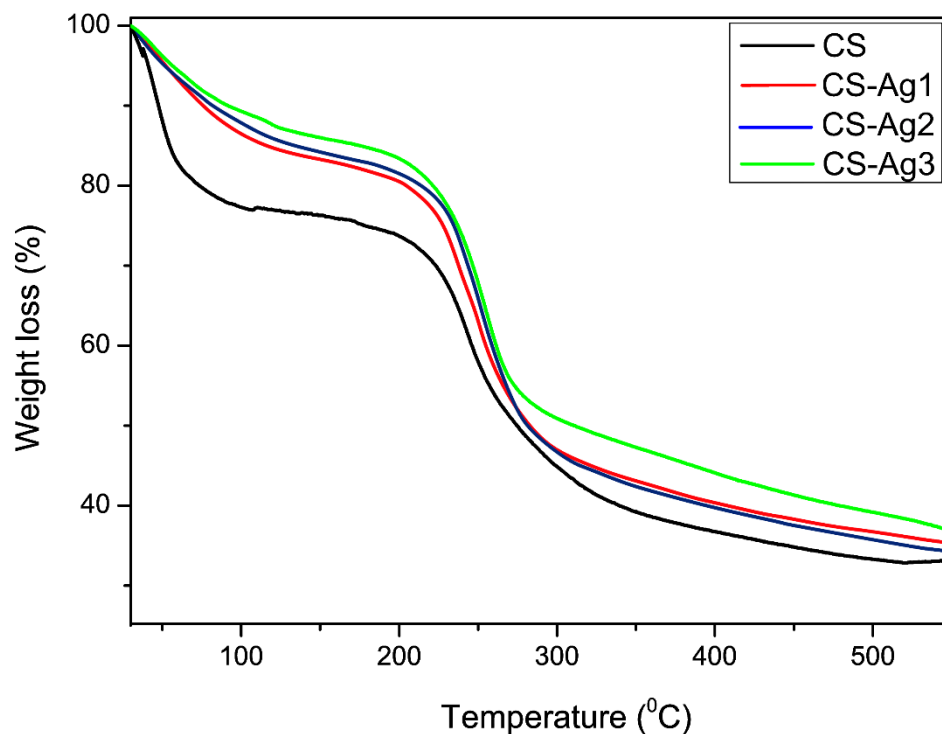


Figure 2.6 TGA curves of CS, CS-Ag1, CS-Ag2 and CS-Ag3 scaffolds.

temperature of CS and CS-Ag scaffolds after 10% weight loss is 50°C and 75°C, respectively, indicating higher stability of CS-Ag scaffolds. Similar pattern of higher thermal stability of silver based chitosan nanocomposites has been reported by Tripathi et al. (2011) and Regiel et al. (2013). The higher stability of CS-Ag scaffolds as compared to CS scaffolds is attributed to the presence of Ag (Tripathi, Mehrotra, and Dutta 2011, Regiel et al. 2012).

2.3.4 *In-vitro* degradation of scaffolds

It is important to understand the degradation kinetics of scaffolds aimed for wound healing applications. *In-vitro* degradation of the scaffolds was studied using lysozyme, an enzyme which cleaves the $\beta(1,4)$ linkages between N-acetyl-D-glucosamines. The degradation profile of the scaffolds estimated after incubation for 7, 14, 21 and 28 days with lysozyme is shown in Figure 2.7. There is no significant difference in the degradation kinetics of CS and CS-Ag scaffolds ($p \leq 0.05$). All the scaffolds exhibited ~20% weight loss after lysozyme treatment over a period of 28 days. The degradation rate

is related to the number of N-acetyl glucosamine residues on the chitosan (>75% deacetylation) which are the primary targets for the lysozyme to cleave the $\beta(1,4)$ glycosidic bonds (Nwe, Furuike, and Tamura 2009, Hsieh, Chang, and Lin 2007).

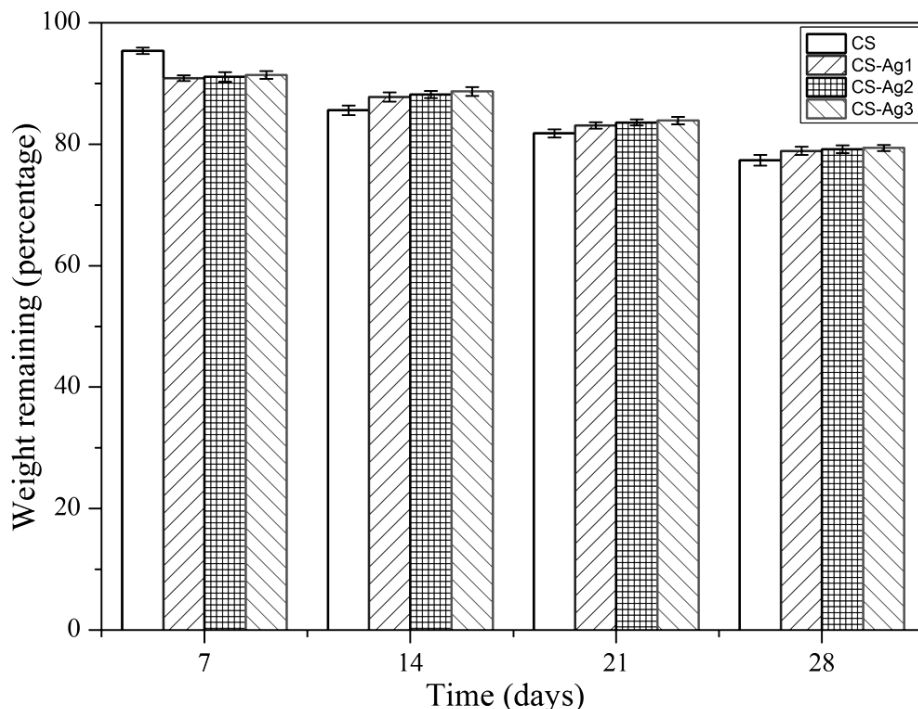


Figure 2.7 Degradation studies of CS, CS-Ag1, CS-Ag2 and CS-Ag3 scaffolds using lysozyme treatment for a period of 7 to 28 days.

2.3.5 Anti-bacterial studies

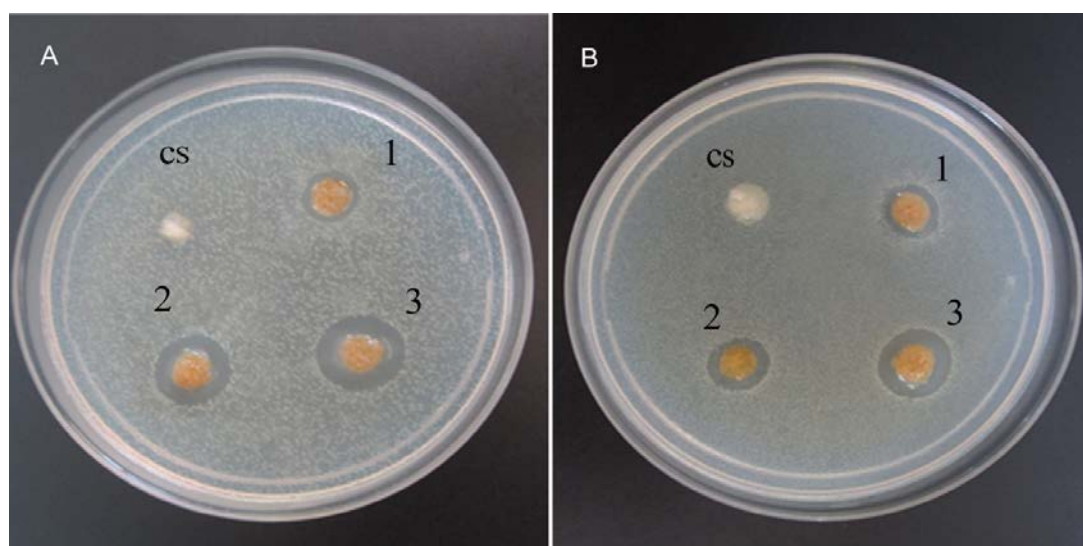


Figure 2.8 Antibacterial effect of CS and CS-Ag (1,2,3) scaffolds against *E.coli* (A) and *S.aureus* (B).

Antibacterial activity was tested against two strains, the Gram-positive *S.aureus* MTCC 737 and Gram-negative *E.coli* NCIM 2345. It was observed that at all the three Ag concentrations; CS-Ag scaffolds exhibited anti-bacterial activity, whereas no inhibition of growth was observed with CS scaffolds (Figure 2.8). An increased anti-bacterial activity was obtained for scaffolds with higher concentration of Ag, and was in the order of CS-Ag3 > CS-Ag2 > CS-Ag1. The antibacterial activity of Ag based scaffolds has been attributed to the release of Ag ions from the matrix into the medium, killing the bacteria by interfering with cellular activities and generating reactive oxygen species. Trapping of Ag nanoparticles within matrices such as collagen, hydroxyapatite, TiO₂ etc., leads to slow and sustained release of the Ag ions resulting in prolonged antibacterial activity (Roy et al. 2012, Saravanan, Vemu, and Barik 2011, Jadalannagari et al. 2014, Naik and Kowshik 2014). The CS-Ag scaffolds exhibited better antibacterial activity against Gram-negative (*E.coli*) as compared to Gram-positive (*S.aureus*) bacteria, and is attributed to the differences in the composition of their cell membranes. Gram-positive bacteria have a thick peptidoglycan layer when compared to Gram-negative bacteria, which hinders the Ag ion diffusion into the cell wall (Jung et al. 2007).

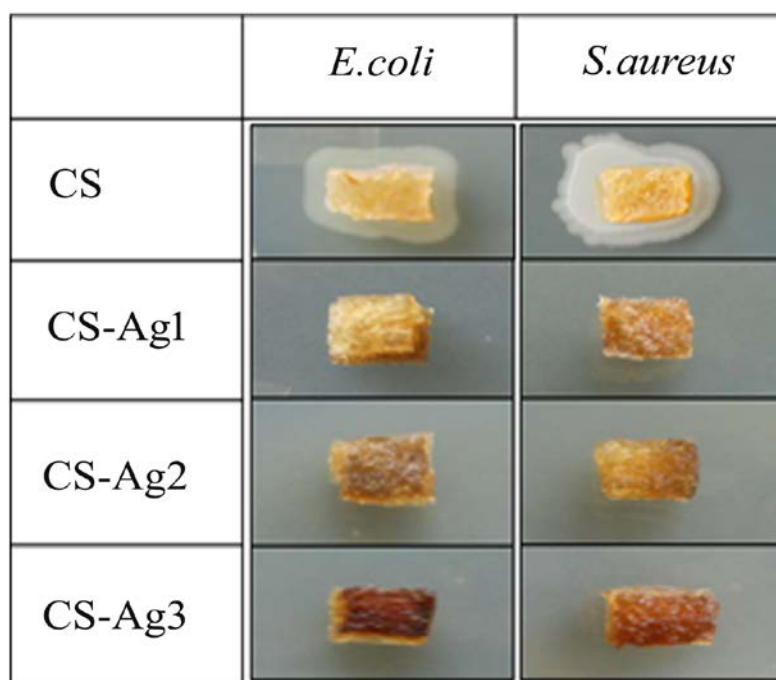


Figure 2.9 Growth of bacterial cells around the CS scaffolds incubated with bacterial suspension for 24 h. No growth is observed around CS-Ag scaffolds.

Antibacterial activity was further confirmed by immersing the scaffolds in MHB inoculated with bacteria (10^6 cells/ml). Inhibition of bacterial growth was observed with

Ag embedded scaffolds, whereas dense growth was noted in the broth containing the CS scaffolds. In order to check whether the CS-Ag scaffolds harbored any live bacteria, the scaffolds were removed from the inoculated medium, placed on fresh MH agar plates and incubated for growth. No growth of bacterial cells was noted with CS-Ag scaffolds indicating complete inhibition of the bacterial cells, whereas luxuriant growth was observed around the CS scaffolds (Figure 2.9).

2.3.6 *In vitro* Ag release studies

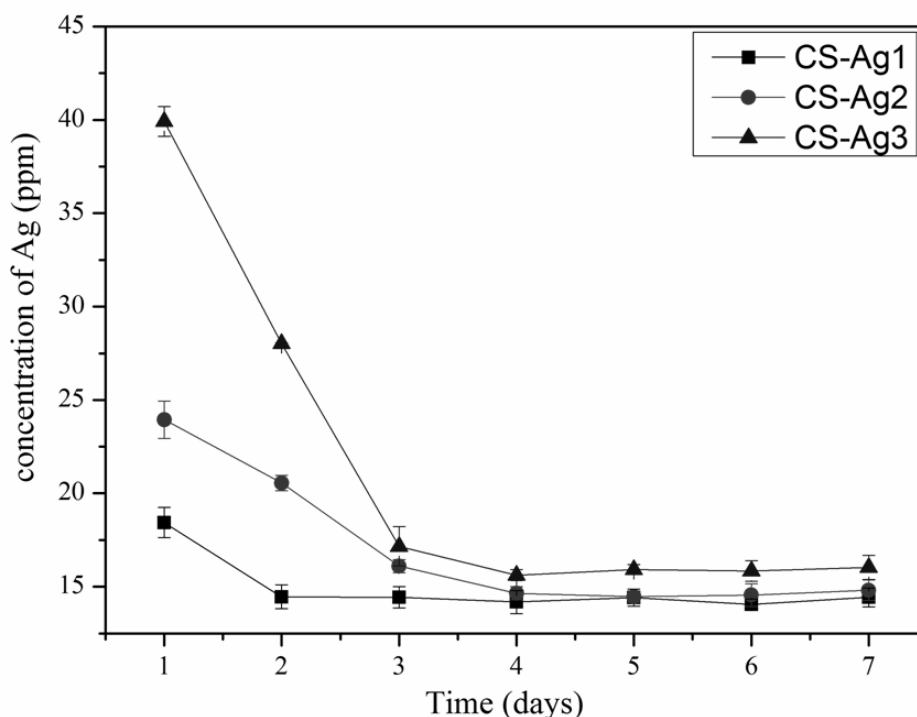


Figure 2.10 Ag release rate from the CS-Ag scaffolds over a period of seven days.

The amount of Ag released from the CS-Ag1, CS-Ag2 and CS-Ag3 scaffolds incubated in SWF for seven days and estimated at intervals of 24h is shown in Figure 2.10. Total Ag released into the medium (ionic and non-ionic) was estimated using FAAS. The non-ionic Ag particles were ionized using ionization buffer containing 1N nitric acid (Kebbekus 2003). The CS-Ag scaffolds showed initial burst release of Ag for two days and later the release was slow and sustained over a period of 7 days. Such an initial high release is favorable for rapid killing of the bacterial cells so that they do not develop resistance while the subsequent slow and sustained release is optimum for a long-term antimicrobial activity in addition to minimizing the Ag toxicity on mammalian cells (Naik et al. 2013). The total cumulative percentage of Ag released after 7 days from the CS-Ag1, CS-Ag2 and CS-Ag3 was 42, 35 and 26 %, respectively. The release of Ag ions is governed by

water diffusion characteristics of the scaffold, thus allowing the surface adsorbed Ag to release first. The Ag ions present in the core of the scaffold require time to be transported to the surface, allowing a slow and sustained release in the later stages. The initial quick release makes the CS-Ag scaffolds ideal candidates for chronic wounds which are prone to bacterial infections and the steady release provides long-term antimicrobial activity (Wu et al. 2010).

2.3.7 Biocompatibility studies

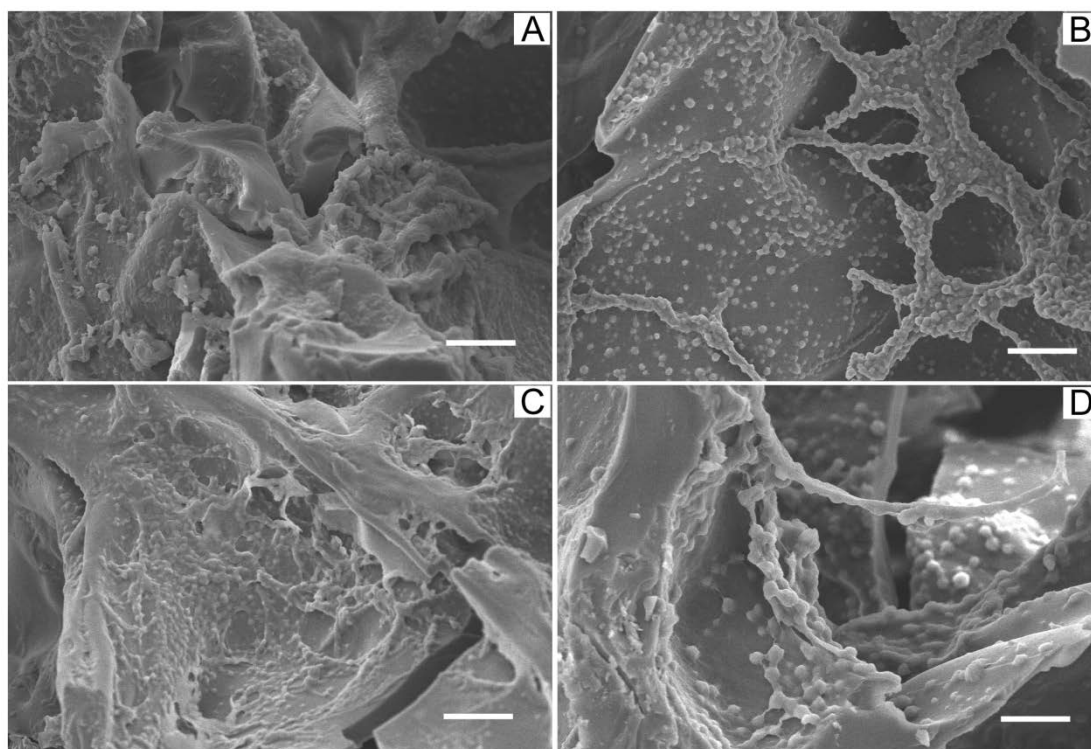


Figure 2.11 SEM micrographs of HaCaT cell attachment and proliferation on CS (A), CS-Ag1, CS-Ag2 and CS-Ag3 scaffolds (scale bar- 10 μ m).

The cell attachment and viability studies on the scaffolds were carried out using HaCaT cells, which are spontaneously transformed keratinocytes. Figure 2.11 shows the attachment of the HaCaT cells on to the walls of polymeric scaffolds as visualized by SEM. As observed from the figures, HaCaT cells have retained their native morphology when grown in three-dimensional scaffolds.

Cell viability is related to microstructure of the scaffold, such as surface property, pore size and connectivity. The cell viability on the scaffolds was analyzed using MTT assay. The MTT reagent is reduced to a blue coloured formazon product by cellular reductases in viable cells. Formazon crystals can be solubilised in organic solvents like DMSO. Thus, the amount of formazon formed is directly proportional to the number of metabolic

cells, and an increase in optical density indicates cell adhesion and proliferation in the scaffolds (Li et al. 2010).

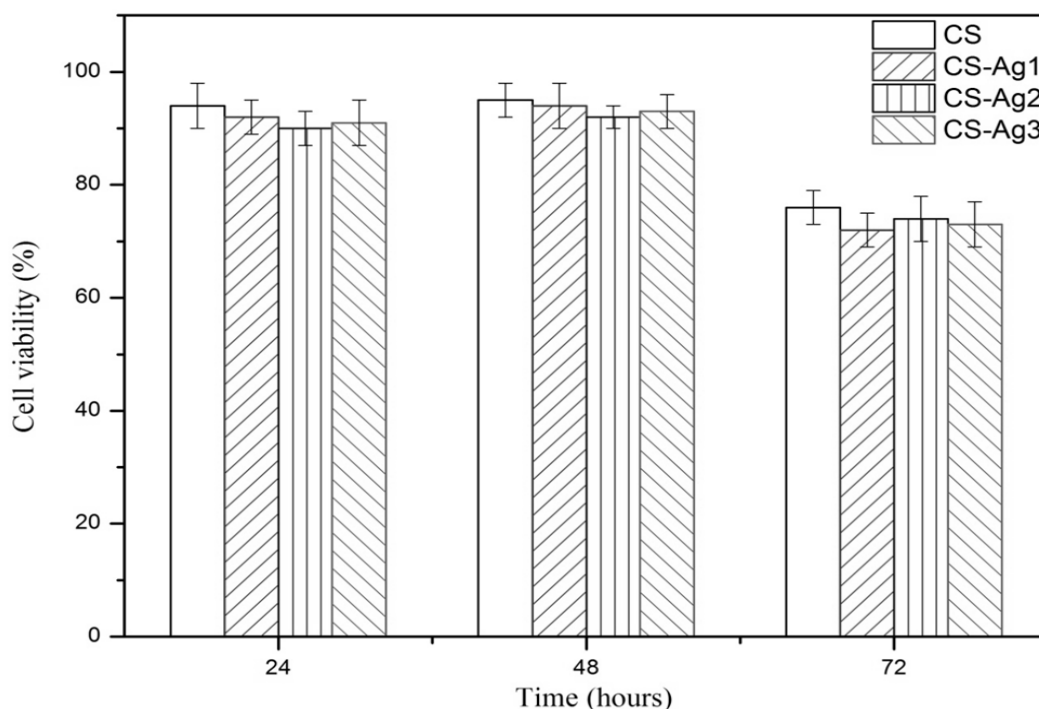


Figure 2.12 Cell viability by MTT assay on CS, CS-Ag1, CS-Ag2 and CS-Ag3.

The viability count of HaCaT cells on the CS-Ag scaffolds was not significantly different ($p \leq 0.05$) from the CS scaffolds (Figure 2.12) and these results are in agreement with the SEM data. The adhesion and proliferation of the mammalian cells on these scaffolds is facilitated by the electrostatic interactions between the amino groups of CS with the negative charge of the cell surface. In addition, biospecific interaction between cell receptors and the CS molecules also contributes towards cell attachment (Tangsadthakun et al. 2017, Correia et al. 2011). The cells at 24 h and 48 h in both control and Ag scaffolds have shown good viability indicating their biocompatible nature. The presence of Ag in the CS scaffolds had no visible effect on HaCaT proliferation. However the cell viability decreased after 72 h, in all the synthesized scaffolds. Similar decline in cell number after 3 days has been widely reported and can majorly due to the cells becoming confluent rather than the Ag toxicity (Bhat, Tripathi, and Kumar 2011). These results show that the CS-Ag scaffolds are biocompatible with good potential for tissue engineering applications.

2.4 Conclusion

The polymeric CS-Ag scaffolds have been synthesized using a novel melt-down neutralization technique. Uniform entrapment of Ag within the polymeric matrix enhances the antibacterial activity, without affecting other physico-chemical and biological properties of the CS. The slow and sustained release of Ag provides long term antibacterial activity and has no toxicity towards keratinocytes. The CS-Ag scaffolds prohibited bacterial cell adhesion on to the scaffolds, while at the same time supported growth of keratinocytes which is an essential characteristic for tissue engineering applications.

Chapter 3: Synthesis and Characterization of Antioxidant Incorporated Chitosan-Collagen Scaffolds

3.1 Introduction

Wound healing is a complex process with cellular and biochemical events of numerous cells uniting to synergize and remodel the compromised tissue. The wound healing niche comprises of many cell types that signal one another in both endocrine and paracrine fashion which ensure the return to normal homeostasis in the damaged area (Gonzalez et al. 2016). Reactive oxygen species (ROS), a group of extremely potent molecules, are rate limiting in successful tissue regeneration. The free radicals of unstable oxygen molecules interact with biopolymers such as proteins, DNA, lipids and carbohydrates causing progressive oxidative damage leading to cell death (Bryan et al. 2012). ROS have a fundamental function in innate immunity and the ability to act in both signaling and host defense capacities. A balanced ROS response will disinfect a tissue and stimulate healthy tissue turnover whereas suppressed or elevated ROS will result in an infection or damage the otherwise healthy tissue. The understanding of the ROS niche within a tissue is an area of emerging research with the aim to aid the healing process through potential exogenous augmentation processes by using new tools such as antioxidants, metal chelators, ion reducing substances etc., to understand the chemical complexity in the biological systems (Dunnill et al. 2017, Sharma et al. 2012).

Antioxidants are substances which help in regulating the ROS-mediated damage of biological molecules and body tissue. The presence of excess ROS or the absence of antioxidant ROS scavenger molecules such as vitamins E, C, and glutathione are the characteristics of a chronic wound environment. Interestingly, levels of wound antioxidants tend to decrease with age, which correlates with the delayed wound healing responses seen in the elderly. Reduced or delayed wound healing occurs as a consequence of lower concentrations of antioxidants allowing the wound ROS reaction to proceed unchecked, thereby progressively compounding tissue damage (Kurahashi and Fujii 2015, Di Mascio, Murphy, and Sies 1991).

Although antioxidants like glutathione, vitamin C, ellagic acid (EA), curcumin (CM), and other phenolic compounds have been studied for their potential to scavenge free radicals, their application in tissue engineering remains largely unexplored (Lee et al. 2010, Gopalakrishnan et al. 2014). SM, the active component of the milk thistle plant (*Silybum*

Chapter 3: Synthesis and Characterization of Antioxidant Incorporated Chitosan-Collagen Scaffolds

marianum) is a polyphenolic flavonolignan with potential antioxidant activity. SM has shown protective effect against oxidative stress generated by ROS in several experimental models by scavenging the free radicals, preventing lipid peroxidation and increasing the expression of antioxidant genes (Tabandeh et al. 2013, Soto et al. 2010). CM, one of the major yellow pigments in turmeric is widely known for its anti-inflammatory and antioxidant properties. In cisplatin induced rats, pre-treatment with CM was found to normalize the levels of lipid peroxidation biomarkers, catalase activity, and renal functions (Kuhad et al. 2007). Endothelial cells treated with CM exhibit an increase in the expression of mRNAs for several antioxidant enzymes which may thereby contribute towards reducing the oxidative stress (Motterlini et al. 2000). Among the phenolic acids, EA, a naturally occurring phenolic compound present in several fruits and nuts, has been found to have antioxidant, anticarcinogenic, chemo-preventive, and radical scavenging activity. In rats, dietary intake of EA has been demonstrated to prevent oxidative stress induced by streptozotocin as observed by a significant reduction in the oxidative stress markers such as MDA, TOS, OSI, and NO (Uzar et al. 2012). Similarly, upon UVA exposure, human epidermal keratinocyte (HaCaT) cells pretreated with EA exhibit reduced DNA fragmentation, and Bcl-2/Bax deregulation along with an increase in the expression of antioxidant enzymes such as heme oxygenase 1 (HO-1), and SOD (Hseu et al. 2012). The antioxidant properties of phenolic compounds are mainly attributed to the H-atom donation from the phenolic group to the ROS and making it less reactive (Kuhad et al. 2007).

Successful tissue engineering solutions to augment healing and remodeling of wounded or diseased tissue rely on naturally derived extracellular matrix (ECM). Recognition of the importance of ECM in wound healing has led to the development of wound management products that aim to stimulate or replace it (Tracy, Minasian, and Caterson 2016). ECM is comprised of various components such as collagen, fibrin, proteoglycans, hyaluronic acid, and other adhesive proteins, such as laminin and fibronectin. It provides structural and mechanical integrity to tissues, and helps in communicating with the surrounding cellular components (Dvořánková et al. 2011, Kim, Turnbull, and Guimond 2011). The use of natural biopolymers such as collagen (CO) and chitosan (CS) has been extensively increasing in the field of tissue engineering. They exhibit advantages of biodegradability and biocompatibility over synthetic polymers (Kobayashi et al. 2010). Moreover, CS exhibits structural similarity to synovial glycosaminoglycans present in the

hyaluronic acid. Charge based polymers such as CO and CS have an added advantage as their hydroxyl (OH^-) and amino (NH_4^+) groups can bind the bioactive molecules forming conjugates that facilitate controlled release at the wound site (Dhandayuthapani, Krishnan, and Sethuraman 2010, Shaik and Kowshik 2016). However, the challenges in biomedical engineering largely depend on the physical and chemical modifications of the polymer and the bioactive molecules (Venkatesan and Kim 2010). Here, we demonstrate the potential of antioxidant incorporated CO/CS scaffolds in providing micro-environment amenable for recovery of cells from oxidative stress.

3.2 Materials and methods

3.2.1 Materials

CS, CO (type 1, hydrolysed peptide), EA, and CM were purchased from HiMedia, India. Acetic acid, sodium hydroxide (NaOH), and glutaraldehyde were purchased from SD-Fine Chemicals Ltd, India. All the cell culture grade chemicals like DMEM, MTT, and PBS were purchased from HiMedia, India. All other chemicals used were of analytical grade and obtained from HiMedia, India.

3.2.2 Synthesis of antioxidant (SM/CM/EA) incorporated collagen chitosan scaffolds

CS (300 mg) was dissolved in 10 mL 1 % (v/v) acetic acid and stirred overnight. SM, EA, and CM solutions of varying concentrations (0.5, 1, and 2 % w/w) were prepared in ethanol (1 mL) and mixed by vortexing for 10 min. Antioxidant solution was added drop-wise to the CS solution under constant stirring on a magnetic stirrer, which was continued for 24 h. Subsequently, 700 mg of CO was added to the reaction mixture and stirred for 4 h. Glutaraldehyde (0.004 M) was used as the cross-linking agent, and the mixture was poured into 50mm borosil petri plates. The viscous gel filled plates were frozen at -80°C for 24 h. The frozen matrix was allowed to thaw in presence of 0.1 M NaOH to facilitate gel formation by the melt-down neutralization technique. The gels were washed with de-ionized (DI) water until the pH of the wash water was maintained at 7.0. The washed gels were frozen at -20°C for 6 h, followed by freezing at -80°C for 12 h. The frozen gels were lyophilized (CHRIST alpha 1–2 LD plus) to obtain scaffolds. The synthesized CO and CS scaffolds with varying concentration of SM (0.5, 1, and 2 w/w %) are abbreviated as CS-CO-SM_(0.5), CS-CO-SM₍₁₎, and CS-CO-SM₍₂₎, while the scaffolds with CM (0.5, 1, and 2 w/w%) are designated as CS-CO-CM_(0.5), CS-CO-CM₍₁₎, and CS-CO-CM₍₂₎, respectively. Similarly, the scaffolds with EA (0.5, 1, and 2 % w/w) are abbreviated as

CS-CO-EA_(0.5), CS-CO-EA₍₁₎, and CS-CO-EA₍₂₎, respectively. Scaffolds without antioxidants (control) are designated as CS-CO.

3.2.3 Characterization

3.2.3.1 Physico-chemical characterization of the scaffolds

The structural characterizations of the synthesized antioxidant scaffolds were carried out by XRD and ATR-FTIR spectroscopy. The crystalline phase of the antioxidant (SM, CM, and EA) incorporated scaffolds were recorded between the 2 theta angular values of 10 to 60° at a scan speed of 3° per second operated at 10kV/mA current. IR spectra of the scaffolds were recorded to identify the chemical interaction between the polymers (CO, CS) and antioxidants (SM/CM/EA). The scaffolds were scanned in the range of 4000 to 400 cm⁻¹ with a resolution of 4 cm⁻¹, and an average of 60 scans per scaffold. The cross-sectional morphology and porosity of the synthesized antioxidant scaffolds was observed by using SEM (FEG Quanta-200) operated at a working voltage of 10 kV. The gold sputtering of the dehydrated scaffolds was carried out using vacuum-controlled gold sputter coater (Leica EM ACE600).

3.2.3.2 Release kinetics of antioxidants

The *in vitro* release of the antioxidant (SM/CM/EA) from the synthesized scaffolds was determined by UV visible spectroscopy (Shimadzu, UV-2450). The synthesized antioxidant incorporated scaffolds were suspended in 10ml PBS (pH 7.4) and incubated at 37° C. At fixed time intervals, the PBS was replaced with fresh PBS and the spent buffer was used to estimate the amount of antioxidant released using UV spectrophotometry. Concentrations of SM, CM, and EA were estimated at 286, 421, and 260 nm, respectively. All the experiments were performed in triplicate.

3.2.3.3 Mammalian cell culture

Fibroblasts cells are majorly dominated in the dermal region of the skin and play an important role in wound healing. The cell line used for this study was fibroblast-like cells derived from monkey kidney tissue, COS-7. The cells were maintained in DMEM supplemented with 10% fetal bovine serum (FBS) and antibiotics. The cells were maintained at 37°C in a humidified 5% CO₂ incubator (Sanyo, Japan) and sub-cultured according to standard cell culture protocol (Freshney 2001).

3.2.3.4 Cytotoxicity of the fabricated scaffolds

The *in vitro* cytotoxicity of the antioxidant (SM, CM and EA) incorporated scaffolds were tested on COS-7 using MTT assay. The scaffolds were soaked in DMEM for 4-6 h followed by seeding with COS-7 cells (10^5 cells/mL) and incubated for 24, 48, and 72 h. For the samples incubated for 72 h, the spent medium was replaced with fresh medium after 48 h. At the specific time points, the media was aspirated and the scaffolds were washed with PBS (pH 7.2). MTT (500 μ L of 0.5 mg/mL in PBS) was added to each well and incubated for 4–6 h for the formation of insoluble formazan crystals. DMSO (1.5 mL) was added and the cell suspension was incubated for 15 min to solubilize the formazan crystals. The absorbance of the supernatant was measured at 570 nm using DMSO as the blank. Three parallel replicates were analyzed for each scaffold before seeding the cells. The percent cell viability of the COS-7 cells was calculated using the following equation where, A_t , and A_c are the absorbance values of test, and control, respectively.

$$\text{Cell viability (\%)} = [(A_c - A_t) / A_c] * 100$$

For the cell attachment studies, the scaffolds were placed in 6-well plates (non-treated) and soaked in complete media for 4 h prior to seeding with COS-7 cells. The cells were allowed to grow on the scaffolds for 24 h. The spent media was discarded from the plates and the scaffolds were washed thrice with PBS. The cells were fixed by placing the scaffolds in 2.5% glutaraldehyde solution for 4 h and were given three washes with PBS followed by dehydration using an ethanol gradient (20, 30, 50, 70, 90 and 100 %), wherein the scaffolds were maintained at each concentration for 10 min. The scaffolds were gold coated and used for SEM imaging.

3.2.3.5 Determination of antioxidant activity of scaffolds

UV irradiation can induce ROS, resulting in an up-regulation of oxidative stress and ultimately an induction of apoptosis. To analyze the effect of *in vitro* antioxidant activity, the synthesized antioxidant incorporated scaffolds seeded with COS-7 cells were subjected to UV irradiation (Philips 15W/G15 T8- 49J/cm²) for varying time, viz., 10, 20, and 30 min. The percentage cell viability on the scaffolds was analyzed 0 h and 24 h, post irradiation using the MTT assay.

3.3 Results and Discussion:

3.3.1 Synthesis of the CS-CO scaffolds

Antioxidants incorporated collagen (CO) and chitosan (CS) scaffolds were synthesized using the melt-down neutralization method followed by freeze drying (Shaik and Kowshik 2016). Natural polymers such as CO and CS have been extensively used as drug carriers due to their large entrapment efficiency. The present investigation was an effort to incorporate antioxidants into the tissue engineering scaffolds and control their release during oxidative stress. The antioxidants (SM, CM, and EA) were incorporated by dissolving them in ethanol prior to addition into the CS solution. CO was added subsequently by maintaining the CS:CO ratio at 3:7, and cross-linking was achieved using glutaraldehyde. Homogeneity was attained by stirring the acidic reaction mixture for 24 h before casting into molds and freezing at -80°C to obtain polymeric gels. The cast gels were thawed in the presence of NaOH to ensure uniform neutralization of the polymeric matrix. The scaffolds were obtained by freeze-drying the gels and used for further studies.

Collagen based scaffolds have a favorable advantage in skin tissue engineering as collagen makes up to 70% of the dry weight of the dermis (Smith, Holbrook, and Madri 1986). Natural biopolymers such as CS, hyaluronic acid, alginate, etc. have been widely used in skin tissue engineering due to their similarities with the native ECM (Dhandayuthapani, Krishnan, and Sethuraman 2010, Sharma et al. 2016). In acidic solution, both collagen and chitosan are positively charged and the CO/CS reaction mixture is homogenous facilitating efficient mixing of biomacromolecules at sub-molecular level. In contrast blends of polycationic polymers like (CS and CO) with polyanionic molecules such as chondroitin sulfate precipitate immediately due to polyelectrolyte complexation, leading to heterogeneity within the scaffolds (Rodrigues et al. 2016). The GAGs present in the ECM also play an important role by providing structural and biochemical support to the surrounding cells. CS being a peptidoglycan shares some characteristics with various GAGs and hyaluronic acid present in the native ECM (Xu et al. 2007).

3.3.2 Physico-chemical characterization of the scaffolds

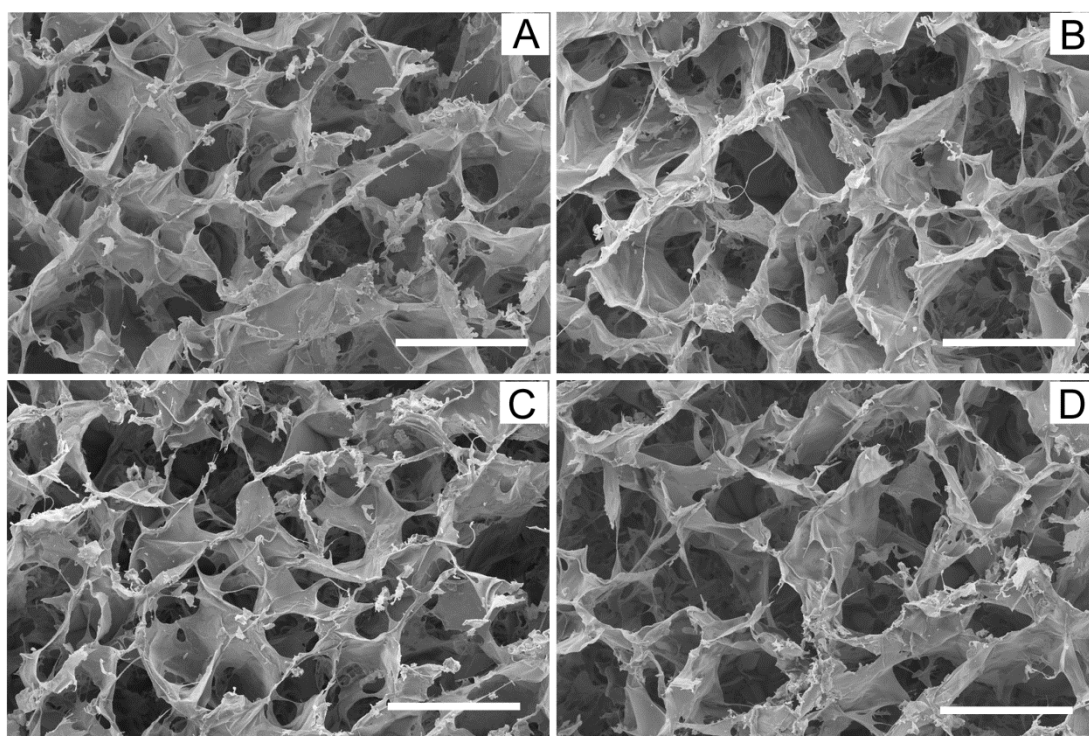


Figure 3.1 SEM micrographs of CS-CO scaffolds (A) along with 2 % w/w SM (B), CM (C) and EA (D), incorporated CS-CO scaffolds (scale bar – 200 μ M).

The inter-connection between the components of the artificial ECM is very important in achieving the structural integrity and mechanical properties of the scaffolds. Crosslinking of the CO/CS scaffold was achieved by using glutaraldehyde, wherein, the amino groups of CO and CS, function as binding sites and increase the glutaraldehyde cross-linking efficiency. It has been reported that scaffolds crosslinked with glutaraldehyde exhibit better pore size, internal porosity and degradation rate as compared to non-crosslinked scaffolds (Kishen et al. 2016). SEM micrographs (Figure. 3.1) of the 2 % w/w SM, CM, and EA incorporated CS-CO scaffolds exhibit a well interconnected pore structure. The incorporation of various antioxidants, viz., SM, CM, or EA did not affect the porous structure of the scaffolds. As mentioned earlier, the optimal pore size of the tissue varies due to the differences in the cellular, biochemical, structural and functional levels of individual tissue, that there is no ideal scaffold for tissue engineering applications (Lien, Ko, and Huang 2009, Samal et al. 2015).

The phase structure of the CO, CS and CS-CO were studied using XRD (Figure 3.2). The CS diffraction spectra has shown the broad peak at 2θ value of 19.83° with the hkl value

of (010) indicating the orthorhombic structure of the CS (ICDD card no.39-1894). The broadening

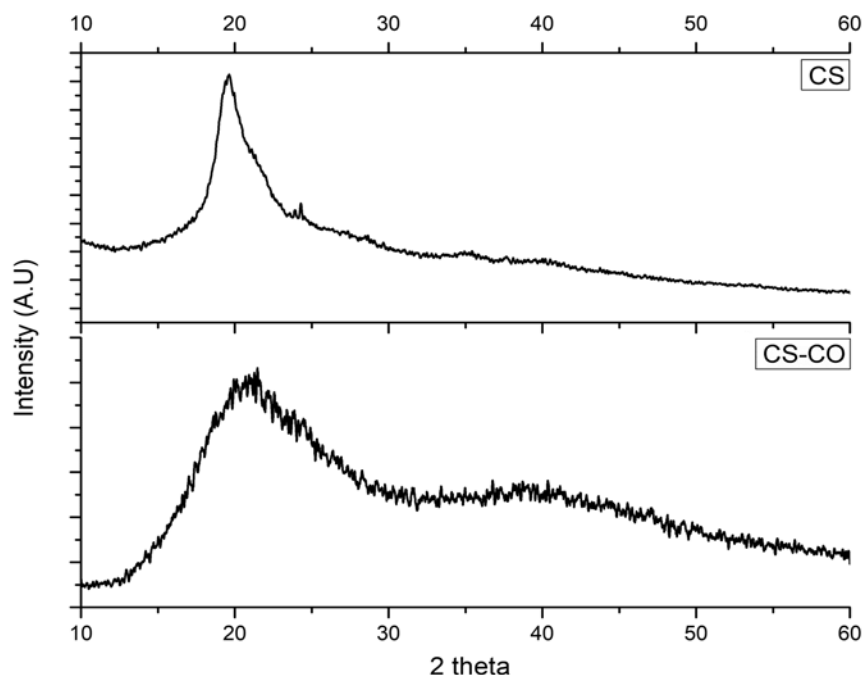


Figure 3.2 XRD pattern of CS and CS-CO scaffolds exhibiting the semi-amorphous nature of the polymers.

of the peak is attributed to its semi-amorphous nature. In CS-CO scaffolds, a broad peak between the 2θ values of 15° to 30° with maxima at 20.92° was observed, and is attributed to the amorphous nature of the polymers (CO; CS) (Chen et al. 2008).

SM incorporated CS-CO scaffolds exhibited diffraction peaks for SM at 19.11° (011), 22.75° (200), and 24.73° (102) which corroborate with the values reported in literature (Yang et al. 2015). The intensity of the peak arising due to SM in the CS-CO-SM₍₁₎ scaffold was found to be lower than that exhibited by CS-CO-SM₍₂₎, while there was no significant difference in the SM peak intensities or phase structure between CS-CO-SM_(0.5) and CS-CO-SM₍₁₎ which may be attributed to the semi- amorphous nature of the SM (Figure 3.3). The amorphous nature of polymeric conjugates facilitates sustained release of the incorporated drug/antioxidant.

CM exhibited many diffraction peaks indicating the highly crystalline nature of the antioxidant. The highest intensity peak at 2θ value 17.22° along with several characteristic diffraction peaks between 10° and 30° correspond with the ICDD card no.09-0816 of CM (Shaikh et al. 2009). The CM incorporated scaffolds exhibited the

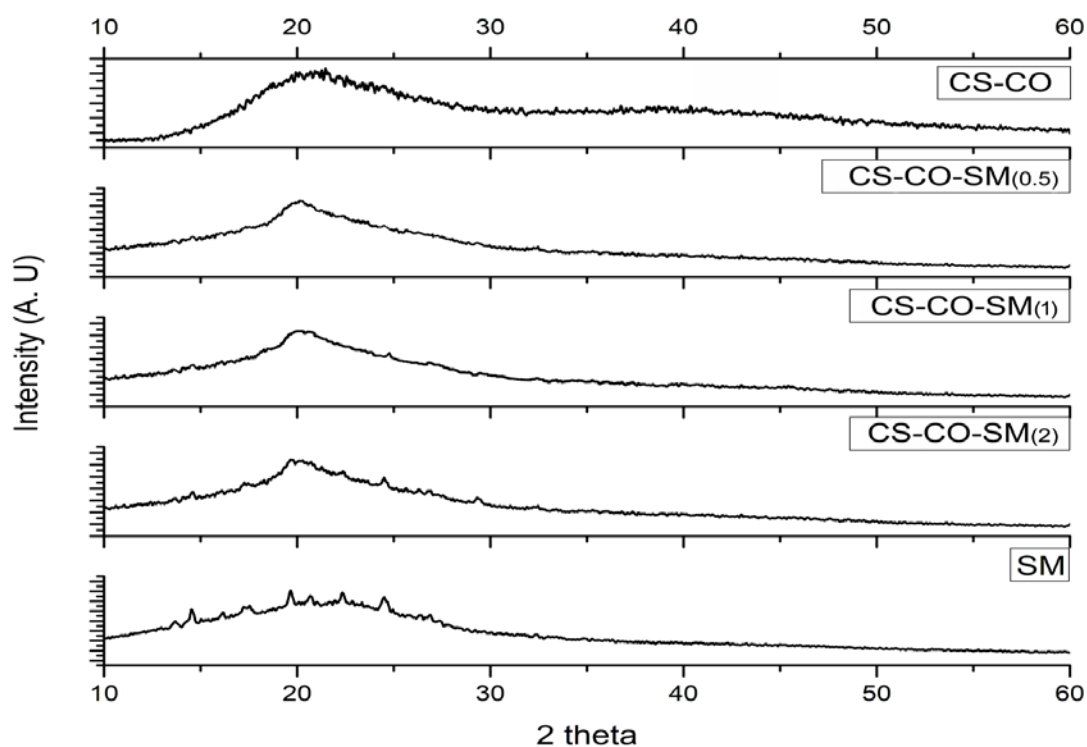


Figure 3.3 XRD pattern of the CS-CO-SM_(0.5), CS-CO-SM₍₁₎ and CS-CO-SM₍₂₎ scaffolds along with the CS-CO scaffolds and SM.

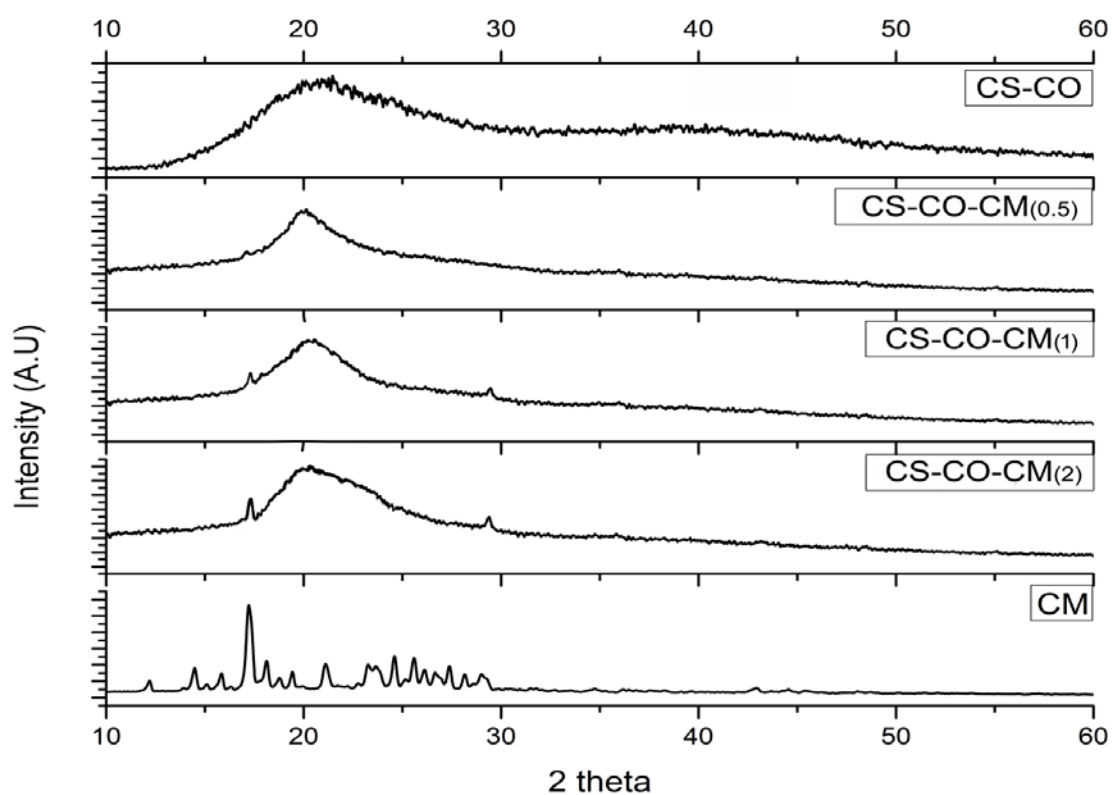


Figure 3.4 XRD patterns of the CS-CO-CM_(0.5), CS-CO-CM₍₁₎ and CS-CO-CM₍₂₎ scaffolds along with the CS-CO scaffolds and CM.

characteristic diffraction peaks of CS, CO and CM, while the intensity of CM at 17.22° increased with the increase in the concentration of CM, besides the broad peak for CS-CO indicating the presence of the antioxidants within the matrix (Figure 3.4).

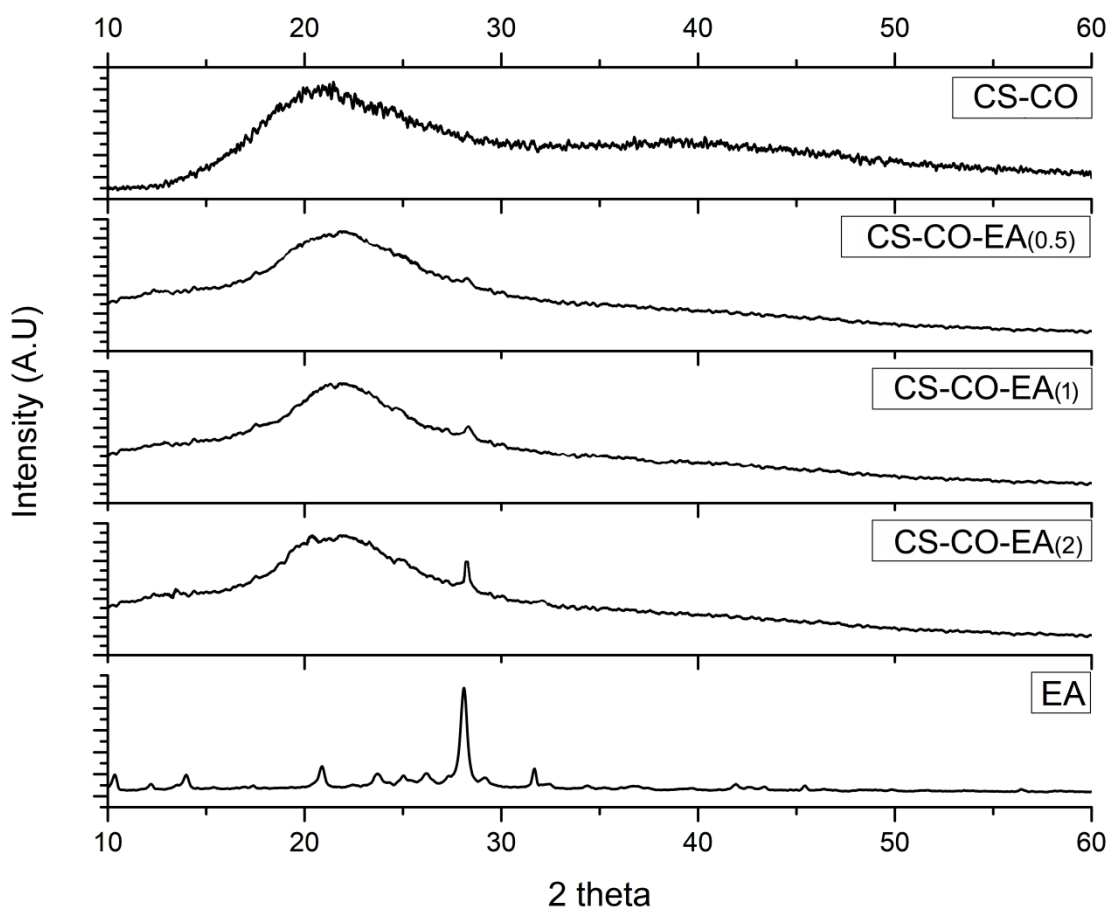


Figure 3.5 XRD pattern of the CS-CO-EA_(0.5), CS-CO-EA₍₁₎ and CS-CO-EA₍₂₎ scaffolds along with the CS-CO scaffolds and EA.

The diffraction pattern of EA show peaks corresponding to 2θ values of 28.32° , 21.86° , 32.43° which are in agreement with the values reported in literature (Kim et al. 2009). The sharp diffraction peaks indicate the crystalline nature of the EA. The scaffolds with EA exhibited the diffraction peak of EA along with broadening peaks of CS and CO which are semi-amorphous in nature. The diffraction intensity of the EA phase was found to vary with the increase in the concentration of the EA in the scaffolds. The EA (0.5, 1 and 2%) incorporated scaffolds showed diffraction peaks corresponding to EA in addition to the broad peak at 2θ value of 20.08° indicating the presence of the antioxidant within the amorphous polymeric matrix (Figure 3.5).

ATR FT-IR for the CO, CS and CS-CO scaffolds are shown in Figure 3.6. CO exhibited peaks associated with its functional groups at frequencies of 3350 cm^{-1} ($-\text{OH}$ stretching), 3298 cm^{-1} (amide A), 3069 cm^{-1} (amide B), 2897 cm^{-1} (aliphatic side chains), 1636 cm^{-1} (amide I $\text{C}=\text{O}$ stretching), 1530 cm^{-1} (amide II N-H bending and C-N stretching), and 1243 cm^{-1} and 1320 cm^{-1} (amide III C-N stretching and N-H bending) are in agreement

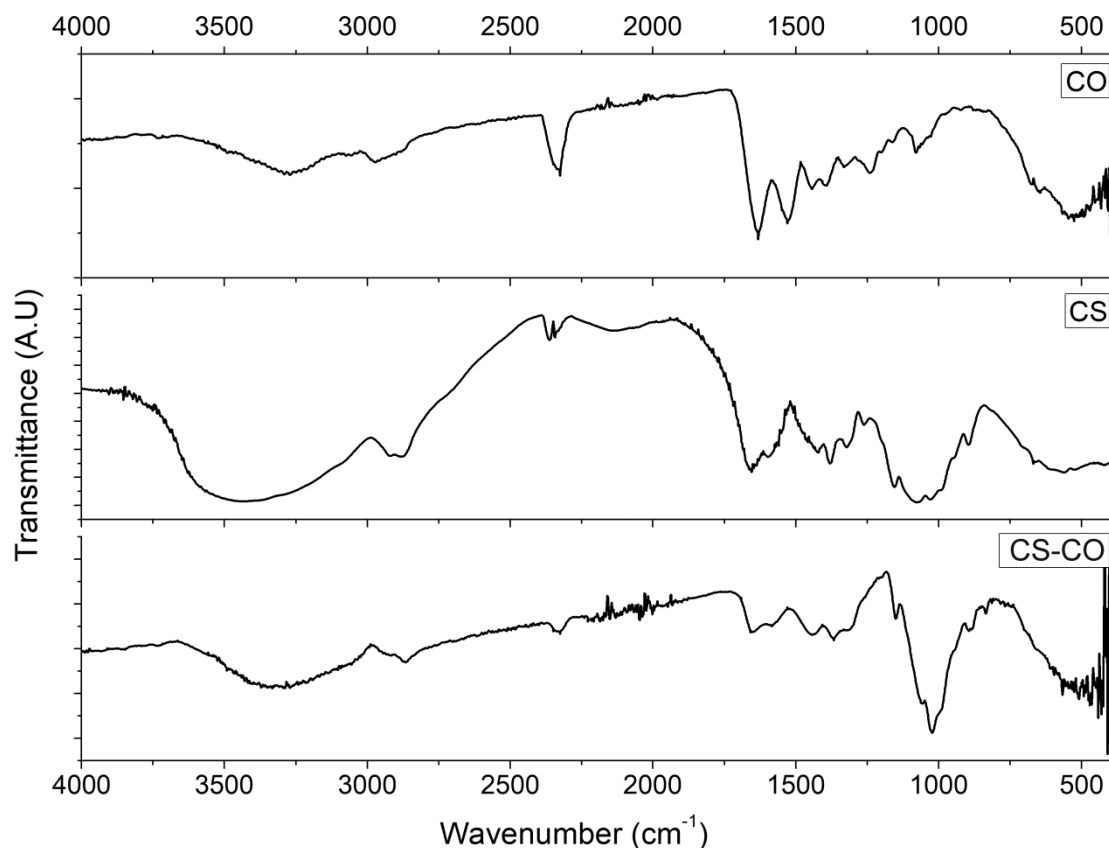


Figure 3.6 FTIR spectra of CS-CO scaffolds along with CO, and CS polymers.

with the literature (Zhang et al. 2004). The IR spectrum of CS exhibited a broad band at 3430 cm^{-1} ($-\text{OH}$ stretching), along with peaks of amine group at 2931 cm^{-1} ; amide bond at 1657 cm^{-1} ; N-H stretching of amide and ether bonds near 1447 cm^{-1} ; and secondary hydroxyl group (characteristic peak of $-\text{C-H}$ in cyclic alcohol, C-O stretch) at 1085 cm^{-1} . In the CS-CO scaffolds, most of the characteristic peaks of CO and CS were observed. The exceptions were a shift in the amide I characteristic absorption band from 1636 cm^{-1} to 1660 cm^{-1} , presence of only one peak representing amide III at 1320 cm^{-1} , absence of amide II peak at 1530 cm^{-1} and a minor shift in the carbonyl groups peaks at 1085 cm^{-1} to 1035 cm^{-1} . Shifts in peaks corresponding to amino and carbonyl groups accompanied with changes in peak intensity have been attributed to hydrogen bond formation between CO and CS. The $-\text{OH}$ and $-\text{NH}_2$ groups in CO and CS can form hydrogen bonds within

themselves. In addition, the $-C=O$ groups and $-NH_2$ groups in collagen may also form hydrogen bonds with $-OH$ and $-NH_2$ groups in chitosan (Sionkowska et al. 2004).

The FT-IR spectra acquired for SM (0.5, 1, and 2%) and the CS-CO scaffold are shown in Figure 3.7. The SM scan showed characteristic peaks at 3457 cm^{-1} (OH stretching vibration), 2946 cm^{-1} (C-H stretching), 1630.40 cm^{-1} (C-O stretching), $1508\text{--}1468\text{ cm}^{-1}$

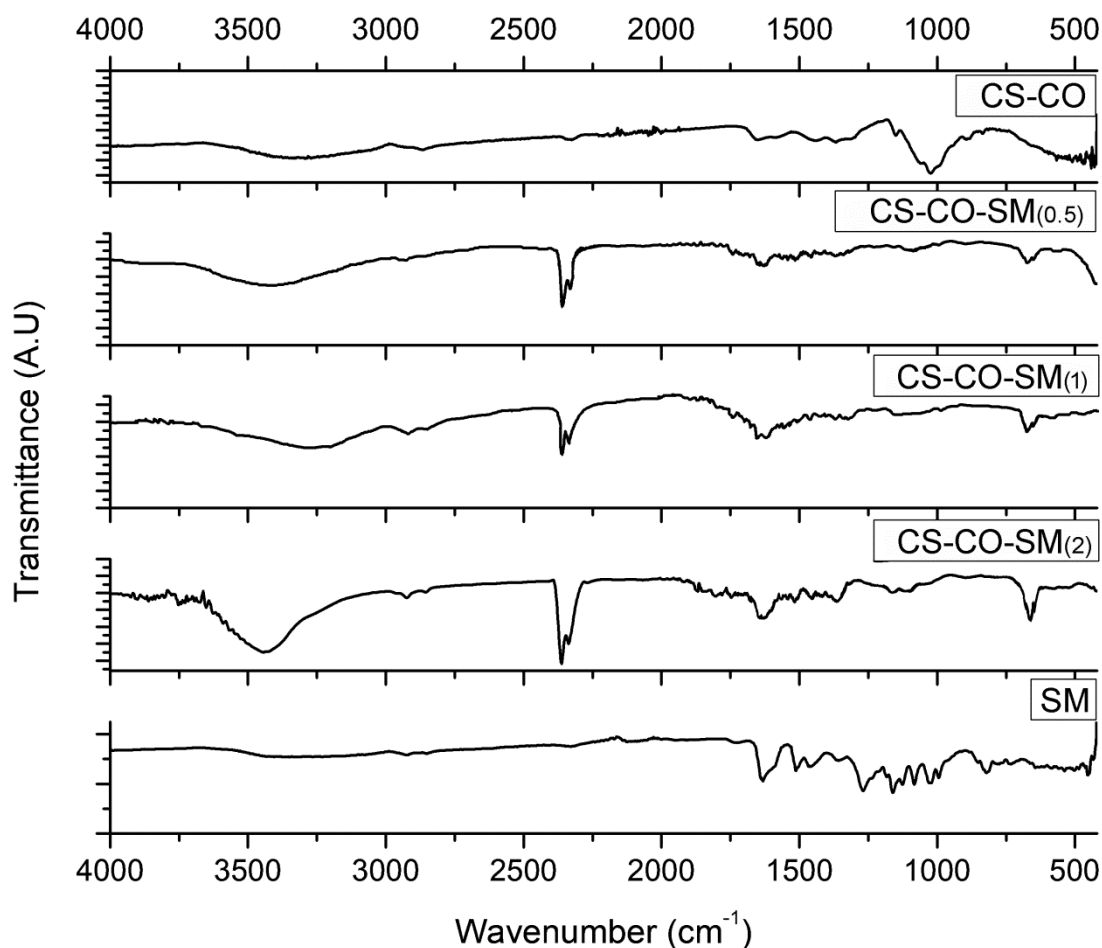


Figure 3.7 FT-IR spectra of the CS-CO-SM_(0.5), CS-CO-SM₍₁₎ and CS-CO-SM₍₂₎ scaffolds along with the CS-CO scaffolds and SM.

(skeleton vibration of aromatic $C=C$ ring stretching), and 1269 cm^{-1} (C-O-C stretching). The scaffolds incorporated with SM exhibited a stretching vibration at 1636 cm^{-1} representing the amide C-O and a peak at 1340 cm^{-1} representing the amide III nature of the bond. The peaks associated to SM were observed in all the scaffolds incorporated with SM (0.5, 1 and 2%). The $C=O$ and $C=C$ bands which are dominant in SM shifted to lower energy and were accompanied with a reduction in peak intensity. Similar shift in the IR frequencies have been reported for SM loaded chitosan based nanoparticles synthesized by ionotropic pre-gelation (Pooja et al. 2014).

FTIR spectrum of CM (0.5, 1 and 2%) incorporated scaffolds along with the CS-CO and CM are shown in Figure 3.8. The IR spectra of CM exhibited characteristic stretching bands at 3504 cm^{-1} (-O-H), 2997 cm^{-1} (-C-H), 1601 cm^{-1} (C=C symmetric aromatic ring), 1507 cm^{-1} (-C=O), 1273 cm^{-1} (enol C-O), and 960 cm^{-1} (benzoate trans-C-H vibration). The CM incorporated scaffolds showed IR absorption at 1247 cm^{-1} and 1031 cm^{-1} which

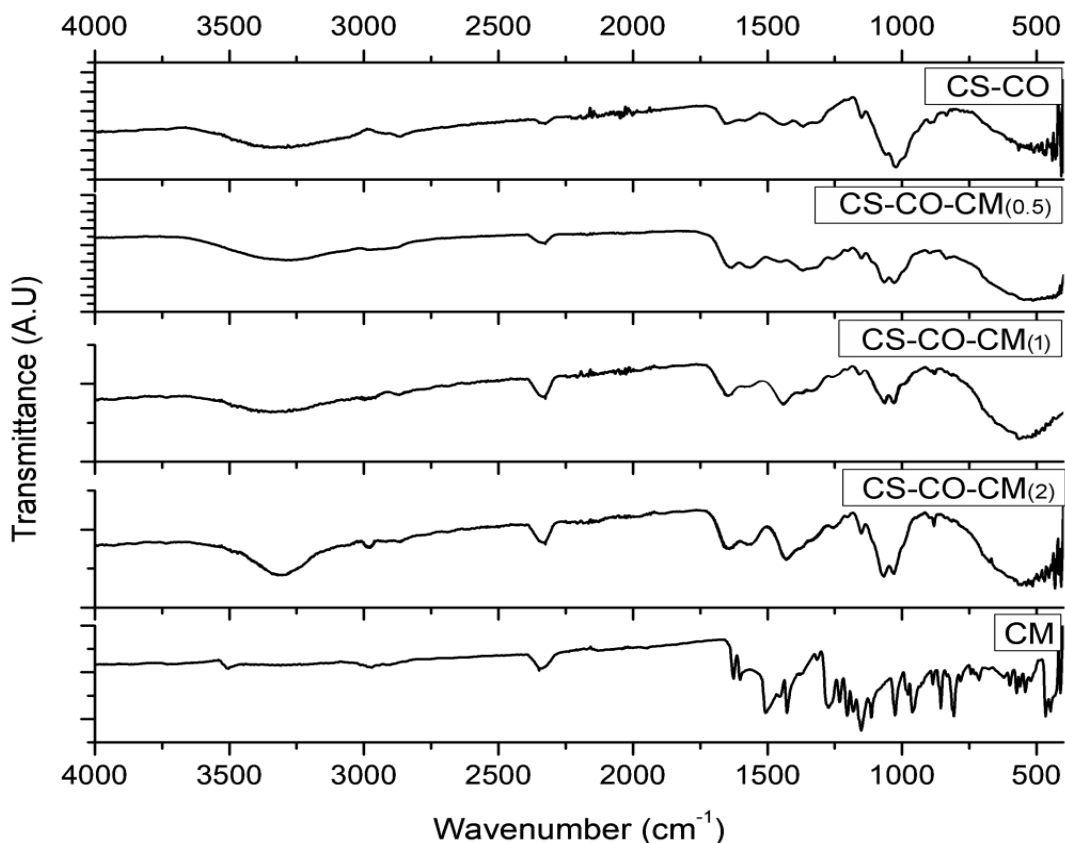


Figure 3.8 FT-IR spectra of the CS-CO-CM_(0.5), CS-CO-CM₍₁₎ and CS-CO-CM₍₂₎ scaffolds along with the CS-CO scaffolds and CM.

corresponds to the C-O-C along with 1447 cm^{-1} (N-H stretching) as observed in the CS-CO scaffold. The C=O and C=C bands which are dominant in CM were shifted to lower energy and were accompanied with a reduction in peak intensity. Similar shift in the IR frequencies have been reported for CM loaded alginate based CS nanoparticles synthesized by ionotropic pre-gelation (Das, Kasoju, and Bora 2010).

The IR spectra of EA (0.5, 1, and 2%) incorporated scaffolds are shown in the Figure 3.9 along with the controls, CS-CO and EA. EA exhibited the characteristic bands at 3472 cm^{-1} (-OH stretching), 1720 cm^{-1} (C=O), and 1617 cm^{-1} (C-C stretching). All the EA incorporated scaffolds exhibit broad -OH stretching and the peaks corresponding to the EA fingerprinting region. A shift in C=O stretching from 1720 cm^{-1} to 1698 cm^{-1} was

observed indicating hydrogen bond formation between the antioxidant and the CO and CS. A similar shift in C=O stretching was observed when ellagic acid and hyaluronic acid hydrogels were synthesized by layer-by-layer assembly method (Barnaby et al. 2013).

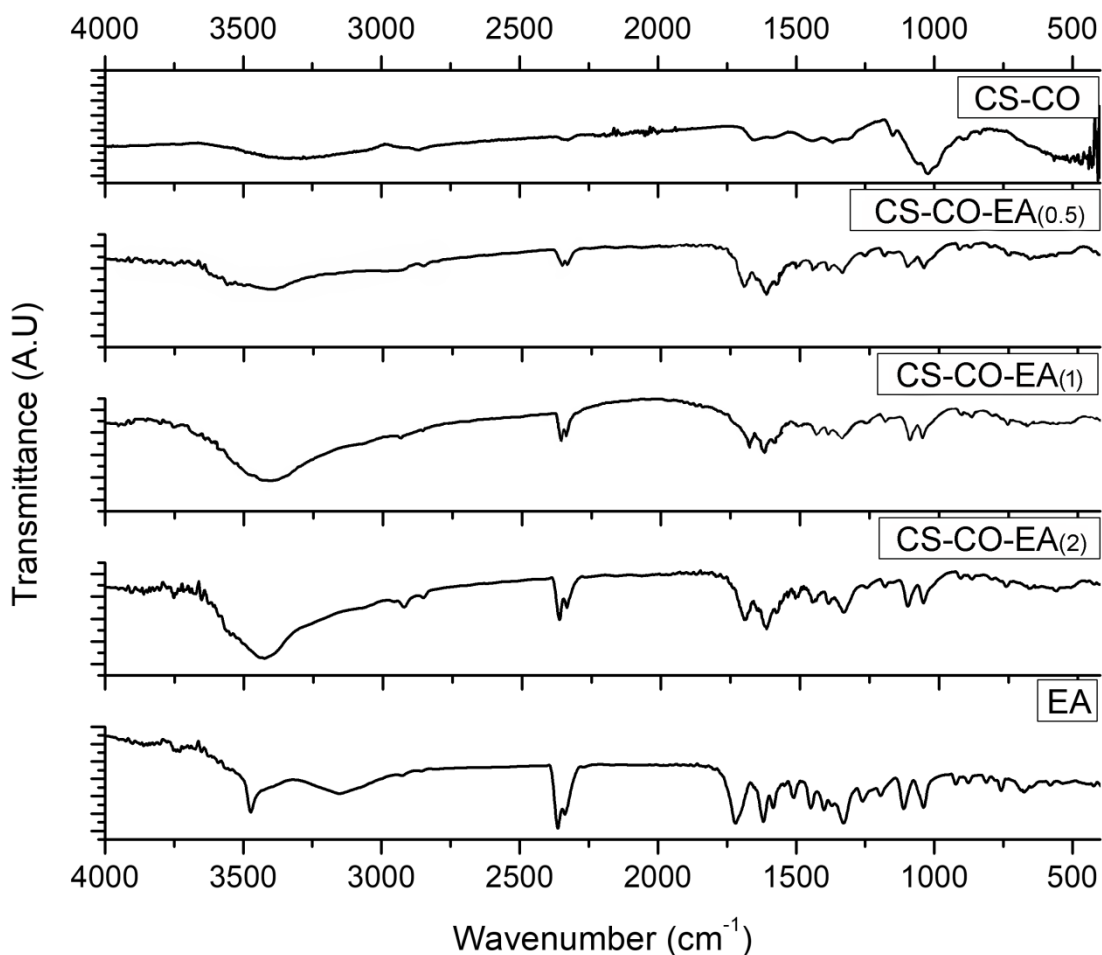


Figure 3.9 FT-IR spectra of the CS-CO-EA_(0.5), CS-CO-EA₍₁₎ and CS-CO-EA₍₂₎ scaffolds along with the CS-CO scaffolds and EA.

3.3.3 Release kinetics of the antioxidants from the antioxidant incorporated scaffolds

The release kinetics plays an important role in the drug delivery, where the optimization of the release concentration can be monitored based on the application. In this study, the release kinetics is studied to understand the rate of release of antioxidants from the polymeric matrix for every 24 h time interval up to 120 h. *In vitro* release kinetics of the SM, CM, and EA from the antioxidant incorporated scaffolds was analyzed by using UV visible spectroscopy [Figure 3.10 (a), (b), (c)]. Sustained release of antioxidants was observed for the scaffolds containing SM, CM and EA over a period of 120 h. In

scaffolds containing 0.5 % and 1.0 % antioxidants, maximal release was observed after 24 h, with a gradual decrease during the following 96h. However, with 2% antioxidant, a higher release of 28%, 30% and 25% for SM, CM, and EA, respectively, was noted during the first 24 h, which was followed by a sustained release. The initial high release could be attributed to the increased adsorption of the antioxidant on to the surface of the scaffold and its immediate release through desorption.

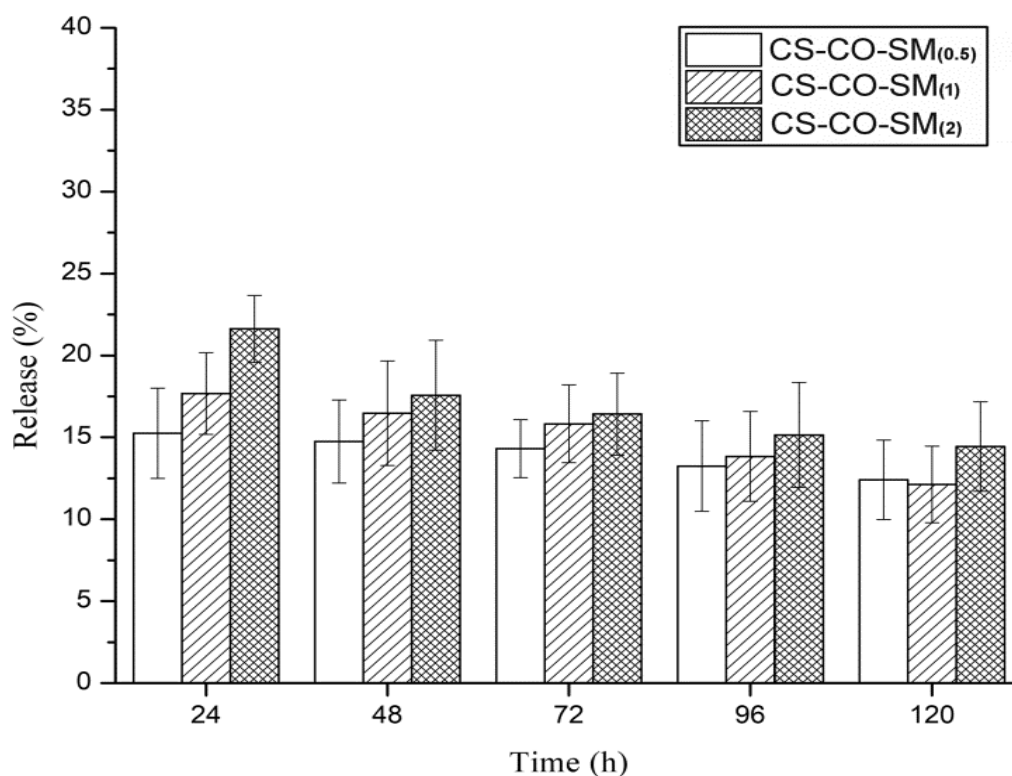


Figure 3.10 (a) *In vitro* release kinetics of SM (%) from the CS-CO-SM_(0.5), CS-CO-SM₍₁₎ and CS-CO-SM₍₂₎ at different time intervals.

The cumulative release at 120 h was higher for scaffolds containing 2% antioxidants (SM- 85%; CM-92%; EA-82%) as compared to scaffold with 0.5% (SM-68%; CM-75%; EA-65%) and 1.0% (SM-77%; CM-80%; EA-71%) antioxidants. Moreover, the scaffolds containing CM exhibited around 10% higher cumulative release as compared to scaffolds with EA and SM. Release kinetics of polymer based scaffolds depends on factors like diffusion co-efficient, rate of hydration, drug binding affinity etc. (Chou, Carson, and Woodrow 2015, Lin and Metters 2006). In the absence of external stimuli, the mechanisms governing controlled release of the bioactive molecule from polymers are basically dissolution and diffusion control (Pundir, Badola, and Sharma 2017). The barrier to diffusion decreases by swelling

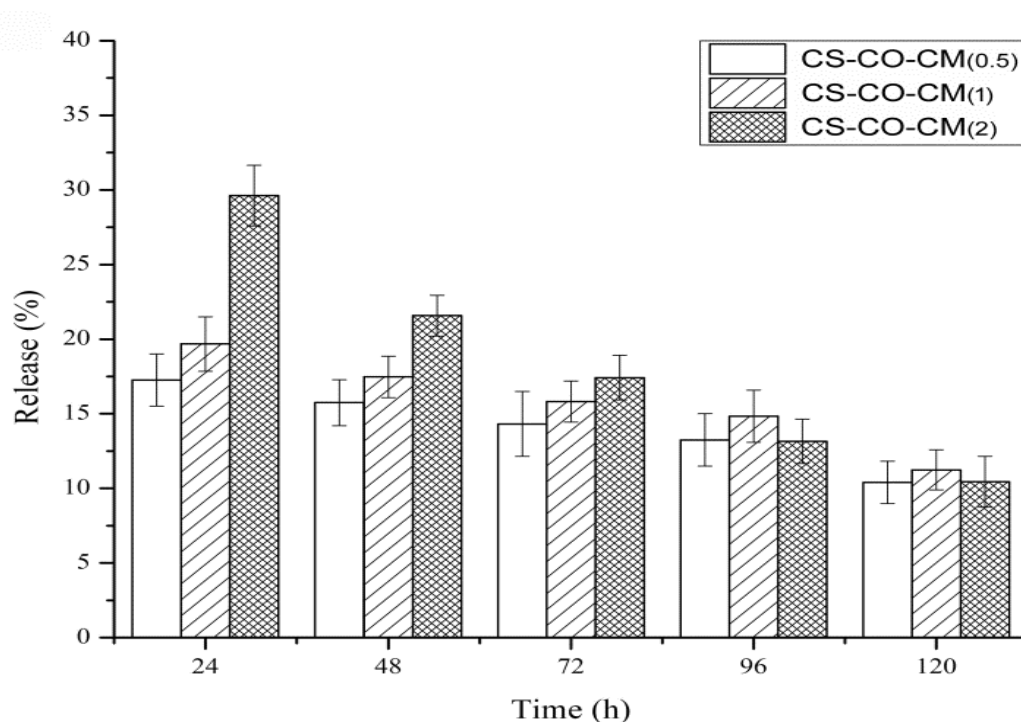


Figure 3.10 (b) *In vitro* release kinetics of CM (%) from the CS-CO-CM_(0.5), CS-CO-CM₍₁₎ and CS-CO-CM₍₂₎ at different time intervals.

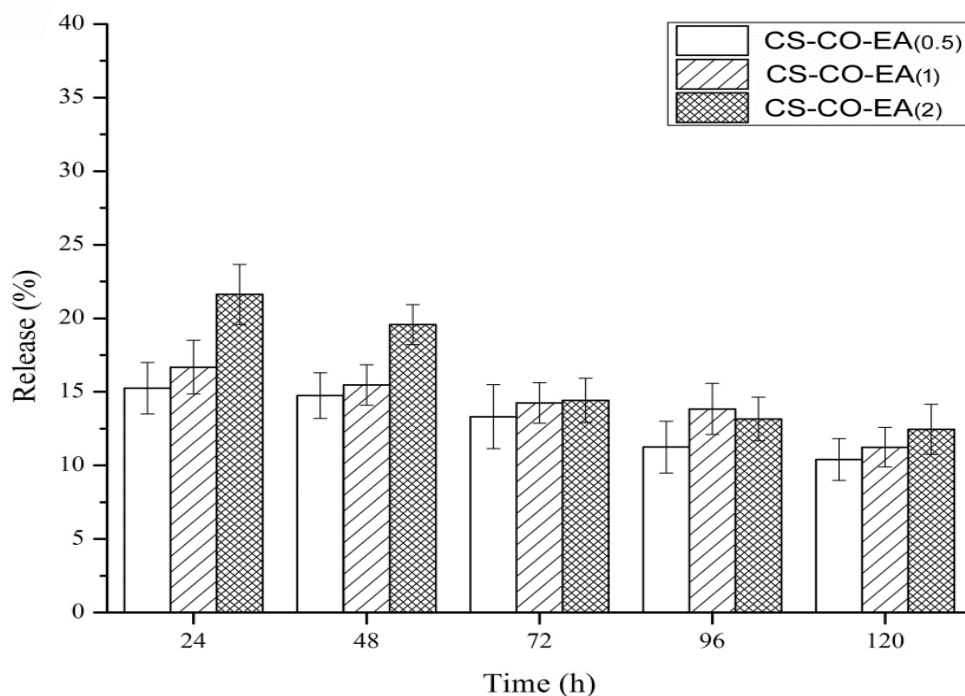


Figure 3.10 (c) *In vitro* release kinetics of EA (%) from the CS-CO-EA_(0.5), CS-CO-EA₍₁₎ and CS-CO-EA₍₂₎ at different time intervals.

of the hydrogel. Within an aqueous solution, polymer chains, such as those in a crosslinked hydrogel form the diffusion barrier that partially slows down diffusion of the biomolecules (Kishen et al. 2016). The adsorption of the biomolecule on to the polymeric matrix results in their early release, whereas, molecules entrapped within the polymeric matrix are governed by diffusion characteristics and contribute towards sustained release.

3.3.4 *In vitro* biocompatibility of the scaffolds

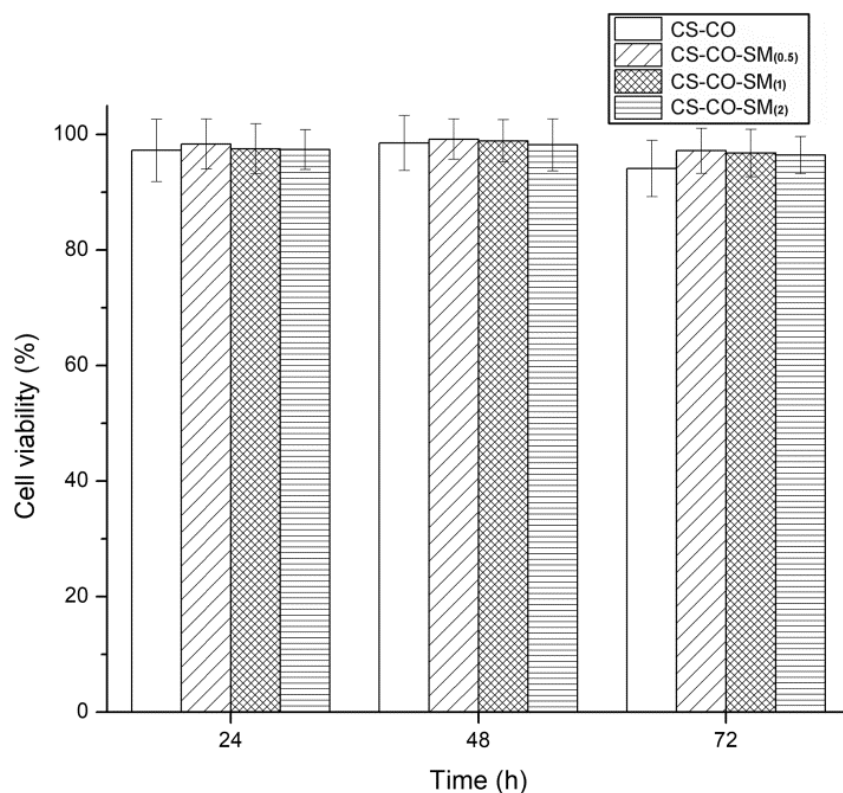


Figure 3.11 *In vitro* cytotoxicity studies of the CS-CO, CS-CO-SM_(0.5), CS-CO-SM₍₁₎ and CS-CO-SM₍₂₎ scaffolds on COS-7 cells at different time intervals.

The cytotoxicity studies of the SM incorporated scaffolds were carried out on COS-7 (fibroblast like) cell line by MTT cell metabolism assay (Figure 3.11). The biocompatibility of the CS-CO-SM_(0.5), CS-CO-SM₍₁₎, and CS-CO-SM₍₂₎ scaffolds were analyzed for up to 72 h. The scaffolds with SM did not exhibit toxicity towards the COS-7 cells as compared to control. SM is widely used in drug delivery because of its biocompatibility. Studies on SM loaded CS nanoparticles have shown to be hepatoprotective in Swiss Albino mice (Gupta, Singh, and Girotra 2014). The SM scaffolds were found to be biocompatible at all the three concentrations, indicating their suitability for use in tissue engineering applications.

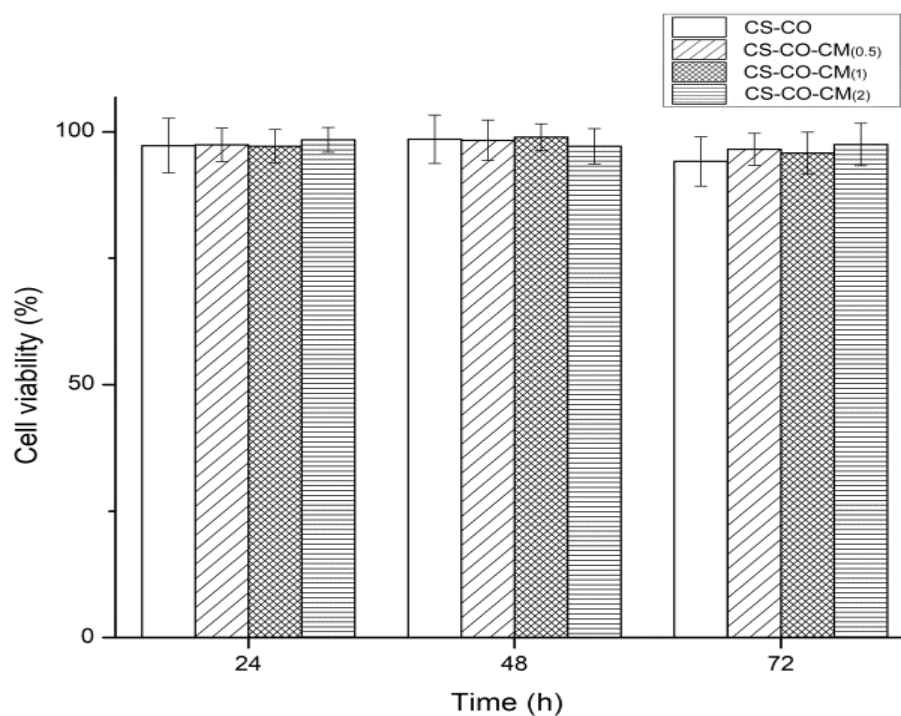


Figure 3.12 *In vitro* cytotoxicity studies of the CS-CO, CS-CO-CM_(0.5), CS-CO-CM₍₁₎ and CS-CO-CM₍₂₎ scaffolds on COS-7 cells at different time intervals.

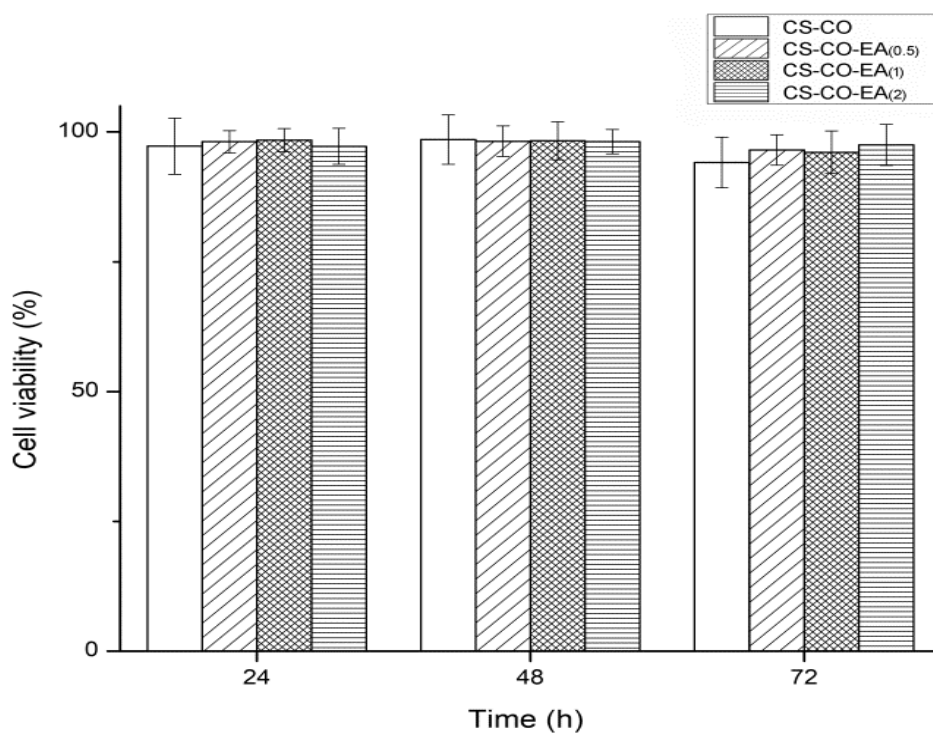


Figure 3.13 *In vitro* cytotoxicity studies of the CS-CO, CS-CO-EA_(0.5), CS-CO-EA₍₁₎ and CS-CO-EA₍₂₎ scaffolds on COS-7 cells at different time intervals.

The cells grown on CM incorporated scaffolds at all the three concentrations (0.5, 1, and 2 % w/w) exhibited cell viability similar to that of control which is indicative of the non-

toxic nature of the antioxidant incorporated scaffold (Figure 3.12). Thus, the synthesized scaffolds were found to be highly biocompatible and amenable for growth and proliferation of cells. Previous studies on CM incorporated polymeric scaffolds, have shown to be cyto-compatible and effectively promoted the cell infiltration and proliferation (Kasoju and Bora 2012, Karri et al. 2016).

EA incorporated scaffolds at all the three concentrations (0.5, 1, and 2 % w/w) were found to be biocompatible when tested on COS-7 cell line for 72 h. The scaffolds promoted the growth of fibroblast cells (Figure 3.13). Similar reports on histidine functionalized ellagic acid microstructures dispersed in hyaluronic acid (HA) were reported to be non-toxic in nature, supported the growth of NRK cells, and proposed as potential drug delivery vehicles (Barnaby et al. 2013).

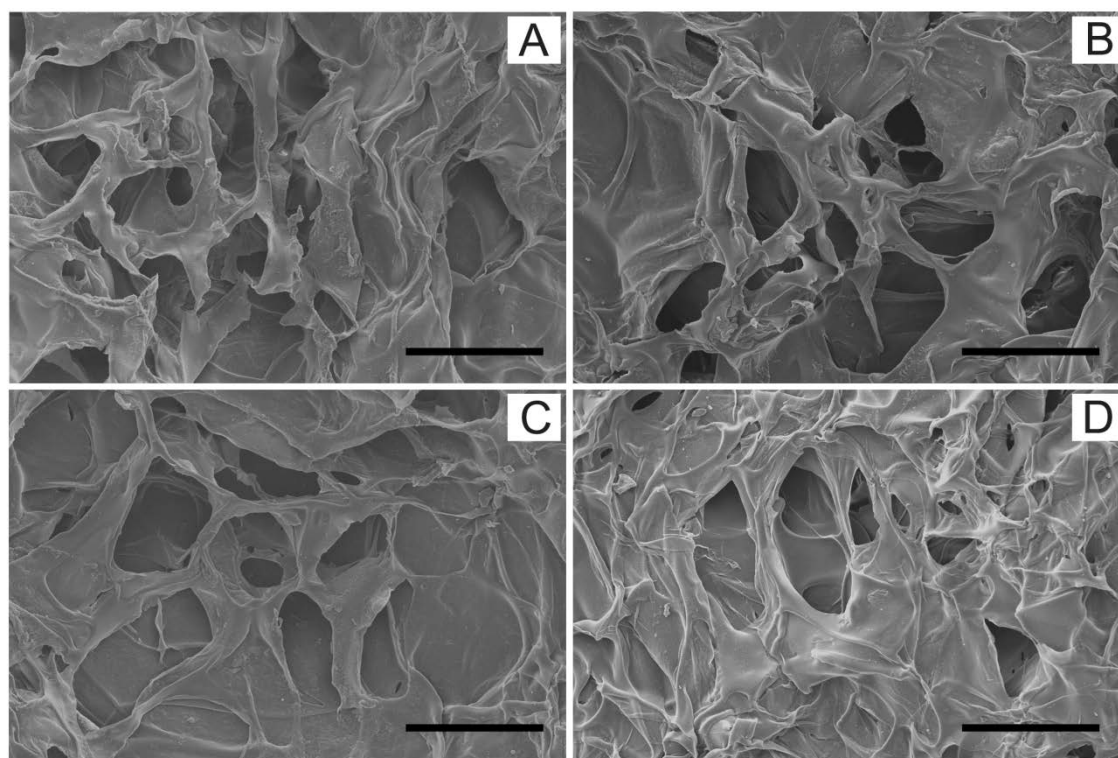


Figure 3.14 SEM images indicating cell adhesion, growth and proliferation of COS7 cells on CS-CO scaffolds (A) along with 2% w/w SM (B), CM (C), and EA (D) incorporated in CS-CO scaffolds (scale bar – 10 μ m).

Further, to better understand the interaction between the antioxidant scaffolds and COS-7 cells, the morphology of the cells on the scaffolds was examined by SEM. As shown in Figure 3.14, the COS-7 cells exhibited proliferation on the scaffolds, with no change in cell morphology as compared to the control. The glutaraldehyde cross-linked CS-CO scaffolds incorporated with antioxidants (SM, CM and EA) exhibited biocompatibility

and an ability to effectively promote cell infiltration and proliferation. These results are in concurrence with the cell viability assays described above. Thus, the synthesized scaffolds were found to be highly biocompatible and amenable for cell growth and proliferation. Similar results were reported for ellagic acid incorporated chitosan nanoparticles have been shown to promote the growth of fibroblast cells in diabetic rat models. Although several antioxidants are widely used in wound healing as drug molecules, their use in tissue engineering is seldom reported. The use of antioxidants in tissue engineering will enhance the cell proliferation by reducing the oxidative stress. The entrapment of the antioxidants into the 3D polymeric matrix will help in controlling the release kinetics thereby lasting the effect for a desired period of time. The use of natural biopolymers based on antioxidant therapies will be a promising alternative for the wounds which are delayed by the oxidative stress.

3.3.5 Application/ anti-oxidant activity of scaffolds

The aim of the antioxidants is to cleanse the ROS, and reduce the inflammation in chronic wounds. In this study, the antioxidants were incorporated in the scaffolds for evaluating their potential applications in treating inflammation arising due to compromised redox potential as is observed in chronic wounds. The functional aspect of the antioxidant based scaffolds was assessed by carrying out the UV irradiation studies. UV irradiation affects biomolecules resulting in the generation of ROS in the form of singlet oxygen ($^1\text{O}_2$), hydrogen peroxide (H_2O_2), superoxide anion (O_2^-), and hydroxyl radical ($\text{HO}\cdot$). Scaffolds with actively growing cells were exposed to UV for 10, 20, and 30 min, respectively and their viability was assessed 0h and 24h, post incubation.

Figure 3.15 (A), shows the effect of UV exposure time on the cell viability on SM incorporated scaffolds. The cells grown on these scaffolds exhibited a decrease in cell viability with increase in UV exposure time. The cell viability on CS-CO scaffolds (control) after 10, 20 and 30 min of UV irradiation is 62, 38, and 11%, respectively. However, the viability of cells on SM incorporated CS-CO scaffolds following respective UV exposure was found to be significantly higher than that of control. Moreover, the cell viability increased with an increase in concentration of SM. The scaffolds with 2% SM exhibited 88%, 79%, and 64% cell viability after 10, 20, and 30 min of UV exposure, respectively. While, 44 and 56% cell viability was observed on scaffolds with 0.5 and 1% SM, respectively, when exposed to 30 min of UV radiation.

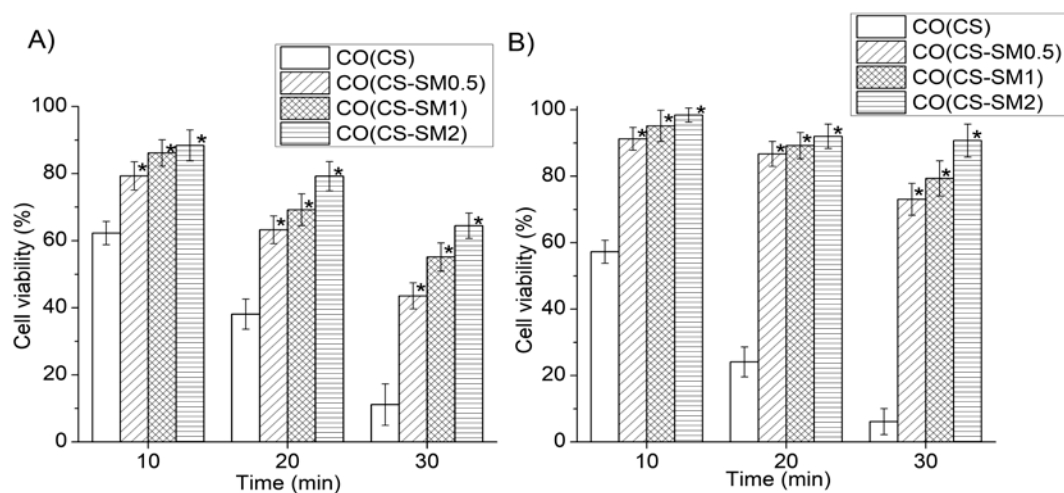


Figure 3.15 Cytotoxicity of COS-7 cells seeded on SM (0.5, 1, 2 % w/w) scaffolds and exposed to UV light for 10, 20 and 30 min. Cell viability was recorded after incubating for 0 h (A) and 24 h (B) post UV exposure. $p < 0.05$ of SM (0.5, 1 and 2 %) scaffolds compared with the CO(CS) scaffold.

In the absence of scavenging systems, the free radicals have the capacity to interact with biomolecules and further radicalize them thereby exaggerating their effects in tissue damage. In order to understand the effect of oxidative stress, the scaffolds with cells were incubated in growth medium for 24 h after respective UV irradiations and analyzed for their cell viability [Figure 3.15 (B)]. The cell viability on CS-CO scaffolds irradiated for 10, 20, and 30 min was 57, 24, and 7 %, respectively post 24 h incubation, while the CS-CO scaffolds without incubation has shown higher cell viability. This indicated the reactivity of the free radicals and their damage if not controlled. Contrarily the scaffolds with SM (0.5, 1 and 2% w/w) have shown an increase in the cell viability after 24 h incubation at all the time points. The cell viability of the CS-CO-SM₍₂₎ scaffolds incubated for 24 h was 99%, 92%, and 90% after 10, 20 and 30 min irradiation, respectively. Similar pattern of increase in the cell viability was observed in the 0.5 and 1 % SM scaffolds after 24 h post irradiation. The significantly higher cell viability on the SM incorporated scaffolds, in contrast to the control demonstrates the antioxidant potential of SM which helped the cells to overcome the oxidative stress. Studies on topical application of SM have shown its ability to inhibit UV induced oxidative stress in *in vitro* and *in vivo* models (Katiyar, Meleth, and Sharma 2008, Svobodová, Walterová, and Psotová 2006). SM inhibits lipid peroxidation and also prevents depletion of glutathione thereby stabilizing the membrane permeability (Jung et al. 2013).

The cell viability of the CM incorporated scaffolds after 10, 20, and 30 min of UV exposure have shown in Figure 3.16 (A). The scaffolds incorporated with CM exhibited concentration dependent increase in the cell viability when compared to the control scaffold at both the incubation times (0 h and 24 h). The CS-CO-CM₍₂₎ scaffolds have shown 90, 70 and 51 % cell viability after exposed to 10, 20, and 30 min UV, respectively. The CS-CO-CM_(0.5) and CS-CO-CM₍₁₎ scaffolds have exhibited 20 and 35%

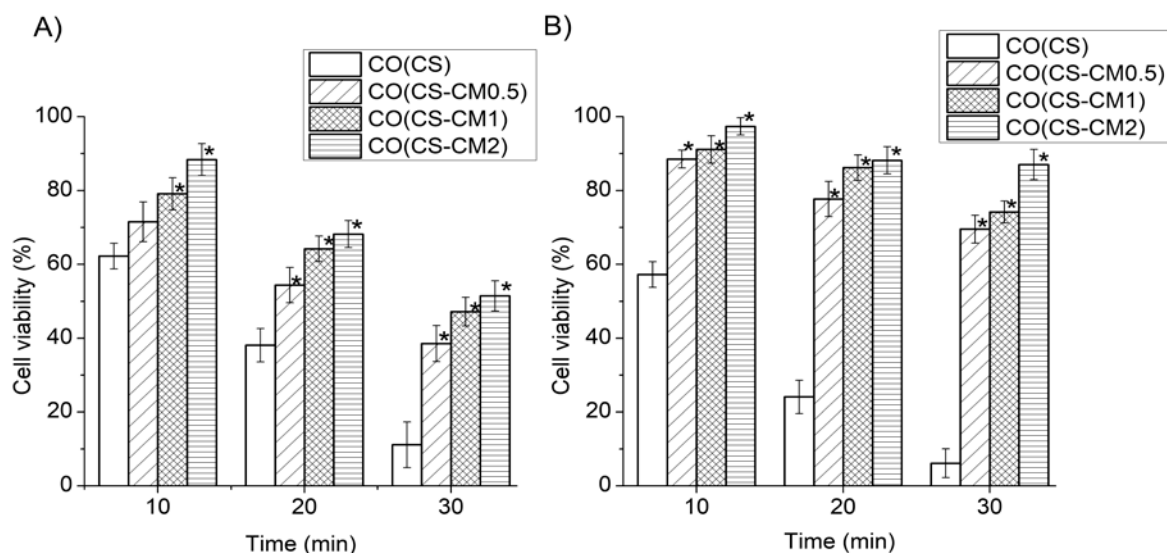


Figure 3.16 Cytocompatibility of COS-7 cells seeded on CM (0.5, 1, 2 % w/w) scaffolds and exposed to UV light for 10, 20 and 30 min. Cell viability was recorded after incubating for 0h (A) and 24h (B) post UV exposure. $p < 0.05$ of SM (0.5, 1 and 2 %) scaffolds compared with the CO(CS) scaffold.

cell viability after 30 min UV irradiation. The cell viability of the CS-CO-CM₍₂₎ scaffolds incubated for 24 h after 10, 20 and 30 min UV irradiation have shown 95, 89, and 85% cell viability, respectively [Figure 3.16 (B)]. The CM incorporated scaffolds incubated for 24 h have shown an increase in the cell viability when compared to the 0 h post UV irradiations. As the concentration of the CM increases, the increase in the cell viability was noted in all the UV irradiation times. Whereas, CS-CO scaffolds incubated for 24 h after UV irradiations have shown decrease in the cell viability when compared to the 0 h. These results indicate that the antioxidant plays a significant role in countering the stress due to ROS, while the scaffolds with CM have shown to increase in the cell viability upon incubation.

The residual cell viability of the scaffolds incorporated with EA when irradiated with UV for 10, 20 and 30 min have shown in Figure 3.17 (A). The CS-CO-EA₍₂₎ scaffolds have

shown the cell survival rate of 77, 69, and 46% after 10, 20 and 30 min of UV exposure, respectively. The cell viability on the synthesized scaffolds increased with the concentration of EA at all the UV irradiation intervals. After 24 h of incubation the control scaffolds have shown a further decrease in the cell viability at all the time intervals of UV exposure [Figure 3.17 (B)]. However, in case of scaffolds with EA, an

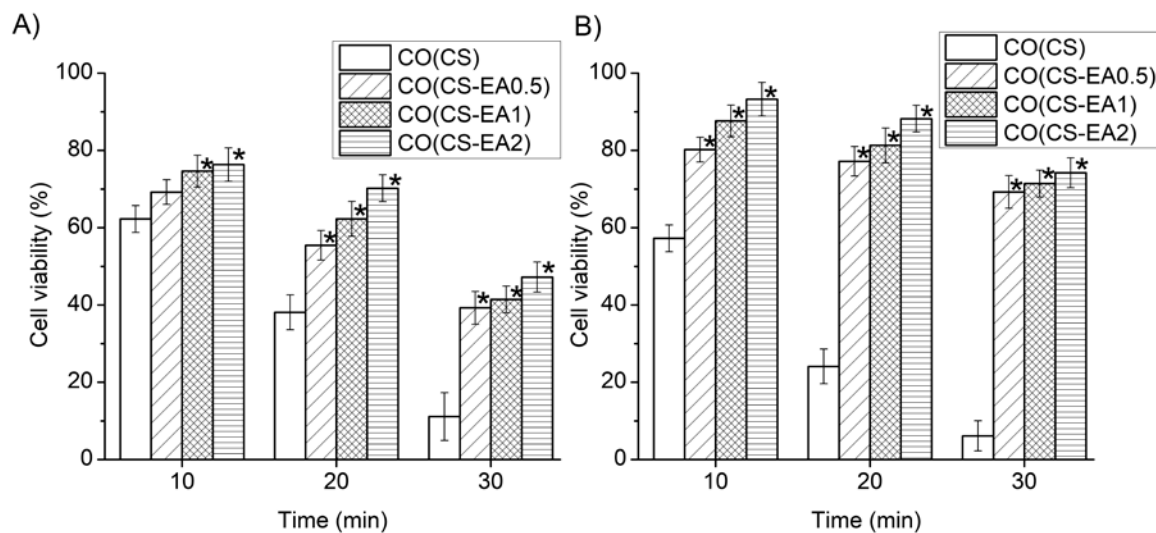


Figure 3.17 Cytocompatibility of COS-7 cells seeded on EA (0.5, 1, 2 % w/w) scaffolds and exposed to UV light for 10, 20 and 30 min. Cell viability was recorded after incubating for 0h (A) and 24h (B) post UV exposure. $p < 0.05$ of SM (0.5, 1 and 2 %) scaffolds compared with the CO(CS) scaffold.

increase in cell viability after 24 h of incubation subsequent to UV exposure was noted. The cell viability of the scaffolds with CM, EA and SM is much higher than the control. The scaffolds containing antioxidant (SM, CM, EA) have significantly reduced the oxidative stress, while in the control scaffold the cytotoxicity is very aggressive which increased with time. The scaffolds with antioxidants probably break the chain reaction of the free radicals thereby restricting and reducing the cell death. The scaffolds with SM exhibited a higher cell revival as compared to the CM and EA scaffolds at all the concentrations and UV exposure times. This may be attributed to the degree of hydroxylation as the SM has more hydroxyl groups when compared to CM and EA which might have helped in decreasing the metabolic activation of ROS, and, secondly, by acting as a chain-breaking antioxidant. In chronic cutaneous wounds 60-70% decrease in anti-oxidant (glutathione, ascorbic acid, and vitamin E) levels has been observed and the strategy of incorporating antioxidant regenerating system to continuously quench the free radicals is being explored (Ojha et al. 2008, Wang et al. 2013). Several antioxidants like

vitamin C, vitamin A, tocopherol, etc., are being tested with an aim to cleanse the free radicals and increase collagen and hyaluronate synthesis (Ha et al. 2010, Kant et al. 2014). Scaffolds with antioxidant can reduce the free radical inflammation and help in maintaining homeostasis of chronic wounds.

3.4 Conclusion

Oxidative stress has adverse effects on the wound healing due to the harmful effects of ROS on the cells and tissues. Antioxidants play an essential role in the reduction, deactivation, and removal of ROS as well as promoting wound-healing process. Antioxidants are widely used in wound healing as drug molecules, but their use in tissue engineering is not widely reported. Although skin possesses an extensive and effective network of antioxidant systems, many of the free radicals can escape this surveillance and induce substantial damage to cutaneous constituents, especially when skin defense mechanisms are compromised. In this study, SM, CM and EA was incorporated into CO-CS matrix with an aim to facilitate their sustained release thereby providing a micro-environment with a potential to overcome oxidative stress and support wound healing. The incorporation of antioxidants (SM; CM; EA) in the CS-CO matrix promotes the adhesion and proliferation of fibroblast cells during oxidative damage. The SM incorporated scaffolds have shown higher cell survival when compared to CM and EA incorporated scaffolds. The revival rate of the cells, post UV exposure was significantly higher in antioxidant incorporated scaffolds exhibiting their potential as promising candidates for tissue engineering applications involving management of oxidative stress.

Chapter 4: Fabrication of Bilayer Scaffolds and Their *In Vivo* Applications

4.1 Introduction

Wounds which do not progress through the healing process in a timely manner are becoming a major challenge to healthcare systems worldwide. Some common features shared by these wounds include prolonged or excessive inflammation, persistent infections, formation of drug-resistant microbial biofilms, and the inability of dermal and/or epidermal cells to respond to repair stimuli (James et al. 2008, Sen et al. 2009). The major factor contributing to delay in wound healing is microbial infections and oxidative stress (Guo and DiPietro 2010). The transition of bacteria from contamination through colonization and, finally, to infection occurs when bacterial proliferation overcomes the host's immune response and host injury occurs. Bacterial infections release metallo-proteases and other mediators of inflammation, thereby damaging the local tissue (Edwards and Harding 2004). The increased levels of inflammation result in elevated levels of ROS, which interact with and damage biomolecules and cells, leading to delayed wound healing. Antioxidants which counter the ROS and maintain the redox balance are depleted in wounds with oxidative stress delaying the healing process. A balance between free radicals and their scavenging systems plays an important role in wound healing. Supplementation of these wound sites with antioxidants has shown to induce the expression of cytoprotective proteins such as SOD, catalase, GPx, HO-1, and GST (Carocho and Ferreira 2013, Ha et al. 2010). The simultaneous incorporation of antibacterial and antioxidant properties may confer an enhanced wound healing property to the biomaterials used for wound care.

Several strategies have been explored to fasten wound healing to facilitate the wound closure and maintain homeostasis. The significance of extracellular matrix (ECM) in wound healing has prompted the utilization of biopolymers to stimulate or replace the damaged or disruptive ECM. Native ECM is composed of various components such as CO, fibrin, GAGs, and other adhesive proteins. The fibrillar molecules of ECM provides the 3D framework while non-fibrillar molecules such as proteoglycans and GAGs, will function to create a charged, dynamic and dynamically active space. The architecture of ECM differs drastically among anatomical locations to facilitate the niche cell adhesion, proliferation and functions by providing mechanical support (Yue 2014). In tissue like skin, the heterogeneity of the ECM distribution varies intra-dermally to accommodate the

niche cells and promote several cell autonomous and non-autonomous processes (Watt and Fujiwara 2011). Recent studies on artificial skin substitutes are attempting to mimic the tissue microenvironment with an aim to reduce the secondary complications arising during the healing process (Edgar et al. 2016). The use of multi-layer matrices incorporating different therapeutic molecules for creating the micro-environment suitable for healing while also addressing the factors delaying it is one such approach (Chaudhari et al. 2016). In this work, we fabricated a bilayer scaffold for skin tissue engineering applications with layer upon layer arrangement of CS-Ag and CS-CO with antioxidant (SM; CM; EA) matrix. In layer 1, conjugation of Ag with CS was aimed at achieving good antibacterial activity, whereas, in layer 2, the incorporation of antioxidants (SM; CM; EA) was to support the scavenging of free radicals during the growth of the tissue. The functional diversity of the bioactive molecules and their release will increase the application of the bilayer scaffold. The *in vivo* topical application of the bilayer scaffolds was analyzed in Wistar rat model.

4.2 Materials and methods

4.2.1 Materials

All the chemicals (cell culture grade) like DMEM, MTT, Hematoxylin, eosin and PBS were purchased from HiMedia, India. Goat Anti-Rabbit Anti-Malondialdehyde antibody (ab6463) and Goat Anti-Rabbit IgG H&L (HRP) were purchased from Abcam, USA and Santa Cruz Biotechnology, USA, respectively.

4.2.2 Synthesis and fabrication of bi-layer scaffolds

4.2.2.1 Synthesis of layer 1 (CS-Ag)

The CS-Ag gels were synthesized by using the protocol described in chapter 2 section 2.2.2, but were frozen at -20° C without lyophilization. The 3% Ag incorporated CS gels were used for the fabrication of the bilayer scaffolds.

4.2.2.2 Synthesis of layer 2 (CS-CO-SM)

The antioxidant (SM; CM; EA) incorporated CS-CO solution were synthesized as per the method given in chapter 3 section 3.2.2. The antioxidant concentration of 2%, which was optimal with respect to the release profile and other functional properties, was selected for fabrication of bilayer scaffolds.

4.2.2.3 Fabrication of bilayer scaffolds:

CS-CO based antioxidant (SM; CM; EA) solution was added to the frozen CS-Ag gels and allowed to freeze at -80 °C for 4 h. The frozen samples were thawed at 8 °C by adding 0.1 M NaOH solution to precipitate and obtain a gel. The gels were repeatedly washed with distilled water until the pH of the wash water remained neutral. These gels were frozen at -80 °C for 4 h and lyophilized using a freeze-drier (CHRIST-MARTIN) to obtain bilayer scaffolds. The synthesized bilayer scaffolds were designated as BS-Ag-SM, BS-Ag-CM and BS-Ag-EA, for scaffolds containing SM, CM, and EA, respectively. Control scaffolds (BS-C) were synthesized using the same protocol but without the addition of antibacterial (Ag) and antioxidant (SM; CM; EA) compounds. All the scaffolds were sterilized by autoclaving at 121 °C, 15 lbs for 15 min, before using them for biological studies.

4.2.3 Swelling studies

The swelling characteristics of bilayer scaffolds were determined by immersing the scaffolds with known weight (I_w) in PBS (pH 7.4) for 24 h at 37 °C separately. The swollen scaffolds were removed at specific time intervals (1, 2, 4, 8, 12, and 24 h) and weighed (F_w) after removal of excess surface water using Whatman filter paper. The degree of swelling of the bilayer scaffolds were calculated by using the following equation.

$$\text{Degree of Swelling (\%)} = (F_w - I_w)/I_w \times 100;$$

Where, F_w is the swollen weight of scaffold, and I_w is the dry weight of scaffold sample.

4.2.4 Assessment of functional performance of the bilayer scaffolds

4.2.4.1 Animal grouping and creation of wound

All the *in vivo* experiments were performed with the approval of the Institutional Animal Ethics Committee of Agharkar Research Institute (ARI/IAEC/2017/08). Animal handling procedures were carried out as per guidelines defined by the Committee for Control and Supervision of Experiments on Animals, Ministry of Environment and Forests, Government of India. The animals were caged individually, provided with food and water, appropriate temperature (23 ± 1 °C), relative humidity 55 ± 5 % and were kept under 14-hour light/10-hour dark cycle.

Wistar rats were randomized into five groups (n=9 animals per group) viz. control wound (no scaffold), BS-C, BS-Ag-SM, BS-Ag-CM, and BS-Ag-EA. The animals were anesthetized with ketamine (80 mg/kg) and xylazine (10mg/kg) prior to the creation of wounds. The fur from dorsal neck region of each rat was trimmed by scissors then shaved using a razor, and disinfected with 70% ethanol. Using a circular stamp (6 mm in diameter), an impression was made in the dorsal thoracic region, 1 cm away from the vertebral column and 5 cm away from the ear, the excision wound was created by cutting out the full thickness of skin that had been marked by the stamp.

4.2.4.2 Estimation of the rate of wound healing (wound closure)

The synthesized scaffolds were placed in the excised skin (representing the wound). Progressive changes in wound healing were assessed by tracing the wound area on transparent tracing paper on days 0, 3, 7 and 10 post-wound surgery. Transparent sheet was laid over the wound and the wound limits were traced on it using a permanent marker. The tracing paper was placed on a sheet of graph paper and the number of squares within the wound area was counted on days 3, 7 and 10. The percentage of wound contraction was measured using the following formula:

$$WC (\%) = [(At_0 - At_{3/7/10}) / At_0] * 100;$$

where, WC is wound contraction, At_0 is wound area in mm at the time of injury, and $At_{3/7/10}$ is the wound area in mm on day 3, 7, and 10 post injury.

After day 10, the healed skin was excised under anesthesia and placed in 10% buffered formalin and used for histological and immunohistochemistry staining.

4.2.4.3 Histological examination

The histological studies of the post-operative tissue obtained at different time intervals (3, 7 and 10 days) were carried out for better understanding of the healing kinetics. The samples were embedded in paraffin, and sliced into 5- μ m sections. Hematoxylin and eosin (H&E) staining was performed, and the sections were observed under an optical microscope.

4.2.4.4 Immunohistochemical staining

Sections were de-paraffinised in xylene 2×10 min and treated with 100, 90 and 70 % (v/v) ethanol for 10 min each. Rehydration was performed by immersing the slides in 1X PBS for 10 min followed by blocking with 5 % bovine serum albumin for 30 min. Sample sections were incubated with 3 % hydrogen peroxide for 5 min to block endogenous peroxidase activity and washed with 1X PBS buffer for 5 min. Subsequently, the slides were treated with rabbit polyclonal anti-MDA primary antibody (1:1000) at 4 °C overnight. The slides were washed in 1X PBS for 10 min and incubated with goat anti-rabbit secondary antibody (1:1000) at 37 °C for 30 min. The slides were washed with 1X PBS, developed with 3,3'-diaminobenzidine tetrahydrochloride (DAB) solution, and counterstained with hematoxylin. Observation of brown color under an optical microscope (Olympus BX60, Olympus, PA, USA) indicates positive staining. The pixels of brown color were analyzed by using ImageJ software and the relative ratio of MDA in BS-C, CS-Ag and BS-Ag-SM samples was calculated with reference to the control group.

4.2.5 Statistical analysis

All the results are expressed as mean \pm standard error. Two-tailed Student's t tests were used to analyze any significant differences between the control and the individual experimental groups. P value of less than 0.05 was considered significant.

4.3 Results and discussion:

The components of skin ECM vary intra-dermally to facilitate native cell growth. The epidermal ECM is a basal lamina whereas the dermal ECM comprises of fibrillar collagen and associated proteins. Thus, skin tissue engineering methodologies need to consider the differences in the ECM while designing scaffolds for wound healing applications. The differences in the ECM components can be minimized by fabricating various ECM components in to bilayer scaffolds thereby providing an amenable environment for niche cells to proliferate and function (Chaudhari et al. 2016). As discussed in chapter 3, the scaffolds containing 2% antioxidants significantly reduced the oxidative stress generated due to UV irradiation at different time intervals as compared to the 0.5% and 1% scaffolds. Hence, the 2% antioxidant concentration was used to fabricate the bilayer scaffolds. The CS-CO based antioxidant matrix was aimed at providing a good platform for the proliferation of dermal fibroblasts, as native dermal ECM is majorly dominated by type 1 CO. The CS-Ag3 scaffolds with 3% Ag exhibited maximum bacterial inhibition

without being toxic to human keratinocytes. Hence, the bilayer scaffolds were fabricated by combining CS-Ag3, and CS-CO-R (R = SM₍₂₎/ CM₍₂₎/ EA₍₂₎); the Ag was incorporated for antibacterial activity and R to provide antioxidant property to reduce the oxidative stress near the wound site. The tendency of the scaffold to retain water is one of the important aspects of skin tissue engineering. The swelling property of scaffold allows the absorption of body fluids, transfer of cell nutrients and metabolites inside the scaffold. This in turn increases the efficacy of the scaffold to become biocompatible.

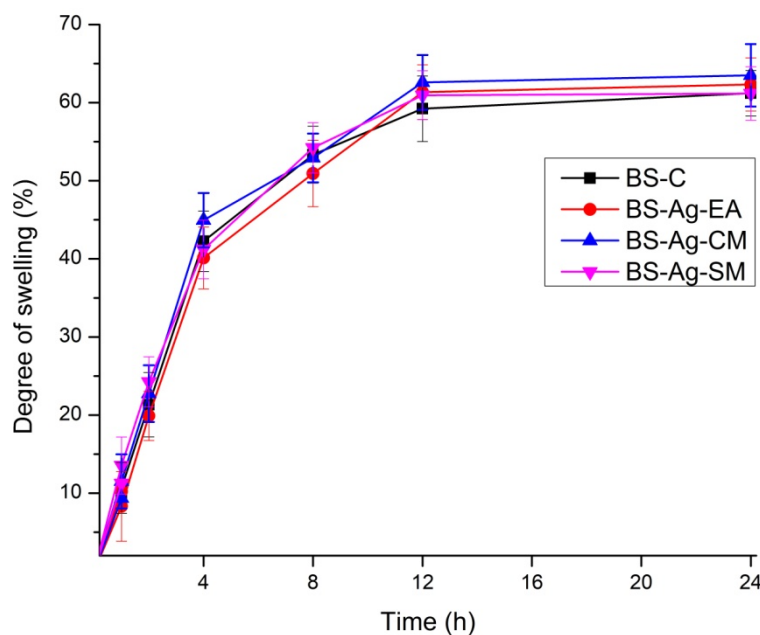


Figure 4.1 Swelling behavior of bilayer scaffolds incorporated with Ag/antioxidants (EA; CM; SM) along with BS-C in PBS at 37° C for 1, 2, 4, 8, 12 and 24 h (data are expressed as standard error of mean).

Swelling characteristics of various bilayer scaffolds were observed as shown in Figure 4.1. It was found that the degree of swelling of antibacterial/antioxidant incorporated bilayer scaffolds were similar to that of BS-C. This indicates that the incorporation of antibacterial and antioxidant compounds did not affect the swelling property of the chitosan–collagen scaffold. To further demonstrate the functional performance of the bilayered scaffolds, *in vivo* experiments on Wistar rats were carried out.

4.3.1 Estimation of the rate of wound healing (wound closure)

The effect on wound healing after topical application of scaffolds was evaluated by photographic images. On day 3 after injury, it was observed that the swelling around the

wound subsided and surface of the wound gradually began to form a pale yellow crust in the treated (BS-Ag-SM, BS-Ag-CM, and BS-Ag-EA) groups. On day 7, after injury, the edges of the wounds contracted in groups treated with BS-Ag-SM, BS-Ag-CM, and BS-Ag-EA. In the control rats, reddening of the wound was observed until 7th day indicating the inflammation near the wound site. In BS-C treated groups, the pale and hard crusts formation was observed on 7th day indicating wound contraction while in control (no scaffold) this phase was visible on 10th day. In the BS-Ag-SM treated group, the wound had almost completely healed with no crust, while a thin crust with the contraction of wound was observed in the BS-Ag-CM, and BS-Ag-EA treated groups (Figure 4.2).

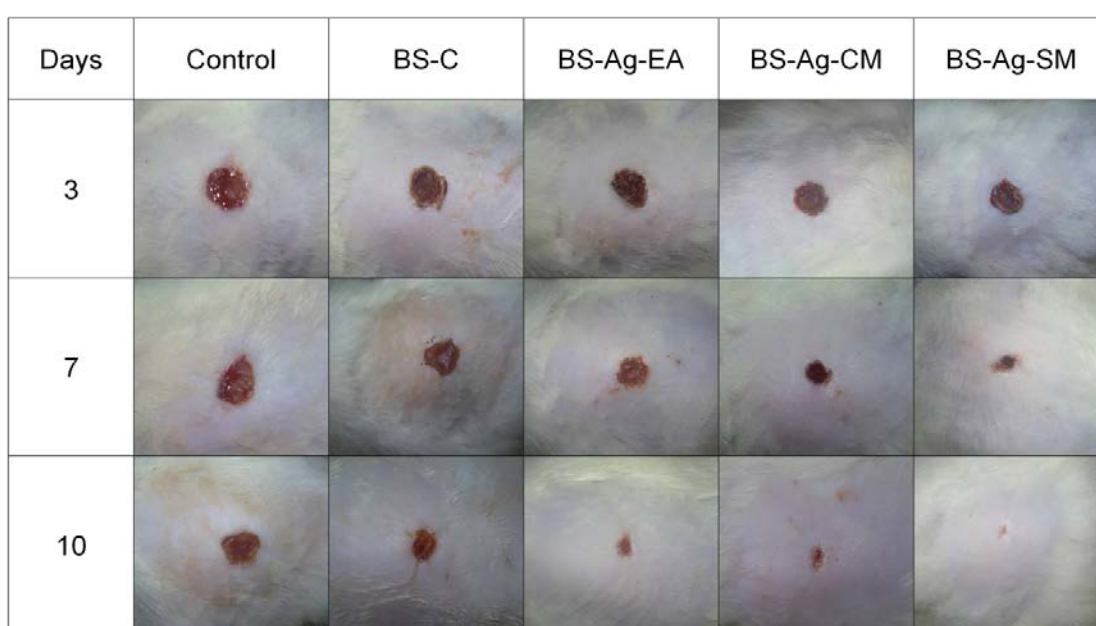


Figure 4.2 Representative images of the Wistar rats skin wounds after the administration of BS-C, BS-Ag-EA, BS-Ag-CM, BS-Ag-SM scaffolds and natural healing (control) on days 3, 7, and 10 days post injury.

Furthermore, changes in the wound size were assessed by tracing the wound area. Rats treated with BS-Ag-SM scaffolds exhibited increased wound contraction from 27.5 % on day 3 to 75.4 % on day 7 with complete epithelialization and closure of wound by day 10. BS-Ag-CM, and BS-Ag-EA treated groups exhibited around 72% and 66% wound contraction on day 7, followed by 91% and 84% on day 10, respectively. The BS-C scaffolds exhibited 65% wound contraction by the end of 10 days post injury (Figure 4.3). Whereas, in the control, although an increase in wound contraction from 13.7% on day 3 to 41.4 % on day 7 was noted, it was only 55 % by the end of the day 10. The classical

symptoms of inflammation such as reddening and edema of the surrounding tissues were clearly observed in the control groups at day 3 and day 7, post injury. In contrast, wounds

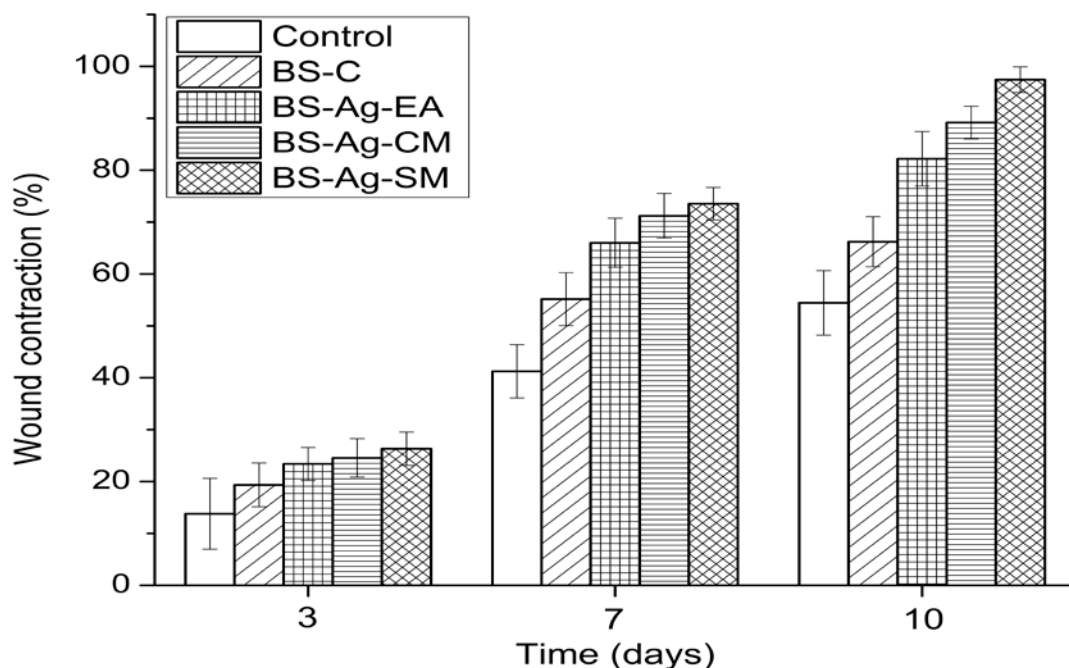


Figure 4.3 Graphical representation of the wound contraction in Wistar rats after the application of BS-C, BS-Ag-EA, BS-Ag-CM, BS-Ag-SM scaffolds and natural healing (control) at 3, 7, and 10 days post injury. All values represent the means and SD; $n = 3$.

treated with BS-Ag-SM, BS-Ag-CM and BS-Ag-EA scaffolds were completely dry and covered with granulation tissue with no obvious swelling. The contraction of the wound was observed in all the groups by the end of the 10th day post injury, and in the order of: BS-Ag-SM > BS-Ag-CM > BS-Ag-EA > BS-C > control. Studies on SM as antioxidant agent has been widely reported, but its applications in *in-vivo* wound healing have not fully studied. Antioxidant activity of polyphenolic compounds such as SM, CM and EA depends on the degree of hydroxylation in their structure, which reduces the free radicals by donating hydrogen atom (Kuhad et al. 2007). The structure of SM has more hydroxyl ions than CM, which might be the reason for the enhanced wound contraction when compared to CM and EA. The use of Ag and antioxidants (SM; CM; EA) in to the bilayer scaffolds reduced the inflammation generated during healing process thereby promoting the wound contraction.

4.3.2 Histological examination of skin excisions

Histological analysis of the wounds after excision of the scaffolds was performed by H&E staining (Figure 4.4). On day 3, all wounds in control groups (positive and negative controls) showed inflammatory and cellular changes in the epidermis with presence of neutrophils and mononuclear cells along with edematous eosinophilic exudate.

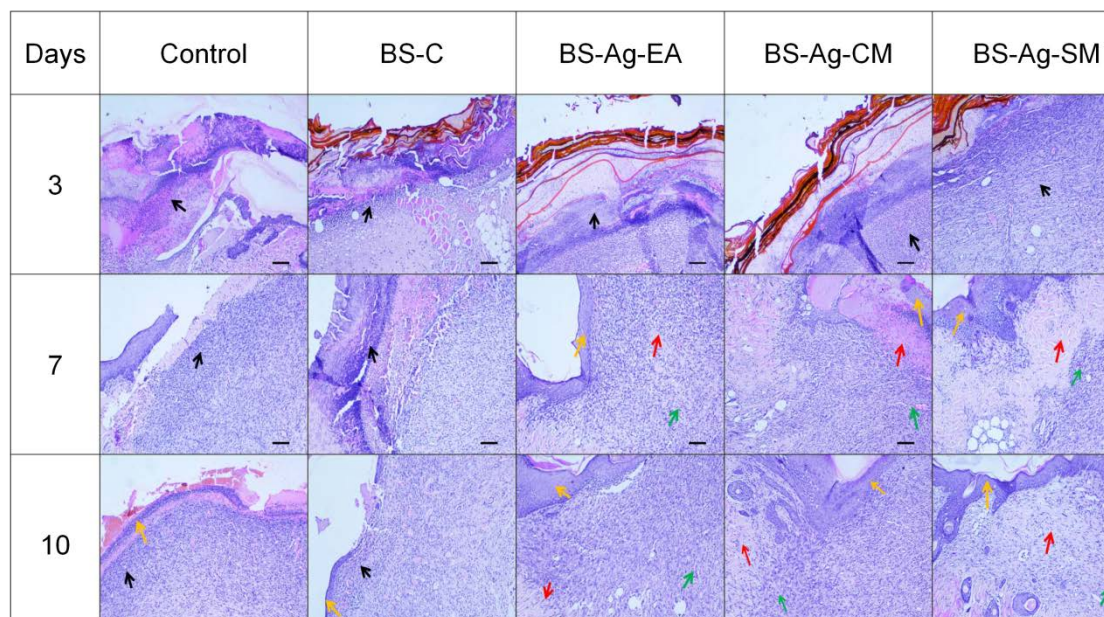


Figure 4.4 Histological evaluation of skin grafts treated with of BS-C, BS-Ag-EA, BS-Ag-CM, BS-Ag-SM scaffolds and natural healing (control) after 3, 7, and 10 days post injury. (Black arrow- inflammatory infiltration; Yellow arrow-epithelialization; Red arrow-fibrogenesis; Green arrow-granulation).

Remnants of scaffolds with irregular layer of necrotic cellular debris and inflammatory cells were observed in the epidermal layer of BS-C scaffolds treated group. While, BS-Ag-EA and BS-Ag-CM treated groups showed mild inflammation in the epidermis with presence of neutrophils and mononuclear cells along with edematous eosinophilic exudate. Inflammatory changes of a lesser degree were found in the epidermis of BS-Ag-SM treated group as compared to control groups. Healing of wound tissue was initiated with diffuse fibroblast, cellular proliferation and neo-vascularization in the dermal tissue layer of BS-Ag-SM treated group. On day 7, incomplete re-epithelialization of epidermal layer with crust comprising of necrotic cellular debris with inflammatory cells was noted in control groups. Rats treated with BS-Ag-SM, BS-Ag-CM and BS-Ag-EA groups showed significant progressive status of wound healing with proliferation of fibroblast, neovascularization and collagen deposition. Moreover, uniform new layer of skin-

epithelium with well formed granulation tissue was observed in BS-Ag-SM group. The scaffolds were not visible in the epidermal tissue suggestive of complete resorption during the wound healing process. On day 10, control groups showed incomplete wound healing with irregular re-epithelization and crust formation in the epidermis. The BS-Ag-SM scaffold treated groups exhibited complete re-epithelization and uniform fibroblast proliferation with the absence of any inflammatory or hemorrhagic changes in the epidermal/dermal layers. The wound healing in BS-Ag-CM and BS-Ag-EA groups was almost complete with re-epithelialization, and diffused fibroblast proliferation/granulation tissue in the dermal layer as observed on day 10.

Among the contributors to delayed wound healing, a prolonged inflammatory response is undoubtedly one of the important factors along with the microbial load (Morgan and Nigam 2013). To accomplish the successful wound repair and tissue regeneration, the inflammatory response must be tightly regulated *in vivo* without undesirable extension or aggravation, which would also avoid scar formation (Guo and DiPietro 2010, Khanna et al. 2010). Several reports have shown that Ag dressings improve wound healing activity, both *in vitro* and *in vivo*, attributed to its antibacterial and anti-inflammatory activity (Jain et al. 2009). The chitosan/collagen scaffolds incorporated with nano-Ag were found to regulate the wound's abnormal activation of macrophages and improve the progress of inflammatory stages thereby accelerating wound healing (You et al. 2017). The BS-Ag-SM scaffolds did not exhibit inflammatory infiltration on the 7th and 10th day of injury. The BS-Ag-CM and BS-Ag-EA treated groups showed a similar pattern but with less fibrogenesis and re-epithelialization at the same time points. Antioxidant compounds promote wound healing process in an oxidatively stressed environment by cleansing the free radicals and also by up-regulating the endogenous antioxidant enzymes (Nencini, Giorgi, and Micheli 2007, Sherif and Al-Gayyar 2013). This in turn promotes collagen deposition, granulation, epithelialization, and wound contraction which are characteristics of the proliferative phase of wound healing (Tabandeh et al. 2013). Ag exerts positive effects through its antimicrobial properties, reduction in wound inflammation, and modulation of fibrogenic cytokines.

4.3.3 Immunohistochemical staining

Lipid peroxidation was observed in wound tissues using immunohistochemical staining with anti-MDA rabbit polyclonal antibody. The MDA positive regions of the tissue

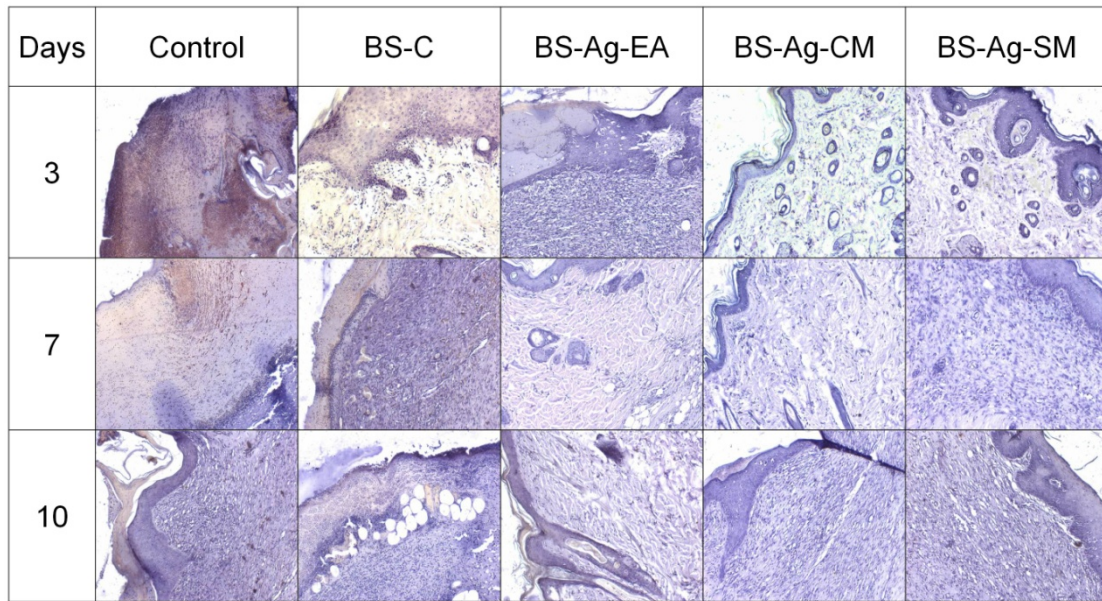


Figure 4.5 (A) Immunohistochemistry staining of anti-MDA performed on the skin grafts treated with BS-C, BS-Ag-EA, BS-Ag-CM, BS-Ag-SM scaffolds and natural healing (control) after 3, 7, and 10 days post injury.

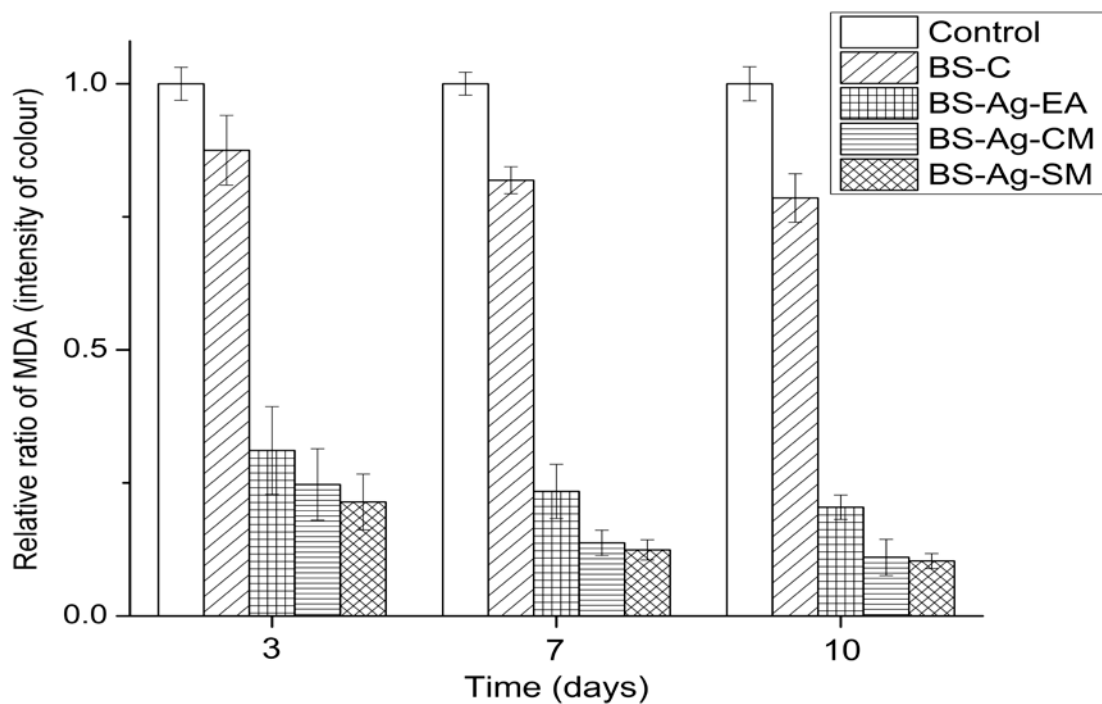


Figure 4.5 (B) Graphical representation of relative colour intensity of MDA in BS-C, BS-Ag-EA, BS-Ag-CM, and BS-Ag-SM scaffolds in context to natural healing (control), analyzed using ImageJ software.

stained brown. The intensity of brown color was higher in the skin wounds of control groups with strong to moderate staining from day 3 to 10. However, a significant decrease

in the intensity of brown color was observed in BS-Ag-SM, BS-Ag-CM and BS-Ag-EA treated group as compared with control groups on all the days. Although, BS-Ag-EA treated group showed a significant decrease in the intensity of brown color as compared to control, it was significantly higher than the BS-Ag-SM group [Figure 4.5 (A) and (B)].

Oxidative stress causes DNA damage and subsequent apoptosis due to the imbalance between production of free radicals and antioxidant defenses. ROS also affects biomolecules such as lipids, essential cellular proteins etc., thereby resulting in damaging the neighboring cells while prolonging the inflammatory stage (Bryan et al. 2012). Products of lipid peroxidation can be easily detected in biological fluids and tissues that can reliably reflect the specific markers of lipid peroxidation that occur *in vivo*. Malondialdehyde (MDA) is a natural polyunsaturated fatty acid formed in all mammalian cells as a product of lipid peroxidation and serves as a biomarker of oxidative stress (Nielsen et al. 1997). MDA is toxic and has been implicated in aging mutagenesis, carcinogenesis, diabetic nephropathy and radiation damage (Feng et al. 2006). Increased levels of MDA formed as a result of the high amount of lipid peroxidation were observed in the control groups (control, and BS-C scaffolds) at all the three time intervals, whereas, the groups treated with BS-Ag-EA, and BS-Ag-CM scaffolds exhibit mild to lesser lipid peroxidation at 7th and 10th day [Figure 4.5 (B)]. The groups treated with BS-Ag-SM showed lesser lipid peroxidation at all the time points. This is attributed to the antioxidant potential of the SM, CM and EA in addressing the oxidative stress due to ROS. The same pattern was confirmed from the wound contraction studies and H&E staining. The antioxidants (SM; CM; EA) in CO and CS matrix contributed towards cleansing of the ROS, while CS-Ag scaffolds prevented microbial colonization of the wound. Such bilayer scaffolds exhibiting therapeutic potentials have the potential to enhance wound healing in compromised situations and can be a promising material for skin tissue engineering applications.

4.4 Conclusion

The understanding of wound healing processes has led to the development of tissue engineering materials which would enhance the native ECM and nullify the factors affecting it. Microbial infections and oxidative stress generated by ROS are the major limiting factors which are affecting the wound healing process. In this chapter, novel bilayer scaffold have been synthesized in order to support the intra dermal nature of the

skin by incorporating Ag and SM/ CM/ EA. The incorporation of antimicrobial (Ag) and antioxidant (SM/ CM/ EA) compounds in to the polymeric matrix helps in enhancing the antibacterial activity and reducing the oxidative stress near the wound site. The bilayer scaffolds containing Ag/SM exhibited complete wound healing by the 10th day post injury with no indicators of oxidative stress, whereas, bilayer scaffolds containing Ag/CM and Ag/EA have shown around 90 % wound contraction while the control bilayer scaffolds without Ag and antioxidants have exhibited around 66% wound healing along with lipid peroxidation. The incorporation of antibacterial and antioxidants compounds enhanced the wound healing process at all the time points when compared to the control groups. Thus, the bilayer scaffolds with a combination of bioactive molecules can be a potential approach in supporting wound healing for skin tissue engineering applications, especially for wounds compromised by bacteria and ROS stress.

Summary of Results and Conclusion

A novel method for synthesis of the CS-Ag and CS-CO based SM, CM and EA was formulated using the melt-down neutralization technique followed by freeze-drying. The incorporation of the melt-down neutralization technique in the synthesis process helped in achieving uniform molding of the scaffold while at the same time ensuring even distribution of the bioactive molecules throughout the polymeric matrix.

The synthesized CS-Ag scaffolds with varying concentrations of Ag (1, 2, 3 % w/w) were characterized by using XRD, FTIR, TGA and SEM. The *in vitro* release kinetics of Ag from the CS scaffolds exhibited an initial high release followed by slow and sustained release. The antimicrobial activity of the CS-Ag scaffolds was studied on Gram positive (*Staphylococcus aureus*) and Gram negative (*Escherichia coli*) bacteria. The antimicrobial activity of the synthesized scaffolds increased with the concentration of the Ag and was maximum at 3% Ag concentration. The antibacterial activity was higher against Gram negative bacteria as compared to Gram positive bacteria. Further, when Ag based CS scaffolds were incubated in *E.coli* and *S.aureus* suspension for up to 24 h, no adherence of the bacteria on the scaffolds was noted confirming the antimicrobial potential of the CS-Ag scaffolds. The scaffolds exhibited a biphasic Ag release profile, wherein an initial high release was followed by subsequent slow and sustained release. The initial high release of Ag will help in combating the higher concentrations of initial bacterial load while the subsequent slow release provides the long term antibacterial activity. The Ag ions concentration in the scaffolds did not exhibit any toxicity towards the HaCaT (keratinocytes) cell lines. Therefore, CS-Ag scaffolds have a lot of potential as antibacterial agents in skin tissue engineering applications where the infections arising due to bacteria can delay the wound healing process.

The CS and CO incorporated with 0.5, 1 and 2% antioxidants (SM; CM; EA) were synthesized for their radical scavenging activity. The incorporation of antioxidants into the CS-CO polymeric matrix was confirmed by XRD and FTIR. The scaffolds exhibited a sustained release kinetics of the antioxidants (SM, CM and EA) monitored for up to 120 h. COS7 cells showed good viability, cell attachment and proliferation on the scaffolds. The *in vitro* antioxidant potential of the scaffolds containing SM/ CM/ EA was effective in reducing the oxidative stress generated by 10, 20 and 30 min, of UV irradiation. The scaffolds containing antioxidants exhibited the potential to reduce the oxidative stress on

the COS7 cell lines at 0 h and 24 h post irradiation incubation. The cell survival increased with increase in the concentration of the antioxidants. Hence, the concentration of 2% antioxidant was selected for the fabrication of the bilayer scaffolds. The antioxidant potential of the compounds was in the order of SM>CM>EA, as estimated in terms of revival of the fibroblasts from oxidative stress. The antioxidant potential of polyphenolic compounds depends up on the degree of hydroxylation; SM has more hydroxyl groups as compared to CM and EA.

The bilayer scaffolds with antibacterial and antioxidant activity were synthesized by combining the CS-Ag3 and CS-CO-R (R= SM₍₂₎/ CM₍₂₎/ EA₍₂₎), and tested for potential *in vivo* applications. The topical application of bilayer scaffolds with antibacterial and antioxidant compounds, studied for 3, 7 and 10 days in Wistar rat models showed better wound healing properties as compared to control scaffolds (positive and negative control). The wound contraction studies of the bilayer scaffolds containing Ag/SM showed complete wound healing by the end of 10th day post injury. The bilayer scaffolds containing Ag/CM and Ag/EA exhibited 91% and 84 % wound contraction, whereas, the control bilayer scaffolds exhibited 65% wound contraction and the groups without any scaffolds exhibited 55% wound contraction. The histological and immunohistochemical (anti-MDA) evaluation of tissue sections containing antibacterial and antioxidant incorporated scaffolds showed complete re-epithelialization and no/minimal lipid peroxidation by the end of the 10th day post injury. The bilayer scaffolds containing Ag/SM exhibited better wound healing with no lipid peroxidation by the 10th day as compared to Ag/CM and Ag/EA. These bilayer scaffolds incorporating antibacterial (Ag) and antioxidant (SM; CM; EA) compounds were designed with an idea of inhibiting bacterial growth and reduce the oxidative stress at the wound site demonstrating their potential application in skin tissue engineering.

Thus, some of the important contributions emerging from the present thesis are as follows:

- 1) In this study, a novel melt-down neutralization method has been developed for the fabrication of the tissue engineering scaffolds. This method of synthesis ensures uniformity of the matrix and the even distribution of bioactive molecules.
- 2) In the present work, incorporation of polyphenolic antioxidants (SM; CM; EA) into the collagen-chitosan matrix has been studied for the first time.

3) Novel bilayer scaffolds have been fabricated to address the infections and oxidative stress at the wound site by incorporating antibacterial (Ag) and antioxidant (SM; CM; EA) compounds. These bilayer scaffolds with an independent release behavior are proposed as ideal candidates for treating chronic wounds.

Future Scope of Work

1) The scaffolds incorporated with polyphenolic antioxidants have demonstrated efficient cell revival rate in oxidative stressed environment. The antioxidant potential of the scaffolds at the molecular level has to be studied to understand the mechanisms of interactions with the free radicals.

2) The bilayer scaffolds with antibacterial and antioxidants have shown excellent wound healing activity in *in vivo* model. As degradation kinetics of the biomaterials plays an important role in the tissue engineering applications a detailed study in understanding the *in vivo* degradation of the bilayer scaffolds is required. The bilayer scaffolds can be further investigated to understand the *in vivo* molecular interactions of the scaffolds with the wound while quantitatively evaluating the components like inflammation, gene expression of ECM components and proteases. A detail evaluation of these bilayer scaffold incorporated into wounds sections, will help in understand the distribution of the cells, and ECM which will further help in designing the scaffolds for tissue engineering applications.

References

- Abbaszadegan, Abbas, Yasamin Ghahramani, Ahmad Gholami, Bahram Hemmateenejad, Samira Dorostkar, Mohammadreza Nabavizadeh, and Hashem Sharghi. 2015. "The effect of charge at the surface of silver nanoparticles on antimicrobial activity against gram-positive and gram-negative bacteria: a preliminary study." *Journal of Nanomaterials* 16 (1):53.
- Annabi, Nasim, Jason W Nichol, Xia Zhong, Chengdong Ji, Sandeep Koshy, Ali Khademhosseini, and Fariba Dehghani. 2010. "Controlling the porosity and microarchitecture of hydrogels for tissue engineering." *Tissue Engineering Part B: Reviews* 16 (4):371-383.
- Balañá, María Eugenia, Hernán Eduardo Charreau, and Gustavo José Leirós. 2015. "Epidermal stem cells and skin tissue engineering in hair follicle regeneration." *World journal of stem cells* 7 (4):711.
- Banerjee, Ena Ray. 2017. "Tissue Engineering and Cell-Based Therapy in Regenerative Medicine." In *Perspectives in Translational Research in Life Sciences and Biomedicine*, 1-55. Springer.
- Barnaby, Stacey N, Nako Nakatsuka, Stephen H Frayne, Karl R Fath, and Ipsita A Banerjee. 2013. "Formation of hyaluronic acid–ellagic acid microfiber hybrid hydrogels and their applications." *Colloid and Polymer Science* 291 (3):515-525.
- Besinis, Alexander, Sanna Dara Hadi, HR Le, Christopher Tredwin, and RD Handy. 2017. "Antibacterial activity and biofilm inhibition by surface modified titanium alloy medical implants following application of silver, titanium dioxide and hydroxyapatite nanocoatings." *Nanotoxicology* 11 (3):327-338.
- Bhat, Sumrita, Anuj Tripathi, and Ashok Kumar. 2011. "Supermacroporous chitosan–agarose–gelatin cryogels: in vitro characterization and in vivo assessment for cartilage tissue engineering." *Journal of the Royal Society Interface* 8 (57):540-554.
- Böttcher-Haberzeth, Sophie, Thomas Biedermann, and Ernst Reichmann. 2010. "Tissue engineering of skin." *Burns* 36 (4):450-460.
- Breitkreutz, Dirk, Isabell Koxholt, Kathrin Thiemann, and Roswitha Nischt. 2013. "Skin basement membrane: the foundation of epidermal integrity—BM functions and diverse roles of bridging molecules nidogen and perlecan." *BioMed research international* 2013.

- Brglez Mojzer, Eva, Maša Knez Hrnčič, Mojca Škerget, Željko Knez, and Urban Bren. 2016. "Polyphenols: extraction methods, antioxidative action, bioavailability and anticarcinogenic effects." *Molecules* 21 (7):901.
- Bryan, Nicholas, Helen Ahswin, Neil Smart, Yves Bayon, Stephen Wohler, and John A Hunt. 2012. "Reactive oxygen species (ROS)—a family of fate deciding molecules pivotal in constructive inflammation and wound healing." *Eur Cell Mater* 24 (249):e65.
- Burdick, Jason A., Robert L. Mauck, Joseph H. Gorman, and Robert C. Gorman. 2013. "Acellular Biomaterials: An Evolving Alternative to Cell-Based Therapies." *Science translational medicine* 5 (176):176ps4-176ps4. doi: 10.1126/scitranslmed.3003997.
- Cao, Zhen, Ce Dou, and Shiwu Dong. 2014. "Scaffolding biomaterials for cartilage regeneration." *Journal of Nanomaterials* 2014:4.
- Carocho, Márcio, and Isabel CFR Ferreira. 2013. "A review on antioxidants, prooxidants and related controversy: natural and synthetic compounds, screening and analysis methodologies and future perspectives." *Food and Chemical Toxicology* 51:15-25.
- Chang, Jai Wong, Choung Soo Kim, Soon Bae Kim, Su Kil Park, Jung Sik Park, and Sang Koo Lee. 2006. "Proinflammatory cytokine-induced NF- κ B activation in human mesangial cells is mediated through intracellular calcium but not ROS: effects of silymarin." *Nephron Experimental Nephrology* 103 (4):e156-e165.
- Chaudhari, Atul A, Komal Vig, Dieudonné Radé Baganizi, Rajnish Sahu, Saurabh Dixit, Vida Dennis, Shree Ram Singh, and Shreekumar R Pillai. 2016. "Future prospects for scaffolding methods and biomaterials in skin tissue engineering: a review." *International journal of molecular sciences* 17 (12):1974.
- Chen, Zonggang, Xiumei Mo, Chuanglong He, and Hongsheng Wang. 2008. "Intermolecular interactions in electrospun collagen–chitosan complex nanofibers." *Carbohydrate polymers* 72 (3):410-418.
- Cheng, Lijia, Feng Ye, Ruina Yang, Xiaofeng Lu, Yujun Shi, Li Li, Hongsong Fan, and Hong Bu. 2010. "Osteoinduction of hydroxyapatite/ β -tricalcium phosphate bioceramics in mice with a fractured fibula." *Acta biomaterialia* 6 (4):1569-1574.
- Chou, Shih-Feng, Daniel Carson, and Kim A Woodrow. 2015. "Current strategies for sustaining drug release from electrospun nanofibers." *Journal of Controlled Release* 220:584-591.

- Coolen, Neeltje A, Kelly CWM Schouten, Esther Middelkoop, and Magda MW Ulrich. 2010. "Comparison between human fetal and adult skin." *Archives of dermatological research* 302 (1):47-55.
- Correia, Clara R, Liliana S Moreira-Teixeira, Lorenzo Moroni, Rui L Reis, Clemens A van Blitterswijk, Marcel Karperien, and João F Mano. 2011. "Chitosan scaffolds containing hyaluronic acid for cartilage tissue engineering." *Tissue Engineering Part C: Methods* 17 (7):717-730.
- Curotto, E., and F. Aros. 1993. "Quantitative Determination of Chitosan and the Percentage of Free Amino Groups." *Analytical Biochemistry* 211 (2):240-241. doi: <https://doi.org/10.1006/abio.1993.1263>.
- Dakal, Tikam Chand, Anu Kumar, Rita S Majumdar, and Vinod Yadav. 2016. "Mechanistic basis of antimicrobial actions of silver nanoparticles." *Frontiers in microbiology* 7:1831.
- Dang, Jiyoung M, and Kam W Leong. 2006. "Natural polymers for gene delivery and tissue engineering." *Advanced drug delivery reviews* 58 (4):487-499.
- Das, Ratul Kumar, Naresh Kasoju, and Utpal Bora. 2010. "Encapsulation of curcumin in alginate-chitosan-pluronic composite nanoparticles for delivery to cancer cells." *Nanomedicine: Nanotechnology, Biology and Medicine* 6 (1):153-160.
- Demidova-Rice, Tatiana N, Michael R Hamblin, and Ira M Herman. 2012. "Acute and impaired wound healing: pathophysiology and current methods for drug delivery, part 1: normal and chronic wounds: biology, causes, and approaches to care." *Advances in skin & wound care* 25 (7):304.
- Deng, Hua, Danielle McShan, Ying Zhang, Sudarson S. Sinha, Zikri Arslan, Paresh C. Ray, and Hongtao Yu. 2016. "Mechanistic Study of the Synergistic Antibacterial Activity of Combined Silver Nanoparticles and Common Antibiotics." *Environmental science & technology* 50 (16):8840-8848. doi: 10.1021/acs.est.6b00998.
- Dhandayuthapani, Brahatheeswaran, Uma Maheswari Krishnan, and Swaminathan Sethuraman. 2010. "Fabrication and characterization of chitosan-gelatin blend nanofibers for skin tissue engineering." *Journal of Biomedical Materials Research Part B: Applied Biomaterials* 94 (1):264-272.

- Dhandayuthapani, Brahatheeswaran, Yasuhiko Yoshida, Toru Maekawa, and D Sakthi Kumar. 2011. "Polymeric scaffolds in tissue engineering application: a review." *International journal of polymer science* 2011.
- Di Mascio, Paolo, Michael E Murphy, and Helmut Sies. 1991. "Antioxidant defense systems: the role of carotenoids, tocopherols, and thiols." *The American journal of clinical nutrition* 53 (1):194S-200S.
- Diegelmann, Robert F, and Melissa C Evans. 2004. "Wound healing: an overview of acute, fibrotic and delayed healing." *Front Biosci* 9 (1):283-289.
- Doillon, CJ, CF Whyne, S Brandwein, and FH Silver. 1986. "Collagen-based wound dressings: Control of the pore structure and morphology." *Journal of Biomedical Materials Research Part A* 20 (8):1219-1228.
- Dunnill, Christopher, Thomas Patton, James Brennan, John Barrett, Matthew Dryden, Jonathan Cooke, David Leaper, and Nikolaos T Georgopoulos. 2017. "Reactive oxygen species (ROS) and wound healing: the functional role of ROS and emerging ROS-modulating technologies for augmentation of the healing process." *International wound journal* 14 (1):89-96.
- Dvořánková, Barbora, Pavol Szabo, Lukas Lacina, Peter Gal, Jana Uhrova, Tomas Zima, Herbert Kaltner, Sabine André, Hans-Joachim Gabius, and Eva Sykova. 2011. "Human galectins induce conversion of dermal fibroblasts into myofibroblasts and production of extracellular matrix: potential application in tissue engineering and wound repair." *Cells Tissues Organs* 194 (6):469-480.
- Edgar, Lauren, Kyle McNamara, Theresa Wong, Riccardo Tamburrini, Ravi Katari, and Giuseppe Orlando. 2016. "Heterogeneity of scaffold biomaterials in tissue engineering." *Materials* 9 (5):332.
- Edwards, Ruth, and Keith G Harding. 2004. "Bacteria and wound healing." *Current opinion in infectious diseases* 17 (2):91-96.
- El Gharas, Hasna. 2009. "Polyphenols: food sources, properties and applications—a review." *International journal of food science & technology* 44 (12):2512-2518.
- Feng, Zhaohui, Wenwei Hu, Lawrence J Marnett, and Moon-shong Tang. 2006. "Malondialdehyde, a major endogenous lipid peroxidation product, sensitizes human cells to UV-and BPDE-induced killing and mutagenesis through inhibition of nucleotide

- excision repair." *Mutation Research/Fundamental and Molecular Mechanisms of Mutagenesis* 601 (1):125-136.
- Freshney, I. 2001. "Application of cell cultures to toxicology." *Cell Biol Toxicol* 17 (4-5):213-30.
- Gayle, William E, C Glen Mayhall, V Archer Lamb, Elaine Apollo, and Jr BW Haynes. 1978. "Resistant *Enterobacter cloacae* in a burn center: the ineffectiveness of silver sulfadiazine." *The Journal of trauma* 18 (5):317-323.
- Gazak, Radek, Daniela Walterova, and Vladimir Kren. 2007. "Silybin and silymarin-new and emerging applications in medicine." *Current medicinal chemistry* 14 (3):315-338.
- Ghasemi-Mobarakeh, Laleh, Molamma P Prabhakaran, Mohammad Morshed, Mohammad-Hossein Nasr-Esfahani, and Seeram Ramakrishna. 2008. "Electrospun poly (ϵ -caprolactone)/gelatin nanofibrous scaffolds for nerve tissue engineering." *Biomaterials* 29 (34):4532-4539.
- Ghosh, Sougata, Sumersing Patil, Mehul Ahire, Rohini Kitture, Sangeeta Kale, Karishma Pardesi, Swaranjit S Cameotra, Jayesh Bellare, Dilip D Dhavale, and Amit Jabgunde. 2012. "Synthesis of silver nanoparticles using *Dioscorea bulbifera* tuber extract and evaluation of its synergistic potential in combination with antimicrobial agents." *International Journal of Nanomedicine* 7:483.
- Gonzalez, Ana Cristina de Oliveira, Tila Fortuna Costa, Zilton de Araújo Andrade, and Alena Ribeiro Alves Peixoto Medrado. 2016. "Wound healing-A literature review." *Anais brasileiros de dermatologia* 91 (5):614-620.
- Gopalakrishnan, Lalitha, Lakshmi Narashimhan Ramana, Swaminathan Sethuraman, and Uma Maheswari Krishnan. 2014. "Ellagic acid encapsulated chitosan nanoparticles as anti-hemorrhagic agent." *Carbohydrate polymers* 111:215-221.
- Govindan, S., E. A. K. Nivethaa, R. Saravanan, V. Narayanan, and A. Stephen. 2012. "Synthesis and characterization of chitosan–silver nanocomposite." *Applied Nanoscience* 2 (3):299-303. doi: 10.1007/s13204-012-0109-5.
- Guest, JF, Kath Vowden, and Peter Vowden. 2017. "The health economic burden that acute and chronic wounds impose on an average clinical commissioning group/health board in the UK." *Journal of wound care* 26 (6):292-303.

- Gunatillake, Pathiraja A, and Raju Adhikari. 2003. "Biodegradable synthetic polymers for tissue engineering." *Eur Cell Mater* 5 (1):1-16.
- Guo, Baolin, Bo Lei, Peng Li, and Peter X Ma. 2015. "Functionalized scaffolds to enhance tissue regeneration." *Regenerative biomaterials* 2 (1):47-57.
- Guo, S al, and Luisa A DiPietro. 2010. "Factors affecting wound healing." *Journal of dental research* 89 (3):219-229.
- Gupta, Siddhi, Thomas J Webster, and Arvind Sinha. 2011. "Evolution of PVA gels prepared without crosslinking agents as a cell adhesive surface." *Journal of Materials Science: Materials in Medicine* 22 (7):1763-1772.
- Gupta, Swati, Shailendra Kumar Singh, and Priti Girotra. 2014. "Targeting silymarin for improved hepatoprotective activity through chitosan nanoparticles." *International journal of pharmaceutical investigation* 4 (4):156.
- Guzman, Maribel, Jean Dille, and Stéphane Godet. 2012. "Synthesis and antibacterial activity of silver nanoparticles against gram-positive and gram-negative bacteria." *Nanomedicine: Nanotechnology, Biology and Medicine* 8 (1):37-45.
- Ha, Hye-Lin, Hye-Jun Shin, Mark A Feitelson, and Dae-Yeul Yu. 2010. "Oxidative stress and antioxidants in hepatic pathogenesis." *World journal of gastroenterology: WJG* 16 (48):6035.
- Han, Chun-mao, Li-ping Zhang, Jin-zhang Sun, Hai-fei Shi, Jie Zhou, and Chang-you Gao. 2010. "Application of collagen-chitosan/fibrin glue asymmetric scaffolds in skin tissue engineering." *Journal of Zhejiang University Science B* 11 (7):524-530.
- Han, Fei, Yang Dong, Zhen Su, Ran Yin, Aihua Song, and Sanming Li. 2014. "Preparation, characteristics and assessment of a novel gelatin–chitosan sponge scaffold as skin tissue engineering material." *International journal of pharmaceutics* 476 (1-2):124-133.
- Harley, Brendan A, Janet H Leung, Emilio CCM Silva, and Lorna J Gibson. 2007. "Mechanical characterization of collagen–glycosaminoglycan scaffolds." *Acta biomaterialia* 3 (4):463-474.
- Haugh, Matthew G, Ciara M Murphy, and Fergal J O'Brien. 2009. "Novel freeze-drying methods to produce a range of collagen–glycosaminoglycan scaffolds with tailored mean pore sizes." *Tissue Engineering Part C: Methods* 16 (5):887-894.

- He, Qing, Qiang Ao, Yandao Gong, and Xiufang Zhang. 2011. "Preparation of chitosan films using different neutralizing solutions to improve endothelial cell compatibility." *Journal of Materials Science: Materials in Medicine* 22 (12):2791-2802.
- Heydarkhan-Hagvall, Sepideh, Katja Schenke-Layland, Andrew P Dhanasopon, Fady Rofail, Hunter Smith, Benjamin M Wu, Richard Shemin, Ramin E Beygui, and William R MacLellan. 2008. "Three-dimensional electrospun ECM-based hybrid scaffolds for cardiovascular tissue engineering." *Biomaterials* 29 (19):2907-2914.
- Hoshiba, Takashi, Hongxu Lu, Naoki Kawazoe, and Guoping Chen. 2010. "Decellularized matrices for tissue engineering." *Expert opinion on biological therapy* 10 (12):1717-1728.
- Howard, Daniel, Lee D Buttery, Kevin M Shakesheff, and Scott J Roberts. 2008. "Tissue engineering: strategies, stem cells and scaffolds." *Journal of anatomy* 213 (1):66-72.
- Hseu, You-Cheng, Chih-Wei Chou, KJ Senthil Kumar, Ke-Ting Fu, Hui-Min Wang, Li-Sung Hsu, Yueh-Hsiung Kuo, Chi-Rei Wu, Ssu-Ching Chen, and Hsin-Ling Yang. 2012. "Ellagic acid protects human keratinocyte (HaCaT) cells against UVA-induced oxidative stress and apoptosis through the upregulation of the HO-1 and Nrf-2 antioxidant genes." *Food and Chemical Toxicology* 50 (5):1245-1255.
- Hsieh, Wen-Chuan, Chih-Pong Chang, and Shang-Ming Lin. 2007. "Morphology and characterization of 3D micro-porous structured chitosan scaffolds for tissue engineering." *Colloids and Surfaces B: Biointerfaces* 57 (2):250-255.
- Intranuovo, Francesca, Roberto Gristina, Francesco Brun, Sara Mohammadi, Giacomo Ceccone, Eloisa Sardella, François Rossi, Giuliana Tromba, and Pietro Favia. 2014. "Plasma Modification of PCL Porous Scaffolds Fabricated by Solvent-Casting/Particulate-Leaching for Tissue Engineering." *Plasma Processes and Polymers* 11 (2):184-195.
- Jadalannagari, Sushma, Ketaki Deshmukh, Sutapa Roy Ramanan, and Meenal Kowshik. 2014. "Antimicrobial activity of hemocompatible silver doped hydroxyapatite nanoparticles synthesized by modified sol-gel technique." *Applied Nanoscience* 4 (2):133-141.
- Jain, Jaya, Sumit Arora, Jyutika M Rajwade, Pratibha Omray, Sanjeev Khandelwal, and Kishore M Paknikar. 2009. "Silver nanoparticles in therapeutics: development of an

antimicrobial gel formulation for topical use." *Molecular Pharmaceutics* 6 (5):1388-1401.

James, Garth A, Ellen Swogger, Randall Wolcott, Patrick Secor, Jennifer Sestrich, John W Costerton, and Philip S Stewart. 2008. "Biofilms in chronic wounds." *Wound Repair and regeneration* 16 (1):37-44.

Jeon, Oju, Su Jin Song, Sun-Woong Kang, Andrew J Putnam, and Byung-Soo Kim. 2007. "Enhancement of ectopic bone formation by bone morphogenetic protein-2 released from a heparin-conjugated poly (L-lactic-co-glycolic acid) scaffold." *Biomaterials* 28 (17):2763-2771.

Ji, Wei, Yan Sun, Fang Yang, Jeroen JJP van den Beucken, Mingwen Fan, Zhi Chen, and John A Jansen. 2011. "Bioactive electrospun scaffolds delivering growth factors and genes for tissue engineering applications." *Pharmaceutical research* 28 (6):1259-1272.

Jung, Kyung-Hye, Man-Woo Huh, Wan Meng, Jiang Yuan, Seok Hee Hyun, Jung-Sook Bae, Samuel M Hudson, and Inn-Kyu Kang. 2007. "Preparation and antibacterial activity of PET/chitosan nanofibrous mats using an electrospinning technique." *Journal of applied polymer science* 105 (5):2816-2823.

Jung, Young Suk, Sun Ju Kim, Young Soon Kim, Dal Woong Choi, and Young Chul Kim. 2013. "Alterations in sulfur amino acid metabolism in mice treated with silymarin: a novel mechanism of its action involved in enhancement of the antioxidant defense in liver." *Planta medica* 79 (12):997-1002.

Kagan, VE, and YY Tyurina. 1998. "Recycling and redox cycling of phenolic antioxidants." *Annals of the New York Academy of Sciences* 854 (1):425-434.

Kant, Vinay, Anu Gopal, Nitya N Pathak, Pawan Kumar, Surendra K Tandan, and Dinesh Kumar. 2014. "Antioxidant and anti-inflammatory potential of curcumin accelerated the cutaneous wound healing in streptozotocin-induced diabetic rats." *International immunopharmacology* 20 (2):322-330.

Karri, Veera Venkata Satyanarayana Reddy, Gowthamarajan Kuppusamy, Siddhartha Venkata Talluri, Sai Sandeep Mannemala, Radhakrishna Kollipara, Ashish Devidas Wadhvani, Shashank Mulukutla, Kalidhindi Rama Satyanarayana Raju, and Rajkumar Malayandi. 2016. "Curcumin loaded chitosan nanoparticles impregnated into collagen-

alginate scaffolds for diabetic wound healing." *International journal of biological macromolecules* 93:1519-1529.

Kasaai, Mohammad R. 2007. "Calculation of Mark–Houwink–Sakurada (MHS) equation viscometric constants for chitosan in any solvent–temperature system using experimental reported viscometric constants data." *Carbohydrate Polymers* 68 (3):477-488. doi: <https://doi.org/10.1016/j.carbpol.2006.11.006>.

Kasoju, Naresh, and Utpal Bora. 2012. "Fabrication and characterization of curcumin-releasing silk fibroin scaffold." *Journal of Biomedical Materials Research Part B: Applied Biomaterials* 100 (7):1854-1866.

Katiyar, Santosh K, Sreelatha Meleth, and Som D Sharma. 2008. "Silymarin, a Flavonoid from Milk Thistle (*Silybum marianum* L.), Inhibits UV-induced Oxidative Stress Through Targeting Infiltrating CD11b+ Cells in Mouse Skin." *Photochemistry and photobiology* 84 (2):266-271.

Kebbekus, Barbara B. 2003. "Preparation of samples for metals analysis." *Sample preparation techniques in analytical chemistry* 162:227.

Khanna, Savita, Sabyasachi Biswas, Yingli Shang, Eric Collard, Ali Azad, Courtney Kauh, Vineet Bhasker, Gayle M Gordillo, Chandan K Sen, and Sashwati Roy. 2010. "Macrophage dysfunction impairs resolution of inflammation in the wounds of diabetic mice." *PloS one* 5 (3):e9539.

Kilic, Ismail, Yeşim Yeşiloğlu, and Yüksel Bayrak. 2014. "Spectroscopic studies on the antioxidant activity of ellagic acid." *Spectrochimica Acta Part A: Molecular and Biomolecular Spectroscopy* 130:447-452.

Kim, GeunHyung, Seunghyun Ahn, YunYoung Kim, Youngseok Cho, and Wook Chun. 2011. "Coaxial structured collagen–alginate scaffolds: fabrication, physical properties, and biomedical application for skin tissue regeneration." *Journal of Materials Chemistry* 21 (17):6165-6172.

Kim, Hong Nam, Do-Hyun Kang, Min Sung Kim, Alex Jiao, Deok-Ho Kim, and Kahp-Yang Suh. 2012. "Patterning methods for polymers in cell and tissue engineering." *Annals of biomedical engineering* 40 (6):1339-1355.

- Kim, Soo-Hwan, Hyeong-Seon Lee, Deok-Seon Ryu, Soo-Jae Choi, and Dong-Seok Lee. 2011. "Antibacterial activity of silver-nanoparticles against *Staphylococcus aureus* and *Escherichia coli*." *Korean J. Microbiol. Biotechnol* 39 (1):77-85.
- Kim, Soo-Hyun, Jeremy Turnbull, and Scott Guimond. 2011. "Extracellular matrix and cell signalling: the dynamic cooperation of integrin, proteoglycan and growth factor receptor." *Journal of Endocrinology* 209 (2):139-151.
- Kim, Sungwoo, Yongxing Liu, M Waleed Gaber, Joel D Bumgardner, Warren O Haggard, and Yunzhi Yang. 2009. "Development of chitosan–ellagic acid films as a local drug delivery system to induce apoptotic death of human melanoma cells." *Journal of Biomedical Materials Research Part B: Applied Biomaterials* 90 (1):145-155.
- Kishen, Anil, Suja Shrestha, Annie Shrestha, Calvin Cheng, and Cynthia Goh. 2016. "Characterizing the collagen stabilizing effect of crosslinked chitosan nanoparticles against collagenase degradation." *Dental Materials* 32 (8):968-977.
- Kobayashi, Ken, Teruhisa Suzuki, Yukio Nomoto, Yasuhiro Tada, Masao Miyake, Akihiro Hazama, Ikuo Wada, Tatsuo Nakamura, and Koichi Omori. 2010. "A tissue-engineered trachea derived from a framed collagen scaffold, gingival fibroblasts and adipose-derived stem cells." *Biomaterials* 31 (18):4855-4863.
- Kuhad, Anurag, Sangeeta Pilkhwal, Sameer Sharma, Naveen Tirkey, and Kanwaljit Chopra. 2007. "Effect of curcumin on inflammation and oxidative stress in cisplatin-induced experimental nephrotoxicity." *Journal of Agricultural and Food Chemistry* 55 (25):10150-10155.
- Kurahashi, Toshihiro, and Junichi Fujii. 2015. "Roles of antioxidative enzymes in wound healing." *Journal of Developmental Biology* 3 (2):57-70.
- Langer, R, and JP Vacanti. 1993. "Tissue engineering." *Science* 260 (5110):920-926. doi: 10.1126/science.8493529.
- Lee, Wen-Jane, Hsiu-Chung Ou, Wen-Cheng Hsu, Min-Min Chou, Jenn-Jhy Tseng, Shih-Lan Hsu, Kun-Ling Tsai, and Wayne Huey-Hereng Sheu. 2010. "Ellagic acid inhibits oxidized LDL-mediated LOX-1 expression, ROS generation, and inflammation in human endothelial cells." *Journal of vascular surgery* 52 (5):1290-1300.
- Li, Jiashen, Yun Chen, Arthur F. T. Mak, Rocky S. Tuan, Lin Li, and Yi Li. 2010. "A one-step method to fabricate PLLA scaffolds with deposition of bioactive hydroxyapatite

- and collagen using ice-based microporogens." *Acta Biomaterialia* 6 (6):2013-2019. doi: <https://doi.org/10.1016/j.actbio.2009.12.008>.
- Li, Xian-Zhi, Hiroshi Nikaido, and Kurt E Williams. 1997. "Silver-resistant mutants of *Escherichia coli* display active efflux of Ag⁺ and are deficient in porins." *Journal of bacteriology* 179 (19):6127-6132.
- Li, Zhensheng, Hassna R Ramay, Kip D Hauch, Demin Xiao, and Miqin Zhang. 2005. "Chitosan–alginate hybrid scaffolds for bone tissue engineering." *Biomaterials* 26 (18):3919-3928.
- Lien, Sio-Mei, Liang-Yu Ko, and Ta-Jen Huang. 2009. "Effect of pore size on ECM secretion and cell growth in gelatin scaffold for articular cartilage tissue engineering." *Acta Biomaterialia* 5 (2):670-679.
- Lin, Chien-Chi, and Andrew T Metters. 2006. "Hydrogels in controlled release formulations: network design and mathematical modeling." *Advanced drug delivery reviews* 58 (12):1379-1408.
- Liu, Weidong, Yingjie Zhai, Xueyuan Heng, Feng Yuan Che, Wenjun Chen, Dezhong Sun, and Guangxi Zhai. 2016. "Oral bioavailability of curcumin: problems and advancements." *Journal of drug targeting* 24 (8):694-702.
- Loh, Qiu Li, and Cleo Choong. 2013. "Three-dimensional scaffolds for tissue engineering applications: role of porosity and pore size." *Tissue Engineering Part B: Reviews* 19 (6):485-502.
- Lok, Chun-Nam, Chi-Ming Ho, Rong Chen, Qing-Yu He, Wing-Yiu Yu, Hongzhe Sun, Paul Kwong-Hang Tam, Jen-Fu Chiu, and Chi-Ming Che. 2006. "Proteomic analysis of the mode of antibacterial action of silver nanoparticles." *Journal of proteome research* 5 (4):916-924.
- López-Carballo, Gracia, Laura Higuera, Rafael Gavara, and Pilar Hernández-Muñoz. 2012. "Silver ions release from antibacterial chitosan films containing in situ generated silver nanoparticles." *Journal of agricultural and food chemistry* 61 (1):260-267.
- Lu, Pengfei, Ken Takai, Valerie M Weaver, and Zena Werb. 2011. "Extracellular matrix degradation and remodeling in development and disease." *Cold Spring Harbor perspectives in biology* 3 (12):a005058.

- Ma, Lie, Changyou Gao, Zhengwei Mao, Jie Zhou, Jiacong Shen, Xueqing Hu, and Chunmao Han. 2003. "Collagen/chitosan porous scaffolds with improved biostability for skin tissue engineering." *Biomaterials* 24 (26):4833-4841.
- Madihally, Sundararajan V, and Howard WT Matthew. 1999. "Porous chitosan scaffolds for tissue engineering." *Biomaterials* 20 (12):1133-1142.
- Malafaya, Patrícia B, Gabriela A Silva, and Rui L Reis. 2007. "Natural–origin polymers as carriers and scaffolds for biomolecules and cell delivery in tissue engineering applications." *Advanced drug delivery reviews* 59 (4-5):207-233.
- Malarkodi, C, S Rajeshkumar, K Paulkumar, G Gnanajobitha, M Vanaja, and G Annadurai. 2013. "Biosynthesis of semiconductor nanoparticles by using sulfur reducing bacteria *Serratia nematodiphila*." *Advances in nano research* 1 (2):83-91.
- Mallikarjuna, K, G Narasimha, GR Dillip, B Praveen, B Shreedhar, C Sree Lakshmi, BVS Reddy, and B Deva Prasad Raju. 2011. "Green synthesis of silver nanoparticles using *Ocimum* leaf extract and their characterization." *Digest Journal of Nanomaterials and Biostructures* 6 (1):181-186.
- Mandal, Manisha Deb, and Shyamapada Mandal. 2011. "Honey: its medicinal property and antibacterial activity." *Asian Pacific Journal of Tropical Biomedicine* 1 (2):154-160.
- Meeran, Syed M, Suchitra Katiyar, Craig A Elmets, and Santosh K Katiyar. 2006. "Silymarin inhibits UV radiation-induced immunosuppression through augmentation of interleukin-12 in mice." *Molecular cancer therapeutics* 5 (7):1660-1668.
- Morgan, Claire, and Yamni Nigam. 2013. "Naturally derived factors and their role in the promotion of angiogenesis for the healing of chronic wounds." *Angiogenesis* 16 (3):493-502.
- Morones-Ramirez, J. Ruben, Jonathan A. Winkler, Catherine S. Spina, and James J. Collins. 2013. "Silver Enhances Antibiotic Activity Against Gram-negative Bacteria." *Science translational medicine* 5 (190):190ra81-190ra81. doi: 10.1126/scitranslmed.3006276.
- Motterlini, Roberto, Roberta Foresti, Rekha Bassi, and Colin J Green. 2000. "Curcumin, an antioxidant and anti-inflammatory agent, induces heme oxygenase-1 and protects endothelial cells against oxidative stress." *Free Radical Biology and Medicine* 28 (8):1303-1312.

- Murphy, William L., Martin C. Peters, David H. Kohn, and David J. Mooney. 2000. "Sustained release of vascular endothelial growth factor from mineralized poly(lactide-co-glycolide) scaffolds for tissue engineering." *Biomaterials* 21 (24):2521-2527. doi: [https://doi.org/10.1016/S0142-9612\(00\)00120-4](https://doi.org/10.1016/S0142-9612(00)00120-4).
- Myllyharju, Johanna, and Kari I Kivirikko. 2004. "Collagens, modifying enzymes and their mutations in humans, flies and worms." *TRENDS in Genetics* 20 (1):33-43.
- Naik, Kshipra, Amrita Chatterjee, Halan Prakash, and Meenal Kowshik. 2013. "Mesoporous TiO₂ nanoparticles containing Ag ion with excellent antimicrobial activity at remarkable low silver concentrations." *Journal of biomedical nanotechnology* 9 (4):664-673.
- Naik, Kshipra, and Meenal Kowshik. 2014. "Anti-biofilm efficacy of low temperature processed AgCl–TiO₂ nanocomposite coating." *Materials Science and Engineering: C* 34:62-68.
- Nair, Lakshmi S, and Cato T Laurencin. 2005. "Polymers as biomaterials for tissue engineering and controlled drug delivery." In *Tissue engineering I*, 47-90. Springer.
- Nencini, C, G Giorgi, and L Micheli. 2007. "Protective effect of silymarin on oxidative stress in rat brain." *Phytomedicine* 14 (2-3):129-135.
- Nielsen, Flemming, Bo Borg Mikkelsen, Jesper Bo Nielsen, Helle Raun Andersen, and Philippe Grandjean. 1997. "Plasma malondialdehyde as biomarker for oxidative stress: reference interval and effects of life-style factors." *Clinical chemistry* 43 (7):1209-1214.
- Nwe, Nitar, Tetsuya Furuike, and Hiroshi Tamura. 2009. "The mechanical and biological properties of chitosan scaffolds for tissue regeneration templates are significantly enhanced by chitosan from *Gongronella butleri*." *Materials* 2 (2):374-398.
- O'brien, Fergal J. 2011. "Biomaterials & scaffolds for tissue engineering." *Materials today* 14 (3):88-95.
- Ojha, Navdeep, Sashwati Roy, Guanglong He, Sabyasachi Biswas, Murugesan Velayutham, Savita Khanna, Periannan Kuppusamy, Jay L Zweier, and Chandan K Sen. 2008. "Assessment of wound-site redox environment and the significance of Rac2 in cutaneous healing." *Free Radical Biology and Medicine* 44 (4):682-691.

- Orrego, Carlos E, and Jesús S Valencia. 2009. "Preparation and characterization of chitosan membranes by using a combined freeze gelation and mild crosslinking method." *Bioprocess and biosystems engineering* 32 (2):197.
- Parenteau-Bareil, Rémi, Robert Gauvin, and François Berthod. 2010. "Collagen-based biomaterials for tissue engineering applications." *Materials* 3 (3):1863-1887.
- Pawar, Harshavardhan V., Joshua S. Boateng, Isaac Ayensu, and John Tetteh. "Multifunctional Medicated Lyophilised Wafer Dressing for Effective Chronic Wound Healing." *Journal of Pharmaceutical Sciences* 103 (6):1720-1733. doi: 10.1002/jps.23968.
- Pellegrini, Graziella, Rosario Ranno, Giorgio Stracuzzi, Sergio Bondanza, Liliana Guerra, Giovanna Zambruno, Giovanni Micali, and Michele De Luca. 1999. "The control of epidermal stem cells (holoclones) in the treatment of massive full-thickness burns with autologous keratinocytes cultured on fibrin1." *Transplantation* 68 (6):868-879.
- Pereira, Rúben F, and Paulo J Bartolo. 2016. "Traditional therapies for skin wound healing." *Advances in wound care* 5 (5):208-229.
- Pooja, Deep, Dileep J. Babu Bikkina, Hitesh Kulhari, Nalla Nikhila, Srinivas Chinde, Y. M. Raghavendra, B. Sreedhar, and Ashok K. Tiwari. 2014. "Fabrication, characterization and bioevaluation of silibinin loaded chitosan nanoparticles." *International Journal of Biological Macromolecules* 69:267-273. doi: <https://doi.org/10.1016/j.ijbiomac.2014.05.035>.
- Powell, Heather M, and Steven T Boyce. 2009. "Engineered human skin fabricated using electrospun collagen–PCL blends: morphogenesis and mechanical properties." *Tissue Engineering Part A* 15 (8):2177-2187.
- Prochazkova, Sabina, Kjell M. Vårum, and Kjetill Ostgaard. 1999. "Quantitative determination of chitosans by ninhydrin." *Carbohydrate Polymers* 38 (2):115-122. doi: [https://doi.org/10.1016/S0144-8617\(98\)00108-8](https://doi.org/10.1016/S0144-8617(98)00108-8).
- Pundir, Sarika, Ashutosh Badola, and Deepak Sharma. 2017. "Sustained release matrix technology and recent advance in matrix drug delivery system: a review." *International Journal of drug research and technology* 3 (1):8.
- Rambhia, Kunal J, and Peter X Ma. 2015. "Controlled drug release for tissue engineering." *Journal of Controlled Release* 219:119-128.

- Rasouli, Hassan, Mohammad Hosein Farzaei, and Reza Khodarahmi. 2017. "Polyphenols and their benefits: A review." *International Journal of Food Properties*:1-42.
- Regiel, Anna, Silvia Irusta, Agnieszka Kyzioł, Manuel Arruebo, and Jesus Santamaria. 2012. "Preparation and characterization of chitosan–silver nanocomposite films and their antibacterial activity against *Staphylococcus aureus*." *Nanotechnology* 24 (1):015101.
- Ricciardi, Rosa, Gerardino D'Errico, Finizia Auriemma, Guylaine Ducouret, Anna Maria Tedeschi, Claudio De Rosa, Françoise Lauprêtre, and Françoise Lafuma. 2005. "Short time dynamics of solvent molecules and supramolecular organization of poly (vinyl alcohol) hydrogels obtained by freeze/thaw techniques." *Macromolecules* 38 (15):6629-6639.
- Rodrigues, Mariana N, Mariana B Oliveira, Rui R Costa, and João F Mano. 2016. "Chitosan/chondroitin sulfate membranes produced by polyelectrolyte complexation for cartilage engineering." *Biomacromolecules* 17 (6):2178-2188.
- Roy, Mainak, Poulomi Mukherjee, Balaji P Mandal, Rajendra K Sharma, Avesh K Tyagi, and Sharad P Kale. 2012. "Biomimetic synthesis of nanocrystalline silver sol using cysteine: stability aspects and antibacterial activities." *RSC Advances* 2 (16):6496-6503.
- Samal, Juhi, Stefan Weinandy, Agnieszka Weinandy, Marius Helmedag, Lisanne Rongen, Benita Hermanns-Sachweh, Subhas C Kundu, and Stefan Jockenhoevel. 2015. "Co-Culture of Human Endothelial Cells and Foreskin Fibroblasts on 3D Silk–Fibrin Scaffolds Supports Vascularization." *Macromolecular bioscience* 15 (10):1433-1446.
- Saraswathy, G, S Pal, C Rose, and TP Sastry. 2001. "A novel bio-inorganic bone implant containing deglued bone, chitosan and gelatin." *Bulletin of Materials Science* 24 (4):415-420.
- Saravanan, M., Anil Kumar Vemu, and Sisir Kumar Barik. 2011. "Rapid biosynthesis of silver nanoparticles from *Bacillus megaterium* (NCIM 2326) and their antibacterial activity on multi drug resistant clinical pathogens." *Colloids and Surfaces B: Biointerfaces* 88 (1):325-331. doi: <https://doi.org/10.1016/j.colsurfb.2011.07.009>.
- Schäfer, Matthias, and Sabine Werner. 2008. "Oxidative stress in normal and impaired wound repair." *Pharmacological Research* 58 (2):165-171.

- Sell, Scott A, Patricia S Wolfe, Koyal Garg, Jennifer M McCool, Isaac A Rodriguez, and Gary L Bowlin. 2010. "The use of natural polymers in tissue engineering: a focus on electrospun extracellular matrix analogues." *Polymers* 2 (4):522-553.
- Sen, Chandan K, Gayle M Gordillo, Sashwati Roy, Robert Kirsner, Lynn Lambert, Thomas K Hunt, Finn Gottrup, Geoffrey C Gurtner, and Michael T Longaker. 2009. "Human skin wounds: a major and snowballing threat to public health and the economy." *Wound repair and regeneration* 17 (6):763-771.
- Shahidi, Fereidoon, PK Janitha, and PD Wanasundara. 1992. "Phenolic antioxidants." *Critical reviews in food science & nutrition* 32 (1):67-103.
- Shaik, M Monsoor, and Meenal Kowshik. 2016. "Novel melt-down neutralization method for synthesis of chitosan–silver scaffolds for tissue engineering applications." *Polymer Bulletin* 73 (3):841-858.
- Shaikh, J, DD Ankola, V Beniwal, D Singh, and MNV Ravi Kumar. 2009. "Nanoparticle encapsulation improves oral bioavailability of curcumin by at least 9-fold when compared to curcumin administered with piperine as absorption enhancer." *European Journal of Pharmaceutical Sciences* 37 (3):223-230.
- Sharma, Chhavi, Amit Kumar Dinda, Pravin D Potdar, Chia-Fu Chou, and Narayan Chandra Mishra. 2016. "Fabrication and characterization of novel nano-biocomposite scaffold of chitosan–gelatin–alginate–hydroxyapatite for bone tissue engineering." *Materials Science and Engineering: C* 64:416-427.
- Sharma, Pallavi, Ambuj Bhushan Jha, Rama Shanker Dubey, and Mohammad Pessaraki. 2012. "Reactive oxygen species, oxidative damage, and antioxidative defense mechanism in plants under stressful conditions." *Journal of botany* 2012.
- Sherif, Imam O, and Mohammed MH Al-Gayyar. 2013. "Antioxidant, anti-inflammatory and hepatoprotective effects of silymarin on hepatic dysfunction induced by sodium nitrite." *European cytokine network* 24 (3):114-121.
- Sin, Bo Young, and Hyun Pyo Kim. 2005. "Inhibition of collagenase by naturally-occurring flavonoids." *Archives of pharmacal research* 28 (10):1152-1155.
- Singh, Braj R, Brahma N Singh, Akanksha Singh, Wasi Khan, Alim H Naqvi, and Harikesh B Singh. 2015. "Mycofabricated biosilver nanoparticles interrupt *Pseudomonas aeruginosa* quorum sensing systems." *Scientific reports* 5:13719.

- Singh, Deepti, Dolly Singh, and Sung Soo Han. 2016. "3D printing of scaffold for cells delivery: advances in skin tissue engineering." *Polymers* 8 (1):19.
- Sionkowska, A, M Wisniewski, J Skopinska, CJ Kennedy, and TJ Wess. 2004. "Molecular interactions in collagen and chitosan blends." *Biomaterials* 25 (5):795-801.
- Smith, Lynne T, Karen A Holbrook, and Joseph A Madri. 1986. "Collagen types I, III, and V in human embryonic and fetal skin." *Developmental Dynamics* 175 (4):507-521.
- Sokolsky-Papkov, Marina, Kapil Agashi, Andrew Olaye, Kevin Shakesheff, and Abraham J. Domb. 2007. "Polymer carriers for drug delivery in tissue engineering." *Advanced Drug Delivery Reviews* 59 (4):187-206. doi: <https://doi.org/10.1016/j.addr.2007.04.001>.
- Soto, C, J Pérez, V García, E Uría, M Vadillo, and L Raya. 2010. "Effect of silymarin on kidneys of rats suffering from alloxan-induced diabetes mellitus." *Phytomedicine* 17 (14):1090-1094.
- Stratton, Scott, Namdev B. Shelke, Kazunori Hoshino, Swetha Rudraiah, and Sangamesh G. Kumbar. 2016. "Bioactive polymeric scaffolds for tissue engineering." *Bioactive Materials* 1 (2):93-108. doi: <https://doi.org/10.1016/j.bioactmat.2016.11.001>.
- Sun, Jinchun, and Huaping Tan. 2013. "Alginate-based biomaterials for regenerative medicine applications." *Materials* 6 (4):1285-1309.
- Surai, Peter F. 2015. "Silymarin as a natural antioxidant: an overview of the current evidence and perspectives." *Antioxidants* 4 (1):204-247.
- Svobodová, Alena, Daniela Walterová, and Jitka Psotová. 2006. "Influence of silymarin and its flavonolignans on H₂O₂-induced oxidative stress in human keratinocytes and mouse fibroblasts." *Burns* 32 (8):973-979.
- Tabandeh, Mohammad Reza, Ahamd Oryan, Adel Mohhammad-Alipour, and Abotorab Tabatabaei-Naieni. 2013. "Silibinin regulates matrix metalloproteinase 3 (stromelysin1) gene expression, hexoseamines and collagen production during rat skin wound healing." *Phytotherapy Research* 27 (8):1149-1153.
- Takagi, Atsuya, Kimie Sai, Takashi Umemura, Ryuichi Hasegawa, and Yuji Kurokawa. 1995. "Inhibitory effects of vitamin E and ellagic acid on 8-hydroxydeoxyguanosine formation in liver nuclear DNA of rats treated with 2-nitropropane." *Cancer Letters* 91 (1):139-144. doi: [https://doi.org/10.1016/0304-3835\(95\)03734-E](https://doi.org/10.1016/0304-3835(95)03734-E).

- Tangsadthakun, Chalonglarp, Sorada Kanokpanont, Neeracha Sanchavanakit, Tanom Banaprasert, and Siriporn Damrongsakkul. 2017. "Properties of collagen/chitosan scaffolds for skin tissue engineering." *Journal of Metals, Materials and Minerals* 16 (1).
- Thakur, Vijay Kumar, Manju Kumari Thakur, and Raju Kumar Gupta. 2013. "Rapid synthesis of graft copolymers from natural cellulose fibers." *Carbohydrate Polymers* 98 (1):820-828. doi: <https://doi.org/10.1016/j.carbpol.2013.06.072>.
- Thombre, Rebecca S, Vinaya Shinde, Elvina Thaiparambil, Samruddhi Zende, and Sourabh Mehta. 2016. "Antimicrobial activity and mechanism of inhibition of silver nanoparticles against extreme halophilic archaea." *Frontiers in microbiology* 7:1424.
- Tracy, Lauren E, Raquel A Minasian, and EJ Caterson. 2016. "Extracellular matrix and dermal fibroblast function in the healing wound." *Advances in wound care* 5 (3):119-136.
- Tripathi, Shipra, GK Mehrotra, and PK Dutta. 2011. "Chitosan–silver oxide nanocomposite film: preparation and antimicrobial activity." *Bulletin of Materials Science* 34 (1):29-35.
- Tsang, Ka-Kit, Enid Wai-Yung Kwong, Kevin Y Woo, Tony Shing-Shun To, Joanne Wai-Yee Chung, and Thomas Kwok-Shing Wong. 2015. "The anti-inflammatory and antibacterial action of nanocrystalline silver and manuka honey on the molecular alternation of diabetic foot ulcer: a comprehensive literature review." *Evidence-Based Complementary and Alternative Medicine* 2015.
- Ulery, Bret D, Lakshmi S Nair, and Cato T Laurencin. 2011. "Biomedical applications of biodegradable polymers." *Journal of polymer science Part B: polymer physics* 49 (12):832-864.
- Umesalma, Syed, and Ganapasam Sudhandiran. 2010. "Differential inhibitory effects of the polyphenol ellagic acid on inflammatory mediators NF- κ B, iNOS, COX-2, TNF- α , and IL-6 in 1, 2-dimethylhydrazine-induced rat colon carcinogenesis." *Basic & clinical pharmacology & toxicology* 107 (2):650-655.
- Uzar, Ertugrul, Harun Alp, Mehmet Ugur Cevik, Ugur Fırat, Osman Evliyaoglu, Adnan Tufek, and Yasar Altun. 2012. "Ellagic acid attenuates oxidative stress on brain and sciatic nerve and improves histopathology of brain in streptozotocin-induced diabetic rats." *Neurological Sciences* 33 (3):567-574.

- Venkatesan, Jayachandran, and Se-Kwon Kim. 2010. "Chitosan composites for bone tissue engineering—an overview." *Marine drugs* 8 (8):2252-2266.
- Wang, Ping, Libin Zhang, Hao Peng, Yongwu Li, Jian Xiong, and Zheyuan Xu. 2013. "The formulation and delivery of curcumin with solid lipid nanoparticles for the treatment of on non-small cell lung cancer both in vitro and in vivo." *Materials Science and Engineering: C* 33 (8):4802-4808.
- Wang, Wei, Shuqin Bo, Shuqing Li, and Wen Qin. 1991. "Determination of the Mark-Houwink equation for chitosans with different degrees of deacetylation." *International Journal of Biological Macromolecules* 13 (5):281-285. doi: [https://doi.org/10.1016/0141-8130\(91\)90027-R](https://doi.org/10.1016/0141-8130(91)90027-R).
- Watt, Fiona M, and Hironobu Fujiwara. 2011. "Cell-extracellular matrix interactions in normal and diseased skin." *Cold Spring Harbor perspectives in biology* 3 (4):a005124.
- Wei, Guobao, Qiming Jin, William V. Giannobile, and Peter X. Ma. 2006. "Nano-fibrous scaffold for controlled delivery of recombinant human PDGF-BB." *Journal of Controlled Release* 112 (1):103-110. doi: <https://doi.org/10.1016/j.jconrel.2006.01.011>.
- Wu, Xia, Jidong Li, Li Wang, Di Huang, Yi Zuo, and Yubao Li. 2010. "The release properties of silver ions from Ag-nHA/TiO₂/PA66 antimicrobial composite scaffolds." *Biomedical Materials* 5 (4):044105.
- Xu, Haitang, Lie Ma, Haifei Shi, Changyou Gao, and Chunmao Han. 2007. "Chitosan–hyaluronic acid hybrid film as a novel wound dressing: in vitro and in vivo studies." *Polymers for advanced technologies* 18 (11):869-875.
- Yang, Gang, Yaping Zhao, Nianping Feng, Yongtai Zhang, Ying Liu, and Beilei Dang. 2015. "Improved dissolution and bioavailability of silymarin delivered by a solid dispersion prepared using supercritical fluids." *Asian Journal of Pharmaceutical Sciences* 10 (3):194-202. doi: <https://doi.org/10.1016/j.ajps.2014.12.001>.
- You, Chuangang, Qiong Li, Xingang Wang, Pan Wu, Jon Kee Ho, Ronghua Jin, Liping Zhang, Huawei Shao, and Chunmao Han. 2017. "Silver nanoparticle loaded collagen/chitosan scaffolds promote wound healing via regulating fibroblast migration and macrophage activation." *Scientific Reports* 7 (1):10489. doi: [10.1038/s41598-017-10481-0](https://doi.org/10.1038/s41598-017-10481-0).

Yu, Hai, Chunjun Qin, Peipei Zhang, Qingfeng Ge, Mangang Wu, Jianping Wu, Miao Wang, and Zhijun Wang. 2015. "Antioxidant effect of apple phenolic on lipid peroxidation in Chinese-style sausage." *Journal of food science and technology* 52 (2):1032-1039.

Yue, Beatrice. 2014. "Biology of the Extracellular Matrix: An Overview." *Journal of glaucoma*:S20-S23. doi: 10.1097/IJG.0000000000000108.

Zhang, Li-Juan, Xu-Sheng Feng, Hong-Guo Liu, Dong-Jin Qian, Li Zhang, Xi-Ling Yu, and Fu-Zhai Cui. 2004. "Hydroxyapatite/collagen composite materials formation in simulated body fluid environment." *Materials Letters* 58 (5):719-722.

List of Publications

- 1) **M. Monsoor Shaik**, Meenal Kowshik. Novel melt-down neutralization method for synthesis of chitosan–silver scaffolds for tissue engineering applications, *Polymer Bulletin*, 2016, 73:841-858.
- 2) **M. Monsoor Shaik**, Meenal Kowshik. Ellagic acid containing collagen-chitosan scaffolds as potential antioxidative bio-materials for tissue engineering applications, *International Journal of Polymeric Materials and Polymeric Biomaterials*, 2018, DOI: 10.1080/00914037.2018.1443927.
- 3) Deshmukh, Ketaki, **M. Monsoor Shaik**, Sutapa Roy Ramanan, Meenal Kowshik. Self-Activated Fluorescent Hydroxyapatite Nanoparticles: A Promising Agent for Bioimaging and Biolabeling, *ACS Biomaterials Science & Engineering*, 2016, 8:1257-1264.
- 4) Kshipra Naik, Pallavee Srivastava, Ketaki Deshmukh, **M Monsoor S**, Meenal Kowshik. Nanomaterial-based approaches for prevention of biofilm-associated infections on medical devices and implants, *Journal of Nanoscience and Nanotechnology*, 2015, 15:10108-10119.

List of Workshops/ Conference

- **M. Monsoor S** and Meenal Kowshik, Preparation and characterization of Chitosan Nano-Silver biocomposites for wound healing applications (Oral presentation at International Conference on Nano Materials: Science, Technology and Applications, ICNM'13, Chennai, Tamil Nadu), organized by B.S. Abdur Rahman University, India, Deakin University, Australia and Universiti Teknologi MARA, Malaysia from 5th-7th December, 2013. **Won Best Paper Presentation.**
- Monsoon International Workshop on Green Nanotechnology from 6th and 7th August, 2013, at Bogmalo Beach Resort Hotel, Goa, organized by Sam Higginbottom Institute of Agriculture, Technology and Sciences- Deemed University, Allahabad, India in partnership with University of Missouri, USA.
- **M. Monsoor S** and Meenal Kowshik, Novel melt-down neutralization method for synthesis of Chitosan-silver scaffolds for wound healing applications (Poster presentation at Indo-UK international workshop at Advanced Materials And Their Applications In Nanotechnology-2014, Goa) organized by University of Leeds, United Kingdom and BITS Pilani K K Birla Goa Campus, India from 17th- 19th May, 2014.

Brief Biography of the Candidate

Mr. Mohammed Monsoor Shaik was born in Andhra Pradesh, India. He received his Bachelor's degree in biochemistry, biotechnology and chemistry as majors from Acharya Nagarjuna University (2005-2008). He finished his Master's degree in biotechnology from Bangalore University in 2010. Successively, he worked as event organizer in Bangalore for a year before joining BITS Pilani K K Birla Goa Campus in 2012. As a researcher he worked on the synthesis of inorganic nanomaterials for bioimaging applications. His research interests include fabrication of biopolymer scaffolds for wound healing applications. He won the 'Best Paper Presentation Award' for his presentation entitled "Preparation and characterization of Chitosan-Silver biocomposites for wound healing applications" in International Conference on Nano Materials: Science, Technology and Applications, ICNM'13.

Brief Biography of the Supervisor

Prof. Meenal Kowshik received her M. Sc. in Microbiology from Goa University in 1997. She worked on the biological synthesis of metallic and metal sulfide nanoparticles using yeasts at Agarkar Research Institute, and obtained her Ph.D. degree from Pune University (1999–2003). Subsequently, she joined Birla Institute of Technology and Science, Pilani K K Birla Goa Campus, and is currently working as Associate Professor in the Department of Biological Sciences. Her research interests include studies on biofunctionalization of silver based nanocomposites for antimicrobial applications; synthesis of biocompatible nanomaterials for tissue engineering; application of nanomaterials in molecular biology research; interactions of nanomaterials and microorganisms with respect to nanomaterial synthesis as well as toxicity, with special emphasis on halophilic archaeobacteria. She has received research grants from Department of Science and technology for two projects and from the Ministry of Earth Sciences. She has been a co–investigator on four other projects sanctioned by the agencies; Department of Biotechnology, DRDO and UGC. She has published 29 research papers in International and National journals of repute; has 3 patents to her credit and has delivered several invited talks at International and National conferences.